On the derivation of guaranteed and p-robust a posteriori error estimates for the Helmholtz equation

Théophile Chaumont-Frelet, Alexandre Ern, Martin Vohralík

ON THE DERIVATION OF GUARANTEED AND p-ROBUST A POSTERIORI ERROR ESTIMATES FOR THE HELMHOLTZ EQUATION*

T. CHAUMONT-FRELET[1,2], A. ERN[3,4], AND M. VOHRALÍK[4,3]

ABSTRACT. We propose a novel *a posteriori* error estimator for conforming finite element discretizations of two- and three-dimensional Helmholtz problems. The estimator is based on an equilibrated flux that is computed by solving patchwise mixed finite element problems. We show that the estimator is reliable up to a prefactor that tends to one with mesh refinement or with polynomial degree increase. We also derive a fully computable upper bound on the prefactor for several common settings of domains and boundary conditions. This leads to a guaranteed estimate without any assumption on the mesh size or the polynomial degree, though the obtained guaranteed bound may lead to large error overestimation. We next demonstrate that the estimator is locally efficient, robust in all regimes with respect to the polynomial degree, and asymptotically robust with respect to the wavenumber. Finally we present numerical experiments that illustrate our analysis and indicate that our theoretical results are sharp.

KEY WORDS. A posteriori error estimates; Finite element methods; Helmholtz problems; High order methods.

1. INTRODUCTION

In this work, we are concerned with the following Helmholtz equation: find $u : \Omega \to \mathbb{C}$ such that

$$\left\{ \begin{array}{rcll} -k^2 u - \Delta u & = & f & \text{in } \Omega, \\ u & = & 0 & \text{on } \Gamma_{\rm D}, \\ \boldsymbol{\nabla} u \cdot \boldsymbol{n} - iku & = & g & \text{on } \Gamma_{\rm A}. \end{array} \right. \tag{1.1}$$

Here $\Omega \subset \mathbb{R}^d$, $d = 2$ or 3, is a Lipschitz domain with polygonal or polyhedral boundary $\partial\Omega$ that is partitioned into two disjoint relatively open sets $\Gamma_{\rm D}$ and $\Gamma_{\rm A}$, $\boldsymbol{n}$ denotes the unit vector normal to $\partial\Omega$ pointing outward Ω, $f : \Omega \to \mathbb{C}$ and $g : \Gamma_{\rm A} \to \mathbb{C}$ are prescribed data, and the real number $k \in (0, +\infty)$ is the wavenumber.

Problem (1.1) can accurately model the propagation of time-harmonic acoustic or polarized electromagnetic waves. It is also insightful for more elaborate wave propagation models employed, for instance, in elasticity and electromagnetics, with industrial applications in acoustics, radar, and medical or subsurface imaging, see, e.g. [16, 19, 23, 41, 54] and the references therein.

*This project has received funding from the European Research Council (ERC) under the European Union's Horizon 2020 research and innovation program (grant agreement No 647134).

[1]Inria, 2004 Route des Lucioles, 06902 Valbonne, France

[2]Laboratoire J.A. Dieudonné, Parc Valrose, 28 Avenue Valrose, 06108 Nice Cedex 02, 06000 Nice, France

[3]CERMICS, Ecole des Ponts, 77455 Marne-la-Vallée, France

[4]Inria, 2 rue Simone Iff, 75589 Paris, France

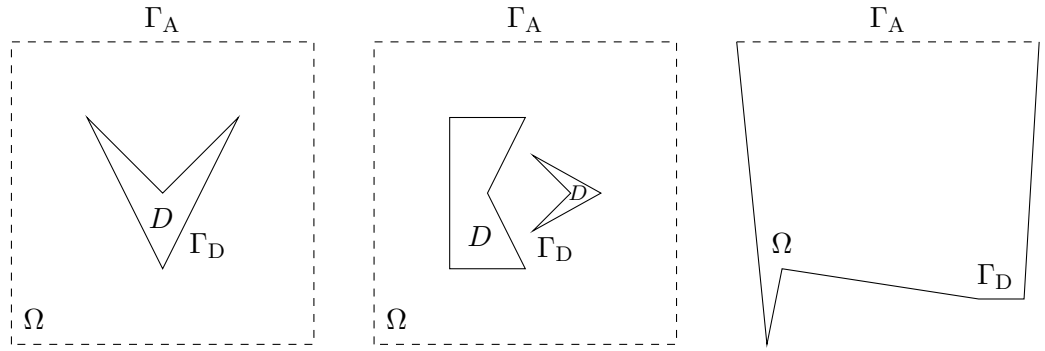

(a) non-trapping obstacle (b) trapping obstacle (c) cavity

FIGURE 1. Examples of domains Ω and boundaries Γ_D and Γ_A

The above setting can represent the *scattering problem* by a sound-soft obstacle D, see Figure 1, (a) and (b). Then $\Gamma_D = \partial D$ represents the boundary of the obstacle, $\Gamma_A = \partial\Omega_0$ where Ω_0 is some "computational box" that includes and surrounds D, and $\Omega = \Omega_0 \setminus D$. An important scenario is the case of a *non-trapping obstacle* D in which both D and Ω_0 are star-shaped with respect to a common center, see Figure 1, (a); for a *trapping obstacle*, see Figure 1, (b), such a condition is not satisfied. In *cavity* problems, see Figure 1, (c), Γ_D represents the basis of a cavity and Γ_A is typically planar. The obstacle-free case with $\Gamma_D = \emptyset$ represents the propagation of a wave in *free space*. Finally, the so-called *interior problem* where $\Gamma_A = \emptyset$ is well-posed provided that k^2 is not an eigenvalue of the Laplace operator in Ω.

Numerical discretizations, often based on the finite element method, are nowadays vastly used to find approximate solutions to (1.1). Here, a finite-dimensional space V_h is constructed which typically consists of piecewise polynomials of degree $p \geq 1$ defined over a computational mesh $\mathcal{T}_h$ of Ω with a maximal cell size h. In this case, $(\frac{kh}{2\pi p})^{-1}$ is a measure of the number of degrees of freedom per wavelength. Another important quantity, following [28, 44], is the approximation factor[1]

$$\sigma_{\mathrm{ba}} := k \sup_{\phi \in L^2(\Omega)\setminus\{0\}} \inf_{v_h \in V_h} \frac{|u_\phi^\star - v_h|_{1,\Omega}}{\|\phi\|_{0,\Omega}},$$

where $u_\phi^\star$ solves an adjoint problem to (1.1) with data $f = \phi$ and $g = 0$ (see Section 2.3 for more details). The real number σ_{ba} describes the ability of the discrete space V_h to approximate (adjoint) solutions to (1.1). This quantity combines a measure of the approximation capacity of V_h in the H^1-seminorm with the stability of the associated adjoint problem. Incidentally we notice that σ_{ba} is bounded uniformly with respect to h and p, as can be seen by taking $v_h = 0$ in the above definition. For the case of scattering by a smooth non-trapping obstacle, the following upper bound is available:

$$\sigma_{\mathrm{ba}} \leq C(\widehat{\Omega}, \widehat{\Gamma}_D) C(\kappa) \left(\frac{kh}{p} + kh_\Omega \left(\frac{kh}{p} \right)^p \right), \tag{1.2}$$

[1]Our definition is slightly different from [44] as we include the wavenumber k in σ_{ba}. This way, the quantity σ_{ba} is adimensional, and invariant under rescaling.

where the constants $C(\widehat{\Omega}, \widehat{\Gamma}_{\mathrm{D}})$ and $C(\kappa)$, respectively, only depend on the shape of the computational domain Ω (but not on its diameter h_Ω) and on the mesh shape-regularity parameter κ, see [44, Proposition 5.3]. We speak of *unresolved regime* when $\frac{kh}{2\pi p} > 1$, and of *resolved regime* when $\frac{kh}{2\pi p} \leq 1$. We also speak of *asymptotic regime* when $\sigma_{\mathrm{ba}} \leq 1$ and *preasymptotic regime* otherwise. We point out that the condition $\sigma_{\mathrm{ba}} \leq 1$ typically translates into stronger requirements on h and p than the resolved regime.

The sesquilinear form $b(\cdot,\cdot)$ associated with the boundary value problem (1.1) is typically not coercive, as it contains a negative $L^2(\Omega)$ contribution, and thus does not lead to an energy norm. The finite element solution (when it exists), is almost meaningless in the unresolved regime, where even the best approximation of the solution u of (1.1) in the discrete space V_h is inaccurate. In the resolved regime, this best approximation already starts to accurately represent u, but the finite element solution $u_h \in V_h$ is not necessarily quasi-optimal and is typically still inaccurate. This phenomena is known in the literature as the "pollution effect". It is only in the asymptotic regime that the quasi-optimality of the finite element solution is ensured, cf. [44] and the references therein. The typical dependence (1.2) encourages the use of finite elements with high polynomial degree p to solve problems with high wavenumber k, and this is a usual practice, cf. [2, 6, 14, 20, 44, 54] and the references therein.

The design of suitable *a posteriori* estimators is of paramount importance both for control of the error between u and u_h and for the efficiency of algorithms adaptively refining h and/or p [24, 56]. Pioneering works on a posteriori error estimation for the Helmholtz equation are reported in [4, 5]. The authors focus on first-order discretizations ($p = 1$) of one-dimensional problems and prove that in the asymptotic regime, the residual [56] and the Zienkiewicz–Zhu [57] estimators are reliable (yielding an error upper bound) and efficient (yielding an error lower bound). Numerous refinements of these results, including goal-oriented estimation and *hp* adaptivity, can be found in [22, 36, 46, 49, 52, 53], see also the references therein.

More recently, *residual estimators* for high-order finite element as well as discontinuous Galerkin discretizations of two- and three-dimensional problems have been studied in [28, 50], where an upper bound is obtained even in the preasymptotic regime, taking the form (when the data f and g are piecewise polynomial)

$$(k^2\|u-u_h\|_{0,\Omega}^2 + |u-u_h|_{1,\Omega}^2)^{\frac{1}{2}} \leq C_{\mathrm{up}}\eta, \quad C_{\mathrm{up}} = C(\kappa) + \theta_0(\sigma_{\mathrm{ba}}), \tag{1.3a}$$

where η is the a posteriori error estimator which is fully computable from u_h and the data. The constant $C(\kappa)$ is not computable, but only depends on the shape-regularity parameter κ of the mesh $\mathcal{T}_h$, and $\lim_{t\to 0}\theta_0(t) = 0$. One sees that in the asymptotic regime where $\sigma_{\mathrm{ba}} \leq 1$, the prefactor C_{up} in (1.3a) simplifies into an (unknown) constant that only depends on the mesh shape-regularity parameter. Moreover, the authors in [28, 50] prove that as long as there are sufficiently many degrees of freedom per wavelength (essentially in the resolved regime where $\frac{kh}{2\pi p} \leq 1$),

$$\eta_K \leq C_{\mathrm{low},\omega_K}(k^2\|u-u_h\|_{0,\omega_K}^2 + |u-u_h|_{1,\omega_K}^2)^{\frac{1}{2}}, \quad C_{\mathrm{low},\omega_K} = C(\kappa_{\mathcal{T}_K}, p)\left(1 + \frac{kh_{\omega_K}}{p}\right), \tag{1.3b}$$

where the factor $(1+\frac{kh_{\omega_K}}{p})$ naturally appears for $\Gamma_{\mathrm{A}} = \emptyset$, $\eta = (\sum_{K\in\mathcal{T}_h}\eta_K^2)^{\frac{1}{2}}$, $\mathcal{T}_K$ is the patch of elements around the mesh element K with shape-regularity $\kappa_{\mathcal{T}_K}$ and the corresponding subdomain ω_K, and the constant $C(\kappa_{\mathcal{T}_K}, p)$ deteriorates as the polynomial degree p increases. We also refer the reader to [35], where the convergence of an adaptive discontinuous Galerkin method based on a residual estimator and Dörfler marking is studied.

Another approach to a posteriori error estimation is based on a construction of an *equilibrated flux*, cf. [25, 38, 47]. In this case, an unknown-constant-free upper bound is obtained for elliptic problems. Moreover, it has been recently shown [7, 29, 30] that such a strategy provides a p-robust estimator which means that the lower bound does not depend on the polynomial degree p. The recent work [20] proposes to use this type of estimators for discontinuous Galerkin discretizations of the Helmhotz problem. The authors consider a simpler configuration of (1.1) with $\Gamma_{\rm D} = \emptyset$ and $d = 2$ and evaluate the error in the $H^1(\Omega)$-seminorm $|u-u_h|_{1,\Omega}$ only. While the proposed estimator is p-robust, both reliability and efficiency only hold up to the uncomputable scaled error terms $k\|u-u_h\|_{0,\Omega}$ and $k^{\frac{1}{2}}\|u-u_h\|_{0,\Gamma_{\rm A}}$. These terms asymptotically vanish, but their actual size is unknown.

In the present work, we follow some of the main arguments developed in [28] but we employ equilibrated flux estimators instead of residual estimators. We establish our results in the *energy norm*

$$|||u-u_h|||_{1,k,\Omega}^2 := k^2\|u-u_h\|_{0,\Omega}^2 + k\|u-u_h\|_{0,\Gamma_{\rm A}}^2 + |u-u_h|_{1,\Omega}^2, \tag{1.4}$$

and prove the global upper bound

$$|||u-u_h|||_{1,k,\Omega} \le C_{\rm up}\eta, \qquad C_{\rm up} = \sqrt{2} + \theta_1(\sigma_{\rm ba}), \tag{1.5a}$$

where η is a fully computable equilibrated flux estimator and $\theta_1(t) := \sqrt{2t+2t^2}$. The factor $\sqrt{2}$ can be further decreased to the optimal value of 1 modulo additional technical developments that we detail in Theorem 2.3 below. Thus, asymptotically, (1.5a) is *unknown-constant-free*, in improvement of (1.3a), and additionally the entire energy norm (including the scaled $L^2(\Omega)$ and $L^2(\Gamma_{\rm A})$ terms) is controlled in contrast to [20]. Though the asymptotic nature of the approximability factor $\sigma_{\rm ba}$ is known, cf. (1.2), $\sigma_{\rm ba}$ cannot be computed or estimated from (1.2), so that the bound (1.5a) is not guaranteed in general. We succeed in removing this remaining deficiency and find a fully computable upper bound on $\sigma_{\rm ba}$ in several configurations of interest, see Theorem 2.7 below. Remarkably, the bound (1.5a) then becomes *guaranteed*, and this in *any regime* (unresolved, resolved, asymptotic), though the upper bound may largely overestimate the error.

The second main property of our estimators is the *local efficiency*

$$\eta_K \le C_{{\rm low},\omega_K}|||u-u_h|||_{1,k,\omega_K}, \quad C_{{\rm low},\omega_K} = C(\kappa_{\mathcal{T}_K})\left(1 + \left(\frac{kh_{\omega_K}}{p}\right)^{\frac{1}{2}} + \frac{kh_{\omega_K}}{p}\right), \tag{1.5b}$$

for every mesh element K, where the term $(\frac{kh_{\omega_K}}{p})^{\frac{1}{2}}$ appears for $\Gamma_{\rm A} \neq \emptyset$. Importantly, in contrast to (1.3b), the constant $C(\kappa_{\mathcal{T}_K})$ in (1.5b) is independent of the polynomial degree p (only depends on the local shape-regularity parameter $\kappa_{\mathcal{T}_K}$), and, in contrast to [20], the scaled $L^2(\Omega)$ and $L^2(\Gamma_{\rm A})$ terms are included. Since $C_{\rm up}$ is also independent of p, we conclude that our a posteriori error estimator is p-robust in all regimes. Moreover the estimator is robust with respect to the wavenumber k in the asymptotic regime where $\sigma_{\rm ba} \le 1$ (and $\frac{kh}{2\pi p} \le 1$).

Our manuscript is organized as follows. In Section 2, we make precise the functional and discrete settings and state our main results. We perform a general analysis of the relationships between the energy error (1.4) and dual norms of the residual in Section 3, and we employ these results in the context of flux equilibration in Section 4. In Section 5, we prove our fully computable upper bounds on the factor $\sigma_{\rm ba}$. We present numerical experiments that illustrate

our findings in Section 6 and draw our conclusions in Section 7. Finally, in Appendix A, we establish an intermediate result related to boundary and volume data.

2. Setting and main results

This section details the setting and presents our main results.

2.1. **Variational formulation.** We recast problem (1.1) into a weak form that consists in finding $u \in H^1_{\Gamma_D}(\Omega)$ such that

$$b(u,v) = (f,v) + (g,v)_{\Gamma_A} \qquad \forall v \in H^1_{\Gamma_D}(\Omega), \tag{2.1}$$

where

$$b(u,v) := -k^2(u,v) - ik(u,v)_{\Gamma_A} + (\boldsymbol{\nabla} u, \boldsymbol{\nabla} v) \tag{2.2}$$

and

$$H^1_{\Gamma_D}(\Omega) := \left\{ v \in H^1(\Omega) |\ v = 0 \text{ on } \Gamma_D \right\}.$$

Above and hereafter, for $m \in \mathbb{N}$ and an open set $\mathcal{O}$, $H^m(\mathcal{O})$ denotes the Sobolev space of order m. We also employ the notations $\|\cdot\|_{m,\mathcal{O}}$ and $|\cdot|_{m,\mathcal{O}}$ for the norm and semi-norm on $H^m(\mathcal{O})$. Also, $(\cdot,\cdot)_{\mathcal{O}}$ denotes the $L^2(\mathcal{O})$ inner-product, and we drop the subscript when $\mathcal{O} = \Omega$. We refer to [1, 18, 31] for the definition and essential properties of the Sobolev spaces. In the following, we assume that the operator $B : H^1_{\Gamma_D}(\Omega) \to (H^1_{\Gamma_D}(\Omega))'$ associated with the sesquilinear form b is a bounded isomorphism. This assumption holds for all $k > 0$ if $|\Gamma_A| > 0$, and it allows for $|\Gamma_A| = 0$ provided that k^2 is not an eigenvalue of the Laplace operator in Ω. We equip $H^1_{\Gamma_D}(\Omega)$ with the *energy norm*

$$|||v|||^2_{1,k,\Omega} := k^2\|v\|^2_{0,\Omega} + k\|v\|^2_{0,\Gamma_A} + |v|^2_{1,\Omega} \qquad \forall v \in H^1_{\Gamma_D}(\Omega). \tag{2.3}$$

Remark that this choice leads to the sharp continuity estimate

$$|b(\phi,v)| \le |||\phi|||_{1,k,\Omega}|||v|||_{1,k,\Omega} \qquad \forall \phi, v \in H^1(\Omega), \tag{2.4}$$

which is of particular interest in the context of goal-oriented error estimation [22, 46, 49].

2.2. **Discrete solution.** Consider a mesh $\mathcal{T}_h$ of Ω that consists of triangular or tetrahedral elements K such that $\bigcup_{K\in\mathcal{T}_h} \overline{K} = \overline{\Omega}$ and such that for two distinct elements $K_\pm \in \mathcal{T}_h$, the intersection $\overline{K_+} \cap \overline{K_-}$ is either empty, a single vertex, a full edge, or a full face of K_+ and K_-. We further require $\mathcal{T}_h$ to be compatible with the partition $\overline{\Gamma_D} \cup \overline{\Gamma_A}$ of $\partial\Omega$, i.e., that each boundary mesh face $\overline{F} \subset \partial\Omega$ is either included in $\overline{\Gamma_D}$ or in $\overline{\Gamma_A}$. For every element $K \in \mathcal{T}_h$, we also define its diameter h_K and its inscribed ball radius ρ_K by

$$h_K := \sup_{\boldsymbol{x},\boldsymbol{y}\in K} |\boldsymbol{x}-\boldsymbol{y}|, \quad \rho_K := \sup\left\{ r > 0 |\ \exists \boldsymbol{x} \in K;\ B(\boldsymbol{x},r) \subset K \right\}.$$

We assume that the mesh is shape-regular in the sense that every $K \in \mathcal{T}_h$ satisfies

$$\kappa_K := \frac{\rho_K}{h_K} \ge \kappa > 0$$

for a fixed constant κ. These hypotheses are standard [18] and not restrictive in particular in the sense that they do not preclude strong grading of the mesh. We will also sometimes use the notation $h := \max_{K\in\mathcal{T}_h} h_K$. If $\mathcal{T} \subset \mathcal{T}_h$ is a subset of cells K, we write $\kappa_{\mathcal{T}} := \min_{K\in\mathcal{T}} \kappa_K$.

For an integer $p \ge 1$, consider the space $\mathcal{P}_p(K)$ of polynomials on K of degree at most p, the broken space

$$\mathcal{P}_p(\mathcal{T}_h) := \left\{ v \in L^2(\Omega) |\ v|_K \in \mathcal{P}_p(K);\ \forall K \in \mathcal{T}_h \right\},$$

and define the approximation space

$$V_h := \mathcal{P}_p(\mathcal{T}_h) \cap H^1_{\Gamma_{\rm D}}(\Omega). \tag{2.5}$$

The discrete version of (2.1) seeks for $u_h \in V_h$ such that

$$b(u_h, v_h) = (f, v_h) + (g, v_h)_{\Gamma_{\rm A}} \qquad \forall v_h \in V_h. \tag{2.6}$$

In what follows we assume that there is at least one solution to (2.6). Uniqueness is not required for the present analysis to hold, i.e., $u_h \in V_h$ can be any solution to (2.6).

2.3. **Approximation properties of adjoint solutions.** The approximation properties of the space V_h from (2.5) play a central role in the forthcoming analysis. Specifically, following [28, 44], we consider the real number $\sigma_{\rm ba}$ defined in the introduction, i.e.

$$\sigma_{\rm ba} := k \sup_{\phi \in L^2(\Omega)\setminus\{0\}} \inf_{v_h \in V_h} \frac{|u^\star_\phi - v_h|_{1,\Omega}}{\|\phi\|_{0,\Omega}}, \tag{2.7}$$

where $u^\star_\phi$ denotes the unique (adjoint) solution in $H^1_{\Gamma_{\rm D}}(\Omega)$ such that

$$b(w, u^\star_\phi) = (w, \phi) \quad \forall w \in H^1_{\Gamma_{\rm D}}(\Omega). \tag{2.8}$$

In strong form, we have $-k^2 u^\star_\phi - \Delta u^\star_\phi = \phi$ in Ω, $u^\star_\phi = 0$ on $\Gamma_{\rm D}$, and $\boldsymbol{\nabla} u^\star_\phi \cdot \boldsymbol{n} + iku^\star_\phi = 0$ on $\Gamma_{\rm A}$. The real number $\sigma_{\rm ba}$ is independent of the data f and g but implicitly depends on Ω, $\Gamma_{\rm D}$, k, and V_h. It combines the ability of the discrete space V_h to approximate the solution $u^\star_\phi$ with the stability of the adjoint problem (2.8). Indeed, we have

$$k \inf_{v_h \in V_h} |u^\star_\phi - v_h|_{1,\Omega} \le \sigma_{\rm ba} \|\phi\|_{0,\Omega} \qquad \forall \phi \in L^2(\Omega). \tag{2.9}$$

The dependence of $\sigma_{\rm ba}$ on Ω, $\Gamma_{\rm D}$, k, and V_h (or less precisely but more concretely on the discretization parameters h and p) is not known in general. As previously stated, $\sigma_{\rm ba}$ is bounded uniformly with respect to h and p (take $v_h = 0$ in (2.7)). However, sharper bounds on $\sigma_{\rm ba}$ are expected to hold by taking other approximating functions $v_h \in V_h$, leading to upper bounds on $\sigma_{\rm ba}$ that depend on h and p. For instance, for the case of scattering by a smooth non-trapping obstacle [44], see also [13, 14], the upper bound (1.2) is available. More generally, as long as the domain Ω features an elliptic regularity shift for the Laplace operator (see e.g. [32]), one can state, cf. Section 5 below, that

$$\sigma_{\rm ba} \le C(\widehat{\Omega}, \widehat{\Gamma}_{\rm D}, k, \kappa) \left(\frac{kh}{p}\right)^{\varepsilon} \tag{2.10}$$

for some $\varepsilon = \varepsilon(\widehat{\Omega}, \widehat{\Gamma}_{\rm D}) > 0$. Here and above, $\widehat{\Omega} := (1/h_\Omega)\Omega$ and $\widehat{\Gamma}_{\rm D} := (1/h_\Omega)\Gamma_{\rm D}$ denote scaled versions of Ω and $\Gamma_{\rm D}$ which are independent of the size of the computational domain Ω. We provide a computable upper bound on $\sigma_{\rm ba}$ in some settings of interest in Theorem 2.7 below.

In addition to (2.7), we also introduce

$$\widetilde{\sigma}_{\rm ba} := k^{\frac{1}{2}} \sup_{\psi \in L^2(\Gamma_{\rm A})\setminus\{0\}} \inf_{v_h \in V_h} \frac{|\widetilde{u}^\star_\psi - v_h|_{1,\Omega}}{\|\psi\|_{0,\Gamma_{\rm A}}}, \tag{2.11}$$

where $\widetilde{u}^\star_\psi$ is the (adjoint) solution in $H^1_{\Gamma_{\rm D}}(\Omega)$ such that

$$b(w, \widetilde{u}^\star_\psi) = (w, \psi)_{\Gamma_{\rm A}} \quad \forall w \in H^1_{\Gamma_{\rm D}}(\Omega). \tag{2.12}$$

In strong form, we have $-k^2\widetilde{u}_\psi^\star - \Delta\widetilde{u}_\psi^\star = 0$ in Ω, $\widetilde{u}_\psi^\star = 0$ on $\Gamma_{\rm D}$, and $\boldsymbol{\nabla}\widetilde{u}_\psi^\star\cdot\boldsymbol{n} + ik\widetilde{u}_\psi^\star = \psi$ on $\Gamma_{\rm A}$. The quantity $\widetilde{\sigma}_{\rm ba}$ is similar to $\sigma_{\rm ba}$ since it measures the best-approximation error and the stability of the adjoint problem (2.12) which features a boundary right-hand side instead of a volume right-hand side as in (2.8). As in the case of volume data, $\widetilde{\sigma}_{\rm ba}$ is bounded uniformly with respect to h and p (take $v_h = 0$ in (2.11)) and if the domain Ω features an elliptic regularity shift, we have

$$\widetilde{\sigma}_{\rm ba} \le C(\widehat{\Omega},\widehat{\Gamma}_{\rm D},k,\kappa)\left(\frac{kh}{p}\right)^{\widetilde{\varepsilon}}, \tag{2.13}$$

where $\widetilde{\varepsilon} = \widetilde{\varepsilon}(\widehat{\Omega},\widehat{\Gamma}_{\rm D}) > 0$. In addition, under a reasonable assumption that is satisfied in all the configurations depicted in Figure 1, we prove in Appendix A the estimate

$$\widetilde{\sigma}_{\rm ba} \le C(\widehat{\Omega},\widehat{\Gamma}_{\rm D})C_{\rm qi}(\kappa)\left(\left(\frac{kh}{p}\right)^{\frac12} + \frac{kh}{p}\right) + \left(C(\widehat{\Omega},\widehat{\Gamma}_{\rm D})\frac{1}{kh_\Omega}\left(1+\frac{1}{kh_\Omega}\right)+2\right)\sigma_{\rm ba}, \tag{2.14}$$

where $C_{\rm qi}(\kappa)$ is a quasi-interpolation constant that only depends on the shape-regularity parameter κ [34, 43]. In particular, in the high-wavenumber regime when $kh_\Omega \to \infty$, we have

$$\widetilde{\sigma}_{\rm ba} \le 2\sigma_{\rm ba} + \mathcal{O}\left(\left(\frac{kh}{p}\right)^{\frac12}\right).$$

2.4. **Equilibrated flux reconstruction.** For each vertex $\boldsymbol{a}$ in the set of vertices $\mathcal{V}_h$ of the mesh $\mathcal{T}_h$, set

$$d_{\boldsymbol{a}} := \psi_{\boldsymbol{a}}\pi_h^p(f) + \psi_{\boldsymbol{a}}k^2u_h - \boldsymbol{\nabla}\psi_{\boldsymbol{a}}\cdot\boldsymbol{\nabla}u_h, \tag{2.15a}$$

and

$$b_{\boldsymbol{a}} := \begin{cases} -\psi_{\boldsymbol{a}}\widetilde{\pi}_h^p(g) - \psi_{\boldsymbol{a}}iku_h & \text{on } \partial\omega_{\boldsymbol{a}}\cap\Gamma_{\rm A},\\ 0 & \text{on } \partial\omega_{\boldsymbol{a}}\setminus\Gamma_{\rm A}.\end{cases} \tag{2.15b}$$

Here u_h is a finite element solution to (2.6) and $\psi_{\boldsymbol{a}}$ is the "hat function" associated with the vertex $\boldsymbol{a}$: the unique function in $\mathcal{P}_1(\mathcal{T}_h)\cap H^1(\Omega)$ such that $\psi_{\boldsymbol{a}}(\boldsymbol{a}) = 1$ and $\psi_{\boldsymbol{a}}(\boldsymbol{a}') = 0$ for all $\boldsymbol{a}' \in \mathcal{V}_h\setminus\{\boldsymbol{a}\}$. Moreover, the elementwise/facewise L^2 projectors π_h^q and $\widetilde{\pi}_h^q$ are respectively defined for any integer $q\ge 0$, any $v\in L^2(\Omega)$, and any $w\in L^2(\Gamma_{\rm A})$ by

$$\pi_h^q(v)|_K \in \mathcal{P}_q(K),\quad (\pi_h^q(v)|_K,\phi)_K = (v|_K,\phi)_K \quad \forall\phi\in\mathcal{P}_q(K),\ \forall K\in\mathcal{T}_h, \tag{2.16a}$$

$$\widetilde{\pi}_h^q(w)|_F \in \mathcal{P}_q(F),\quad (\widetilde{\pi}_h^q(w)|_F,\phi)_F = (v|_F,\phi)_F \quad \forall\phi\in\mathcal{P}_q(F),\ \forall F\in\mathcal{F}_h,\ F\subset\overline{\Gamma_{\rm A}}, \tag{2.16b}$$

where $\mathcal{F}_h$ is the set of mesh faces.

For an integer $q\ge 0$, let $\boldsymbol{\mathcal{P}}_q(K)$ be the set of vector-valued functions that have all components in $\mathcal{P}_q(K)$. We introduce the space $\boldsymbol{RT}_q(K) := \boldsymbol{x}\mathcal{P}_q(K) + \boldsymbol{\mathcal{P}}_q(K)$ from [45, 48] and define

$$\begin{aligned}\mathcal{P}_q(\mathcal{T}) &:= \left\{v\in L^2(\omega)|\ v|_K\in\mathcal{P}_q(K);\ \forall K\in\mathcal{T}\right\},\\ \boldsymbol{RT}_q(\mathcal{T}) &:= \left\{\boldsymbol{v}\in\boldsymbol{L}^2(\omega)|\ \boldsymbol{v}|_K\in\boldsymbol{RT}_q(K);\ \forall K\in\mathcal{T}\right\}\end{aligned}$$

for any subset of mesh elements $\mathcal{T}\subset\mathcal{T}_h$ with the corresponding open subdomain ω. In particular, for each vertex $\boldsymbol{a}\in\mathcal{V}_h$, we denote by $\mathcal{T}_{\boldsymbol{a}}$ the patch of all elements $K\in\mathcal{T}_h$ having $\boldsymbol{a}$ as a vertex and by $\omega_{\boldsymbol{a}}$ the corresponding open subdomain.

Following [7, 25, 29], we consider the following inexpensive and fully parallel post-processing procedure:

Definition 2.1 (Equilibrated flux reconstruction)**.** *For every vertex $\boldsymbol{a} \in \mathcal{V}_h$, let*

$$\boldsymbol{\sigma}_h^{\boldsymbol{a}} := \underset{\substack{\boldsymbol{\tau}_h^{\boldsymbol{a}} \in \boldsymbol{RT}_{p+1}(\mathcal{T}_{\boldsymbol{a}}) \cap \boldsymbol{H}(\mathrm{div},\omega_{\boldsymbol{a}}) \\ \boldsymbol{\nabla}\cdot\boldsymbol{\tau}_h^{\boldsymbol{a}} = d_{\boldsymbol{a}} \text{ in } \omega_{\boldsymbol{a}} \\ \boldsymbol{\tau}_h^{\boldsymbol{a}}\cdot\boldsymbol{n} = b_{\boldsymbol{a}} \text{ on } \Gamma_{\boldsymbol{a}}}}{\operatorname{argmin}} \|\boldsymbol{\tau}_h^{\boldsymbol{a}} + \psi_{\boldsymbol{a}}\boldsymbol{\nabla} u_h\|_{0,\omega_{\boldsymbol{a}}}, \tag{2.17}$$

where $\Gamma_{\boldsymbol{a}}$ is the boundary $\partial\omega_{\boldsymbol{a}}$ without those faces of Γ_{D} sharing the vertex $\boldsymbol{a}$. The equilibrated flux reconstruction is computed by summing up the patchwise contributions (after zero extension) as

$$\boldsymbol{\sigma}_h := \sum_{\boldsymbol{a}\in\mathcal{V}_h} \boldsymbol{\sigma}_h^{\boldsymbol{a}} \in \boldsymbol{RT}_{p+1}(\mathcal{T}_h) \cap \boldsymbol{H}(\mathrm{div},\Omega). \tag{2.18}$$

Since $d_{\boldsymbol{a}} \in \mathcal{P}_{p+1}(\mathcal{T}_{\boldsymbol{a}})$ and $b_{\boldsymbol{a}} \in \mathcal{P}_{p+1}(F)$ for each face $F \subset \partial\omega_{\boldsymbol{a}}$, we see that the minimization set in (2.17) is non-empty when

$$(d_{\boldsymbol{a}}, 1)_{\omega_{\boldsymbol{a}}} = (b_{\boldsymbol{a}}, 1)_{\partial\omega_{\boldsymbol{a}}} \qquad \forall \boldsymbol{a} \notin \overline{\Gamma_{\mathrm{D}}}. \tag{2.19}$$

Since $\psi_{\boldsymbol{a}} \in V_h$ when $\boldsymbol{a} \notin \overline{\Gamma_{\mathrm{D}}}$, we have from (2.6) in combination with (2.16)

$$(\psi_{\boldsymbol{a}}\pi_h^p(f), 1)_{\omega_{\boldsymbol{a}}} = (f, \psi_{\boldsymbol{a}}) = b(u_h, \psi_{\boldsymbol{a}}) - (g, \psi_{\boldsymbol{a}})_{\Gamma_{\mathrm{A}}} = b(u_h, \psi_{\boldsymbol{a}}) - (\psi_{\boldsymbol{a}}\widetilde{\pi}_h^p(g), 1)_{\Gamma_{\mathrm{A}}}.$$

As a result, the compatibility condition (2.19) follows from the definition (2.2) of $b(\cdot,\cdot)$ and

$$\begin{aligned}(\psi_{\boldsymbol{a}}\pi_h^p(f), 1)_{\omega_{\boldsymbol{a}}} =& -k^2(u_h, \psi_{\boldsymbol{a}})_{\omega_{\boldsymbol{a}}} - ik(u_h, \psi_{\boldsymbol{a}})_{\partial\omega_{\boldsymbol{a}}\cap\Gamma_{\mathrm{A}}} + (\boldsymbol{\nabla} u_h, \boldsymbol{\nabla}\psi_{\boldsymbol{a}})_{\omega_{\boldsymbol{a}}} - (\psi_{\boldsymbol{a}}\widetilde{\pi}_h^p(g), 1)_{\Gamma_{\mathrm{A}}} \\ =& (\boldsymbol{\nabla}\psi_{\boldsymbol{a}}\cdot\boldsymbol{\nabla} u_h - k^2\psi_{\boldsymbol{a}} u_h, 1)_{\omega_{\boldsymbol{a}}} + (b_{\boldsymbol{a}}, 1)_{\partial\omega_{\boldsymbol{a}}}.\end{aligned}$$

Then the uniqueness of the minimizer in (2.17) follows from standard convexity arguments.

Remark 2.2 (Equilibrated flux)**.** *In practice, the local fluxes $\boldsymbol{\sigma}_h^{\boldsymbol{a}}$ are obtained by invoking the Euler–Lagrange conditions of the constrained minimization problem* (2.17)*. This leads to the problem of finding the unique pair $(\boldsymbol{\sigma}_h^{\boldsymbol{a}}, r_h^{\boldsymbol{a}}) \in \boldsymbol{RT}_{p+1}(\mathcal{T}_{\boldsymbol{a}}) \cap \boldsymbol{H}(\mathrm{div},\omega_{\boldsymbol{a}}) \times \mathcal{P}_{p+1}^0(\mathcal{T}_{\boldsymbol{a}})$ such that $\boldsymbol{\sigma}_h^{\boldsymbol{a}}\cdot\boldsymbol{n} = b_{\boldsymbol{a}}$ on $\Gamma_{\boldsymbol{a}}$ and*

$$\begin{cases} (\boldsymbol{\sigma}_h^{\boldsymbol{a}}, \boldsymbol{v}_h)_{\omega_{\boldsymbol{a}}} - (r_h^{\boldsymbol{a}}, \boldsymbol{\nabla}\cdot\boldsymbol{v}_h)_{\omega_{\boldsymbol{a}}} &=& -(\psi_{\boldsymbol{a}}\boldsymbol{\nabla} u_h, \boldsymbol{v}_h)_{\omega_{\boldsymbol{a}}} & \forall \boldsymbol{v}_h \in \boldsymbol{RT}_{p+1}(\mathcal{T}_{\boldsymbol{a}}) \cap \boldsymbol{H}_{\Gamma_{\mathrm{A}}}(\mathrm{div},\omega_{\boldsymbol{a}}), \\ (\boldsymbol{\nabla}\cdot\boldsymbol{\sigma}_h^{\boldsymbol{a}}, v_h)_{\omega_{\boldsymbol{a}}} &=& (d_{\boldsymbol{a}}, v_h)_{\omega_{\boldsymbol{a}}} & \forall v_h \in \mathcal{P}_{p+1}^0(\mathcal{T}_{\boldsymbol{a}}), \end{cases}$$

where $\boldsymbol{H}_{\Gamma_{\mathrm{A}}}(\mathrm{div},\omega_{\boldsymbol{a}})$ imposes zero normal flux through $\Gamma_{\boldsymbol{a}}$ and where $\mathcal{P}_{p+1}^0(\mathcal{T}_{\boldsymbol{a}})$ is composed of the functions $v_h \in \mathcal{P}_{p+1}(\mathcal{T}_{\boldsymbol{a}})$ such that $(v_h, 1)_{\omega_{\boldsymbol{a}}} = 0$ if $\boldsymbol{a} \notin \overline{\Gamma_{\mathrm{D}}}$ whereas $\mathcal{P}_{p+1}^0(\mathcal{T}_{\boldsymbol{a}}) := \mathcal{P}_{p+1}(\mathcal{T}_{\boldsymbol{a}})$ otherwise.

2.5. **Data oscillation.** For each element $K \in \mathcal{T}_h$, we define

$$\mathrm{osc}_K(f,g) := \frac{h_K}{\pi}\|f - \pi_h^p(f)\|_{0,K} + C_{\mathrm{tr},K}\left(\frac{h_K}{\pi}\right)^{\frac{1}{2}}\|g - \widetilde{\pi}_h^p(g)\|_{0,\partial K\cap\Gamma_{\mathrm{A}}} \tag{2.20}$$

with

$$C_{\mathrm{tr},K}^2 := N_{K,\Gamma_{\mathrm{A}}}\frac{3}{4\pi}\left(1 + \frac{1}{\pi}\right)\left(\frac{h_K}{\rho_K}\right)^d,$$

where $N_{K,\Gamma_{\mathrm{A}}}$ is the number of faces of K that belong to Γ_{A}, and the remaining part of $C_{\mathrm{tr},K}$ comes from the standard trace inequality for one face of K, cf. [17, Section 4.2]. Owing to this definition of $\mathrm{osc}_K(f,g)$ and to the Poincaré inequality (recall that K is convex)

$$\|v\|_{0,K} \le \frac{h_K}{\pi}|v|_{1,K}$$

as well as to the trace inequality

$$\|v\|_{0,\partial K\cap\partial\Gamma_{\mathrm{A}}} \le C_{\mathrm{tr},K}\left(\frac{h_K}{\pi}\right)^{\frac{1}{2}}|v|_{1,K},$$

we have

$$\|f-\pi_h^p(f)\|_{0,K}\|v\|_{0,K} + \|g-\widetilde{\pi}_h^p(g)\|_{0,\partial K\cap\Gamma_{\mathrm{A}}}\|v\|_{0,\partial K\cap\Gamma_{\mathrm{A}}} \le \mathrm{osc}_K(f,g)|v|_{1,K}, \tag{2.21}$$

for any function $v\in H^1(K)$ with zero mean value on K. If $\mathcal{T}=\{K\}$ is a collection of several elements K, we set

$$\mathrm{osc}_{\mathcal{T}}(f,g) := \left(\sum_{K\in\mathcal{T}}\mathrm{osc}_K(f,g)^2\right)^{\frac{1}{2}},$$

and we omit the subscript when $\mathcal{T}=\mathcal{T}_h$.

2.6. **Main results.** Let u be the weak solution to (2.1) and let u_h be any conforming finite element approximation solving (2.6). Let the equilibrated flux reconstruction $\boldsymbol{\sigma}_h$ be prescribed by Definition 2.1 and define the local and global error estimators as

$$\eta_K := \|\boldsymbol{\sigma}_h+\boldsymbol{\nabla}u_h\|_{0,K},\quad \eta := \left(\sum_{K\in\mathcal{T}_h}\eta_K^2\right)^{\frac{1}{2}}. \tag{2.22}$$

Recall finally the approximability factors σ_{ba} and $\widetilde{\sigma}_{\mathrm{ba}}$ defined respectively by (2.7) and (2.11). Our main result on the error upper bound is the following.

Theorem 2.3 (Upper bounds)**.** *The following global upper bound holds true:*

$$|||u-u_h|||_{1,k,\Omega} \le C_{\mathrm{up}}\left(\eta+\mathrm{osc}(f,g)\right), \tag{2.23}$$

where

$$C_{\mathrm{up}} := \min(\sqrt{2}+\tilde{\theta}_1(\sigma_{\mathrm{ba}}), 1+\tilde{\theta}_2(\sigma_{\mathrm{ba}},\widetilde{\sigma}_{\mathrm{ba}})) \tag{2.24}$$

and

$$\begin{aligned} 0\le\tilde{\theta}_1(t) &:= \sqrt{\left(\frac{1}{2}+\sqrt{\frac{1}{4}+t^2}\right)+\left(\frac{1}{2}+\sqrt{\frac{1}{4}+t^2}\right)^2+t^2}-\sqrt{2} \\ &\le \theta_1(t) := \sqrt{2t+2t^2}, \end{aligned} \tag{2.25}$$

together with

$$\begin{aligned} 0\le\tilde{\theta}_2(t,\tilde{t}) &:= \sqrt{\left(\frac{1}{2}+\sqrt{\frac{1}{4}+t^2}\right)^2+t^2+\tilde{t}^2}-1 \\ &\le \theta_2(t,\tilde{t}) := \sqrt{t+2t^2+\tilde{t}^2}. \end{aligned} \tag{2.26}$$

Note that the bounds $0\le\tilde{\theta}_1(t)\le\theta_1(t)$ and $0\le\tilde{\theta}_2(t,\tilde{t})\le\theta_2(t,\tilde{t})$ in (2.25) and (2.26), respectively, are straightforward, so that the only estimate to prove is (2.23). This result is established in Propositions 3.4, 3.6, and 4.1.

Remark 2.4 (Upper bounds in the asymptotic regime)**.** *When $\sigma_{\rm ba} \to 0$ and $\widetilde{\sigma}_{\rm ba} \to 0$, the presence of $\tilde{\theta}_2$ in* (2.24) *implies that $C_{\rm up} \to 1$. This indeed happens in most configurations of practical interest when $\frac{h}{p} \to 0$ at fixed k, see* (2.10) *and* (2.13) *or* (2.14)*. Thus, the a posteriori error estimate* (2.23) *is asymptotically constant-free. Unfortunately, the approximation factors $\sigma_{\rm ba}$ and $\widetilde{\sigma}_{\rm ba}$ cannot be computed explicitly. To circumvent this issue, we establish a computable estimate on $\sigma_{\rm ba}$ in Theorem 2.7 below, to be used in conjunction with $\tilde{\theta}_1$ in* (2.24)*. This will make the bound* (2.23) *guaranteed but, unfortunately, the computable bound on $\sigma_{\rm ba}$ is in general too rough and leads to a large error overestimation. This is in particular reflected by the fact that this computable bound does not tend to zero as $\frac{h}{p} \to 0$ at fixed k in some cases.*

Our main result on the error lower bound is as follows.

Theorem 2.5 (Lower bounds)**.** *The following local lower bounds also hold true:*

$$\eta_K \le C_{{\rm low},\omega_K} |||u - u_h|||_{1,k,\omega_K} + C(\kappa_{\mathcal{T}_K}) \operatorname{osc}_{\mathcal{T}_K}(f,g) \quad \forall K \in \mathcal{T}_h \tag{2.27}$$

with

$$C_{{\rm low},\omega_K} := C(\kappa_{\mathcal{T}_K}) \left(1 + \left(\frac{kh_{\omega_K}}{p}\right)^{\frac{1}{2}} + \frac{kh_{\omega_K}}{p}\right),$$

where $C(\kappa_{\mathcal{T}_K})$ only depends on the shape-regularity parameter $\kappa_{\mathcal{T}_K}$ of the mesh in the patch $\mathcal{T}_K$ of elements sharing a vertex with K and where h_{ω_K} is the diameter of the corresponding subdomain ω_K.

In addition, the following global lower bound holds true:

$$\eta \le C_{\rm low} |||u - u_h|||_{1,k,\Omega} + C(\kappa) \operatorname{osc}(f,g), \tag{2.28}$$

where

$$C_{\rm low} := C(\kappa) \left(1 + \left(\frac{kh}{p}\right)^{\frac{1}{2}} + \frac{kh}{p}\right),$$

and $C(\kappa)$ only depends on the shape regularity-parameter κ of the mesh.

Remark 2.6 (p-robustness, k-robustness)**.** *Since the approximation factor $\sigma_{\rm ba}$ defined in* (2.7) *is bounded independently of the mesh size h and polynomial degree p (taking $v_h = 0$ in* (2.7)*), the same holds for $C_{\rm up}$. Moreover, trivially, $\frac{kh}{p} \le kh_\Omega$. Then,* (2.23) *and either* (2.27) *or* (2.28) *establish the equivalence of the error and the estimator independently of the mesh size h and polynomial degree p, leading in particular to polynomial-degree robustness in all regimes. More precisely, for any wavenumber k, there exists a constant C, independent of h and p, such that the effectivity index $C_{\rm up}\eta/|||u - u_h|||_{1,k,\Omega}$ is bounded by C for any h and p; here C can depend on k and h_Ω. Moreover, robustness with respect to the wavenumber k is achieved in the asymptotic regime where $\sigma_{\rm ba} \le 1$ (and $\frac{kh}{p} \le 1$), so that $C_{\rm up}$ and $C_{{\rm low},\omega_K}$ or $C_{\rm low}$ are bounded independently of k, h, and p. Indeed, $\sigma_{\rm ba} \le 1$ (and $\frac{kh}{p} \le 1$), there exists a constant C, independent of k, h, and p, such that the effectivity index $C_{\rm up}\eta/|||u - u_h|||_{1,k,\Omega}$ is bounded by C for any k, h, and p; here C is of order 1 for shape-regular meshes.*

The local lower bound (2.27) is established in Proposition 4.5. Though (2.28) is easily obtained from (2.27) by summation over the mesh cells, we provide an estimate with a sharper constant in Proposition 4.6.

Crucially, for several configurations of interest, the upper bound of Theorem 2.3 can be turned into a *guaranteed estimate* in *any regime* starting from the unresolved one (on any

mesh $\mathcal{T}_h$ and for any polynomial degree p) through the following computable upper bounds on the approximability factor $\sigma_{\rm ba}$.

Theorem 2.7 (Computable bounds on $\sigma_{\rm ba}$)**.**

Case 1a) (Scattering by a non-trapping obstacle). *Assume that $\Omega = \Omega_0 \setminus \overline{D}$, $\Gamma_{\rm A} = \partial\Omega_0$, and $\Gamma_{\rm D} = \partial D$, where $\Omega_0, D \subset \mathbb{R}^d$ are two open, bounded, connected sets such that $\overline{D}$ is a proper subset of Ω_0 and assume that the subset*

$$\mathcal{O}_{\Gamma_{\rm D},\Gamma_{\rm A}} := \{\boldsymbol{x}_0 \in \mathbb{R}^d \mid (\boldsymbol{x}-\boldsymbol{x}_0)\cdot\boldsymbol{n} \le 0 \ \forall \boldsymbol{x} \in \Gamma_{\rm D},\ (\boldsymbol{x}-\boldsymbol{x}_0)\cdot\boldsymbol{n} > 0 \ \forall \boldsymbol{x} \in \Gamma_{\rm A}\} \tag{2.29}$$

is nonempty (recall that $\boldsymbol{n}$ points outward Ω). Let

$$C_{\rm stab}(\widehat{\Omega},\widehat{\Gamma}_{\rm D}) := \inf_{\boldsymbol{x}_0 \in \mathcal{O}_{\Gamma_{\rm D},\Gamma_{\rm A}}} C_{\rm stab}(\widehat{\Omega},\widehat{\Gamma}_{\rm D},\boldsymbol{x}_0), \tag{2.30}$$

with

$$C_{\rm stab}(\widehat{\Omega},\widehat{\Gamma}_{\rm D},\boldsymbol{x}_0) := \frac{1}{h_\Omega}\left\{\sup_{\boldsymbol{x}\in\Omega}|\boldsymbol{x}-\boldsymbol{x}_0| + \sup_{\boldsymbol{x}\in\Gamma_{\rm A}}\left(2(\boldsymbol{x}-\boldsymbol{x}_0)\cdot\boldsymbol{n} + \frac{|(\boldsymbol{x}-\boldsymbol{x}_0)\times\boldsymbol{n}|^2}{(\boldsymbol{x}-\boldsymbol{x}_0)\cdot\boldsymbol{n}}\right)\right\}.$$

Then, we have

$$\sigma_{\rm ba} \le \left(\Big((d-1) + C_{\rm stab}(\widehat{\Omega},\widehat{\Gamma}_{\rm D})kh_\Omega\Big) + \Big((d-1) + C_{\rm stab}(\widehat{\Omega},\widehat{\Gamma}_{\rm D})kh_\Omega\Big)^2\right)^{\frac{1}{2}}. \tag{2.31}$$

Case 1b) (Wave propagation in free space). *Assume that Ω is convex and $\Gamma_{\rm D} = \emptyset$, so that $\mathcal{O}_{\Gamma_{\rm D},\Gamma_{\rm A}} = \Omega$. Let $C_{\rm stab}(\widehat{\Omega},\widehat{\Gamma}_{\rm D})$ be defined as above. Then, we have*

$$\sigma_{\rm ba} \le C_{\rm i}(\kappa)\left(d + C_{\rm stab}(\widehat{\Omega},\widehat{\Gamma}_{\rm D})kh_\Omega\right)\frac{kh}{p^\beta}, \tag{2.32}$$

where $C_{\rm i}(\kappa)$ is any approximation constant satisfying

$$\inf_{v_h\in V_h}|v-v_h|_{1,\Omega} \le C_{\rm i}(\kappa)\frac{h}{p^\beta}|v|_{2,\Omega} \qquad \forall v \in H^1_{\Gamma_{\rm D}}(\Omega)\cap H^2(\Omega), \tag{2.33}$$

and such that it only depends on the mesh regularity parameter κ; typically $\beta = 0$ or $\beta = 1$ in (2.32) *and* (2.33).

Case 2a) (Interior problem). *Assume that $\Gamma_{\rm A} = \emptyset$. Then*

$$\sigma_{\rm ba} \le k\max_{j\in\mathbb{N}}\frac{\sqrt{\lambda_j}}{|\lambda_j - k^2|}, \tag{2.34}$$

where λ_j is the j-th eigenvalue of the Laplace operator in Ω with Dirichlet boundary conditions.

Case 2b) (Convex interior problem). *Assume that $\Gamma_{\rm A} = \emptyset$ and that Ω is convex. Then*

$$\sigma_{\rm ba} \le C_{\rm i}(\kappa)\left(1 + \frac{k^2}{\min_{j\in\mathbb{N}}|\lambda_j - k^2|}\right)\frac{kh}{p^\beta}, \tag{2.35}$$

where $C_{\rm i}(\kappa)$ is any approximation constant satisfying (2.33).

Remark 2.8 (Bounds of Theorem 2.7)**.** *In contrast to the a priori bound* (2.10) *which gives $\sigma_{\rm ba} \to 0$ when $\frac{h}{p} \to 0$ with fixed k, our computable upper bounds on $\sigma_{\rm ba}$ of Theorem 2.7 do not share this property in cases 1a) and 2a). Further work is needed to close this gap, and we leave it here as an open question.*

The proof of Theorem 2.7 is carried out in Section 5. The estimates (2.34) and (2.35) follow from standard properties of spectral decomposition and we only sketch the proof at the beginning of Section 5. The more involved upper bounds (2.31) and (2.32) are respectively established in Sections 5.2 and 5.3.

Finally, the constant $C_{\rm stab}(\widehat{\Omega},\widehat{\Gamma}_{\rm D})$ can be easily bounded when $\Gamma_{\rm A}$ has a simple geometry (which is usually the case in scattering applications):

Remark 2.9 (Constant $C_{\rm stab}(\widehat{\Omega},\widehat{\Gamma}_{\rm D})$)**.** *In the Case 1a) (resp. 1b) above, if Ω_0 (resp. Ω) is a circle or a ball centered at $\boldsymbol{x}_0$, then $C_{\rm stab}(\widehat{\Omega},\widehat{\Gamma}_{\rm D}) \leq \frac{3}{2}$. If Ω_0 (resp. Ω) is a square centered at $\boldsymbol{x}_0$, then $C_{\rm stab}(\widehat{\Omega},\widehat{\Gamma}_{\rm D}) \leq \frac{3+\sqrt{2}}{2\sqrt{2}}$. Finally, if Ω_0 (resp. Ω) is a cube centered at $\boldsymbol{x}_0$, then $C_{\rm stab}(\widehat{\Omega},\widehat{\Gamma}_{\rm D}) \leq \frac{3+\sqrt{3}}{2\sqrt{3}}$.*

Similarly, several expressions for the constant $C_{\rm i}(\kappa)$ can be found in the literature [3, 10, 37, 40], leading to (2.33) with $\beta = 0$:

Remark 2.10 (Constant $C_{\rm i}(\kappa)$)**.** *A more precise definition than* (2.33) *is*

$$C_{\rm i}(\kappa) := \frac{p^\beta}{h} \sup_{v\in H^1_{\Gamma_{\rm D}}(\Omega)\cap H^2(\Omega)\setminus\{0\}} \inf_{v_h\in V_h} \frac{|v-v_h|_{1,\Omega}}{|v|_{2,\Omega}}.$$

The value of $C_{\rm i}(\kappa)$ can then be estimated by considering any interpolation operator. For any $v \in H^1_{\Gamma_{\rm D}}(\Omega)\cap H^2(\Omega)$, we can define its $\mathcal{P}_1$ nodal interpolant $\mathcal{I}_h(v) \in V_h$ by

$$(\mathcal{I}_h(v))(\boldsymbol{a}) = v(\boldsymbol{a}) \qquad \forall \boldsymbol{a} \in \mathcal{V}_h.$$

Then we have (with $\beta = 0$)

$$C_{\rm i}(\kappa) \leq \sup_{v\in H^1_{\Gamma_{\rm D}}(\Omega)\cap H^2(\Omega)\setminus\{0\}} \frac{|v-\mathcal{I}_h(v)|_{1,\Omega}}{h|v|_{2,\Omega}},$$

where $C_{\rm i}(\kappa)$ only depends on κ. In particular, following Theorem 1.1 of [3]*, we have $C_{\rm i}(\kappa) \leq 3/\kappa$ if $d = 2$ and $C_{\rm i}(\kappa) \leq 8/\kappa$ if $d = 3$. Furthermore, sharper estimates are available for the specific case of triangles when $d = 2$, and we refer the reader to* [10, 37, 40]*. In particular, for a mesh formed by isosceles right-angled triangles, we will employ the estimate $C_{\rm i}(\kappa) \leq 0.493/\sqrt{2}$ from* [40]*.*

Remark 2.11 (Eigenvalues)**.** *Apart from very simple domain geometries, analytic expressions of the eigenvalues λ_j appearing in* (2.34) *and* (2.35) *are not available. However, guaranteed a posteriori error estimators can be employed to reliably estimate their value, and thus $\sigma_{\rm ba}$, see* [8, 9, 39] *and the references therein. We also refer the reader to* [11]*, where related arguments are employed in the context of least-squares discretizations.*

Remark 2.12 (Data oscillation)**.** *Actually, a slightly sharper upper bound than* (2.23)*, with data oscillation integrated to the local error estimators, follows from* (4.1) *below. Also, upon modifying the treatment of the data f and g as in* [27, 29]*, one could replace in $\mathrm{osc}_K(f,g)$ in* (2.20) *the projections π_h^p and $\widetilde{\pi}_h^p$ by π_h^{p+1} and $\widetilde{\pi}_h^{p+1}$ and gain an additional order for data oscillation in the upper bound* (2.23)*. This is, however, not possible in the lower bounds* (2.27) *and* (2.28)*. We do not present these extensions here for the clarity of exposition.*

3. Relation between the error and the dual norm of the residual

The aim of this section is to obtain lower and upper bounds on the error between u and u_h by dual residual norms. We define the *residual* $\mathcal{R}(u_h) \in \left(H^1_{\Gamma_D}(\Omega)\right)'$ stemming from the weak formulation (2.1) by

$$\langle \mathcal{R}(u_h), v\rangle := b(u-u_h,v) = (f,v) + (g,v)_{\Gamma_A} - b(u_h,v) \qquad \forall v \in H^1_{\Gamma_D}(\Omega). \tag{3.1}$$

We further introduce the residual norm

$$\|\mathcal{R}(u_h)\|_{-1,\Omega} := \sup_{v\in H^1_{\Gamma_D}(\Omega)\setminus\{0\}} \frac{|\langle \mathcal{R}(u_h), v\rangle|}{|v|_{1,\Omega}}. \tag{3.2}$$

Note that in virtue of (2.6), we have

$$\langle \mathcal{R}(u_h), v_h\rangle = 0 \qquad \forall v_h \in V_h. \tag{3.3}$$

3.1. **Global upper bounds.** We start by an upper bound on the $L^2(\Omega)$-norm using the approximation factor $\sigma_{\rm ba}$ defined in (2.7). The proof follows the lines of Lemma 4.7 of [28] and employs the usual Aubin–Nitsche duality argument.

Lemma 3.1 ($L^2(\Omega)$-norm upper bound by the dual norm of the residual)**.** *We have*

$$k\|u-u_h\|_{0,\Omega} \le \sigma_{\rm ba}\|\mathcal{R}(u_h)\|_{-1,\Omega}. \tag{3.4}$$

Proof. We introduce ξ as the unique element of $H^1_{\Gamma_D}(\Omega)$ such that $b(w,\xi) = (w, u-u_h)$ for all $w \in H^1_{\Gamma_D}(\Omega)$. Selecting the test function $w = u-u_h$ and using (3.1) and (3.3), we see that

$$k\|u-u_h\|^2_{0,\Omega} = k\langle \mathcal{R}(u_h), \xi\rangle = k\langle \mathcal{R}(u_h), \xi-\xi_h\rangle \le k\|\mathcal{R}(u_h)\|_{-1,\Omega}|\xi-\xi_h|_{1,\Omega}$$

for all $\xi_h \in V_h$. Hence, using (2.7) and its consequence (2.9) and recalling the definition of ξ, we have

$$k\|u-u_h\|^2_{0,\Omega} \le \|\mathcal{R}(u_h)\|_{-1,\Omega}\left(k\inf_{\xi_h\in V_h}|\xi-\xi_h|_{1,\Omega}\right) \le \sigma_{\rm ba}\|\mathcal{R}(u_h)\|_{-1,\Omega}\|u-u_h\|_{0,\Omega},$$

and (3.4) follows. □ □

We now record a useful quadratic inequality.

Lemma 3.2 (Quadratic inequality)**.** *Assume that $x \ge 0$ satisfies*

$$ax^2 \le c + bx,$$

for some constants $a, b, c > 0$. Then we have

$$ax \le \frac{b}{2} + \sqrt{\frac{b^2}{4} + ac}.$$

With the help of Lemmas 3.1 and 3.2, we obtain an upper bound on the $H^1(\Omega)$ semi-norm.

Lemma 3.3 ($H^1(\Omega)$ semi-norm upper bound by the dual norm of the residual)**.** *We have*

$$|u-u_h|_{1,\Omega} \le \left(\frac{1}{2} + \sqrt{\frac{1}{4} + \left(\sigma_{\rm ba}\right)^2}\right)\|\mathcal{R}(u_h)\|_{-1,\Omega}. \tag{3.5}$$

Proof. Using the definition (2.2) of b, (3.1), and Lemma 3.1, we have

$$\begin{aligned}|u-u_h|_{1,\Omega}^2 &= \operatorname{Re} b(u-u_h,u-u_h)+k^2\|u-u_h\|_{0,\Omega}^2\\ &\le \|\mathcal{R}(u_h)\|_{-1,\Omega}|u-u_h|_{1,\Omega}+\big(\sigma_{\rm ba}\big)^2\|\mathcal{R}(u_h)\|_{-1,\Omega}^2,\end{aligned}$$

and (3.5) follows from Lemma 3.2 with $a=1$, $b=\|\mathcal{R}(u_h)\|_{-1,\Omega}$, and $c=\big(\sigma_{\rm ba}\big)^2\|\mathcal{R}(u_h)\|_{-1,\Omega}^2$. □ □

We are now ready to establish global upper bounds in the energy norm. Our first estimate is explicit in terms of $\sigma_{\rm ba}$.

Proposition 3.4 (First upper bound by the dual norm of the residual)**.** *We have*

$$|||u-u_h|||_{1,k,\Omega}\le(\sqrt{2}+\tilde\theta_1(\sigma_{\rm ba}))\|\mathcal{R}(u_h)\|_{-1,\Omega},$$

with $\tilde\theta_1$ *defined in* (2.25)*.*

Proof. Employing the definitions (2.2) and (3.1), we have

$$k\|u-u_h\|_{0,\Gamma_{\rm A}}^2=-\operatorname{Im} b(u-u_h,u-u_h)\le\|\mathcal{R}(u_h)\|_{-1,\Omega}|u-u_h|_{1,\Omega},$$

and using Lemma 3.3, it follows that

$$k\|u-u_h\|_{0,\Gamma_{\rm A}}^2\le\left(\frac12+\sqrt{\frac14+(\sigma_{\rm ba})^2}\right)\|\mathcal{R}(u_h)\|_{-1,\Omega}^2.$$

Hence, from (2.3) and (3.4)–(3.5), we infer that

$$|||u-u_h|||_{1,k,\Omega}^2\le\left((\sigma_{\rm ba})^2+\left(\frac12+\sqrt{\frac14+(\sigma_{\rm ba})^2}\right)+\left(\frac12+\sqrt{\frac14+(\sigma_{\rm ba})^2}\right)^2\right)\|\mathcal{R}(u_h)\|_{-1,\Omega}^2,$$

and the claim follows from the definition of $\tilde\theta_1$. □ □

Proposition 3.4 is not completely satisfactory, since the asymptotic value for vanishing $\sigma_{\rm ba}$ of the prefactor is $\sqrt{2}$. We now provide a sharper analysis that shows that the asymptotic constant can be brought to the optimal value of 1. Recall the definition (2.11) of $\widetilde{\sigma}_{\rm ba}$.

Lemma 3.5 ($L^2(\Gamma_{\rm A})$-norm upper bound by the dual norm of the residual)**.** *We have*

$$k^{\frac12}\|u-u_h\|_{0,\Gamma_{\rm A}}\le\widetilde{\sigma}_{\rm ba}\|\mathcal{R}(u_h)\|_{-1,\Omega}. \tag{3.6}$$

Proof. We use again a duality argument. We define χ as the unique element of $H^1_{\Gamma_{\rm D}}(\Omega)$ such that $b(w,\chi)=(w,u-u_h)_{\Gamma_{\rm A}}$ for all $w\in H^1_{\Gamma_{\rm D}}(\Omega)$. Selecting the test function $w=u-u_h$, employing the definition of the residual (3.1), and taking advantage of Galerkin's orthogonality (3.3), we have

$$k\|u-u_h\|_{0,\Gamma_{\rm A}}^2=kb(u-u_h,\chi)=k\langle\mathcal{R}(u_h),\chi-\chi_h\rangle\le k\|\mathcal{R}(u_h)\|_{-1,\Omega}|\chi-\chi_h|_{1,\Omega}$$

for all $\chi_h\in V_h$. Then, recalling the above definition of χ and the definition (2.11) of $\widetilde{\sigma}_{\rm ba}$, we obtain (3.6) by taking the infinimum over all $\chi_h\in V_h$. □ □

Our second estimate is explicit in terms of the two constants $\sigma_{\rm ba}$ and $\widetilde{\sigma}_{\rm ba}$:

Proposition 3.6 (Second upper bound by the dual norm of the residual)**.** *We have*

$$|||u-u_h|||_{1,k,\Omega} \le (1+\tilde{\theta}_2(\sigma_{\rm ba},\widetilde{\sigma}_{\rm ba}))\|\mathcal{R}(u_h)\|_{-1,\Omega},$$

where $\tilde{\theta}_2$ *is defined in* (2.26)*.*

Proof. The proof combines (3.4), (3.5), and (3.6). □ □

3.2. **Local lower bounds.** Define the local Sobolev space $H^1_\star(\omega_{\boldsymbol{a}})$ as

$$H^1_\star(\omega_{\boldsymbol{a}}) := \begin{cases} \{v\in H^1(\omega_{\boldsymbol{a}}) \mid \int_{\omega_{\boldsymbol{a}}} v = 0\} & \text{when } \boldsymbol{a}\notin\overline{\Gamma_{\rm D}},\\ \{v\in H^1(\omega_{\boldsymbol{a}}) \mid v=0 \text{ on the part of } \Gamma_{\rm D} \text{ where } \psi_{\boldsymbol{a}}\neq 0\} & \text{when } \boldsymbol{a}\in\overline{\Gamma_{\rm D}}.\end{cases}$$

We will now employ a localized dual norm of the residual from (3.1) that is defined for each $\boldsymbol{a}\in\mathcal{V}_h$ by

$$\|\mathcal{R}(u_h)\|_{-1,\boldsymbol{a}} := \sup_{v\in H^1_\star(\omega_{\boldsymbol{a}})\setminus\{0\}} \frac{|\langle\mathcal{R}(u_h),\psi_{\boldsymbol{a}}v\rangle|}{|v|_{1,\omega_{\boldsymbol{a}}}}, \tag{3.7}$$

recalling that $\psi_{\boldsymbol{a}}$ is the hat function associated with the vertex $\boldsymbol{a}\in\mathcal{V}_h$.

We record that there exists a (Poincaré or Poincaré–Friedrichs) constant $C_{{\rm PF},\boldsymbol{a}}$ that depends only on the local shape-regularity parameter $\kappa_{\mathcal{T}_{\boldsymbol{a}}} := \min_{K\in\mathcal{T}_{\boldsymbol{a}}}\kappa_K$ such that

$$\|v\|_{0,\omega_{\boldsymbol{a}}} \le C_{{\rm PF},\boldsymbol{a}} h_{\boldsymbol{a}} |v|_{1,\omega_{\boldsymbol{a}}} \qquad \forall v\in H^1_\star(\omega_{\boldsymbol{a}}), \tag{3.8}$$

where $h_{\boldsymbol{a}} := \sup_{\boldsymbol{x},\boldsymbol{y}\in\omega_{\boldsymbol{a}}}|\boldsymbol{x}-\boldsymbol{y}|$ is the diameter of the patch subdomain $\omega_{\boldsymbol{a}}$. When $\omega_{\boldsymbol{a}}$ is convex and $\boldsymbol{a}\notin\overline{\Gamma_{\rm D}}$, we have $C_{{\rm PF},\boldsymbol{a}} = 1/\pi$, and we refer the reader to [55] and the references therein for a discussion on the value of the constant $C_{{\rm PF},\boldsymbol{a}}$ in the case of non-convex patches or patches around a Dirichlet boundary vertex. As observed in [7, 29], Leibniz's rule in conjunction with (3.8) shows that

$$|\psi_{\boldsymbol{a}}v|_{1,\omega_{\boldsymbol{a}}} \le C_{{\rm cont,PF},\boldsymbol{a}}|v|_{1,\omega_{\boldsymbol{a}}} \qquad \forall v\in H^1_\star(\omega_{\boldsymbol{a}}), \tag{3.9}$$

where the constant $C_{{\rm cont,PF},\boldsymbol{a}} := 1 + C_{{\rm PF},\boldsymbol{a}}|\psi_{\boldsymbol{a}}|_{1,\infty,\omega_{\boldsymbol{a}}}h_{\boldsymbol{a}}$ only depends on $\kappa_{\mathcal{T}_{\boldsymbol{a}}}$. We will also employ the trace inequality

$$\|v\|_{0,\partial\omega_{\boldsymbol{a}}\cap\Gamma_{\rm A}} \le C_{{\rm tr},\boldsymbol{a}} h_{\boldsymbol{a}}^{\frac12}|v|_{1,\omega_{\boldsymbol{a}}} \qquad \forall v\in H^1_\star(\omega_{\boldsymbol{a}}), \tag{3.10}$$

where the constant $C_{{\rm tr},\boldsymbol{a}}$ again only depends on $\kappa_{\mathcal{T}_{\boldsymbol{a}}}$. Finally, we introduce for each vertex $\boldsymbol{a}\in\mathcal{V}_h$ the local norm

$$|||v|||^2_{1,k,\omega_{\boldsymbol{a}}} := k^2\|v\|^2_{0,\omega_{\boldsymbol{a}}} + k\|v\|^2_{0,\partial\omega_{\boldsymbol{a}}\cap\Gamma_{\rm A}} + |v|^2_{1,\omega_{\boldsymbol{a}}} \quad \forall v\in H^1(\omega_{\boldsymbol{a}}).$$

For all vertices $\boldsymbol{a}\in\mathcal{V}_h$, if $v\in H^1_{\Gamma_{\rm D}}(\Omega)$ with $\operatorname{supp} v\subset\omega_{\boldsymbol{a}}$, there exists a discrete function $Q^{\boldsymbol{a}}_{hp}(v)\in V_h$ with $\operatorname{supp}(Q^{\boldsymbol{a}}_{hp}(v))\subset\omega_{\boldsymbol{a}}$ such that

$$\left|||v-Q^{\boldsymbol{a}}_{hp}(v)|||_{1,k,\omega_{\boldsymbol{a}}} \le C_{{\rm qi},\boldsymbol{a}}\left(1+\frac{kh_{\boldsymbol{a}}}{p}+\left(\frac{kh_{\boldsymbol{a}}}{p}\right)^2\right)^{\frac12}|v|_{1,\omega_{\boldsymbol{a}}}, \tag{3.11}$$

where the constant $C_{{\rm qi},\boldsymbol{a}}$ only depends on $\kappa_{\mathcal{T}_{\boldsymbol{a}}}$. We can use a quasi-interpolation operator $Q^{\boldsymbol{a}}_{hp}$ to achieve (3.11). The construction of such an operator is presented in Theorem 3.3 of [43] in two space dimensions. For three space dimensions, the corresponding operator is constructed in [34].

Lemma 3.7 (Local lower bounds of the error by the dual norm of the residual)**.** *For all vertices $\boldsymbol{a} \in \mathcal{V}_h$, we have*

$$\|\mathcal{R}(u_h)\|_{-1,\boldsymbol{a}} \leq C_{\mathrm{lb},\boldsymbol{a}} |\!|\!| u - u_h |\!|\!|_{1,k,\omega_{\boldsymbol{a}}},$$

where $C_{\mathrm{lb},\boldsymbol{a}} := \min(C_{\mathrm{lb,hat},\boldsymbol{a}}, C_{\mathrm{lb,qi},\boldsymbol{a}})$ and

$$C_{\mathrm{lb,hat},\boldsymbol{a}} := C_{\mathrm{cont,PF},\boldsymbol{a}} \left(1 + \frac{C_{\mathrm{tr},\boldsymbol{a}}^2}{C_{\mathrm{cont,PF},\boldsymbol{a}}^2} k h_{\boldsymbol{a}} + \frac{C_{\mathrm{PF},\boldsymbol{a}}^2}{C_{\mathrm{cont,PF},\boldsymbol{a}}^2} (k h_{\boldsymbol{a}})^2\right)^{\frac{1}{2}},$$

$$C_{\mathrm{lb,qi},\boldsymbol{a}} := C_{\mathrm{cont,PF},\boldsymbol{a}} C_{\mathrm{qi},\boldsymbol{a}} \left(1 + \frac{k h_{\boldsymbol{a}}}{p} + \left(\frac{k h_{\boldsymbol{a}}}{p}\right)^2\right)^{\frac{1}{2}}.$$

Proof. Let $v \in H^1_\star(\omega_{\boldsymbol{a}})$. From (2.4) and (3.1), we observe that

$$|\langle \mathcal{R}(u_h), \psi_{\boldsymbol{a}} v\rangle| = |b(u - u_h, \psi_{\boldsymbol{a}} v)| \leq |\!|\!| u - u_h |\!|\!|_{1,k,\omega_{\boldsymbol{a}}} |\!|\!| \psi_{\boldsymbol{a}} v |\!|\!|_{1,k,\omega_{\boldsymbol{a}}}. \tag{3.12}$$

Then, using (3.8), (3.9), and (3.10), we have

$$\begin{aligned} |\!|\!| \psi_{\boldsymbol{a}} v |\!|\!|^2_{1,k,\omega_{\boldsymbol{a}}} &= k^2 \|\psi_{\boldsymbol{a}} v\|^2_{0,\omega_{\boldsymbol{a}}} + k \|\psi_{\boldsymbol{a}} v\|^2_{0,\partial\omega_{\boldsymbol{a}} \cap \Gamma_{\mathrm{A}}} + |\psi_{\boldsymbol{a}} v|^2_{1,\omega_{\boldsymbol{a}}} \\ &\leq k^2 \|v\|^2_{0,\omega_{\boldsymbol{a}}} + k \|v\|^2_{0,\partial\omega_{\boldsymbol{a}} \cap \Gamma_{\mathrm{A}}} + |\psi_{\boldsymbol{a}} v|^2_{1,\omega_{\boldsymbol{a}}} \\ &\leq \left(C_{\mathrm{PF},\boldsymbol{a}}^2 k^2 h_{\boldsymbol{a}}^2 + C_{\mathrm{tr},\boldsymbol{a}}^2 k h_{\boldsymbol{a}} + C_{\mathrm{cont,PF},\boldsymbol{a}}^2\right) |v|^2_{1,\omega_{\boldsymbol{a}}} \\ &= C_{\mathrm{lb,hat},\boldsymbol{a}}^2 |v|^2_{1,\omega_{\boldsymbol{a}}}. \end{aligned}$$

On the other hand, since $Q_{hp}^{\boldsymbol{a}}(\psi_{\boldsymbol{a}} v) \in V_h$ with $\mathrm{supp}(Q_{hp}^{\boldsymbol{a}}(\psi_{\boldsymbol{a}} v)) \subset \omega_{\boldsymbol{a}}$, using Galerkin's orthogonality (3.3) in (3.12) and (3.11) with (3.9), we have

$$\begin{aligned} |\langle \mathcal{R}(u_h), \psi_{\boldsymbol{a}} v\rangle| &\leq |\!|\!| u - u_h |\!|\!|_{1,k,\omega_{\boldsymbol{a}}} |\!|\!| \psi_{\boldsymbol{a}} v - Q_{hp}^{\boldsymbol{a}}(\psi_{\boldsymbol{a}} v) |\!|\!|_{1,k,\omega_{\boldsymbol{a}}} \\ &\leq C_{\mathrm{qi},\boldsymbol{a}} \left(1 + \frac{k h_{\boldsymbol{a}}}{p} + \left(\frac{k h_{\boldsymbol{a}}}{p}\right)^2\right)^{\frac{1}{2}} |\!|\!| u - u_h |\!|\!|_{1,k,\omega_{\boldsymbol{a}}} |\psi_{\boldsymbol{a}} v|_{1,\omega_{\boldsymbol{a}}} \\ &\leq C_{\mathrm{cont,PF},\boldsymbol{a}} C_{\mathrm{qi},\boldsymbol{a}} \left(1 + \frac{k h_{\boldsymbol{a}}}{p} + \left(\frac{k h_{\boldsymbol{a}}}{p}\right)^2\right)^{\frac{1}{2}} |\!|\!| u - u_h |\!|\!|_{1,k,\omega_{\boldsymbol{a}}} |v|_{1,\omega_{\boldsymbol{a}}} \\ &= C_{\mathrm{lb,qi},\boldsymbol{a}} |\!|\!| u - u_h |\!|\!|_{1,k,\omega_{\boldsymbol{a}}} |v|_{1,\omega_{\boldsymbol{a}}}. \end{aligned}$$

The expected result follows by combining the two bounds together with the definition (3.7) of the localized dual norm. □ □

4. Bounds on the dual norm of the residual by equilibrated fluxes

In the previous section, we derived upper and lower bounds for the finite element error based on dual norms of the residual. These dual norms are not directly computable, as they are defined using a supremum over infinite-dimensional spaces. In this section, we use the technique of equilibrated flux construction to achieve guaranteed computable upper and lower bounds of these dual norms.

4.1. **Global upper bound.** Recall the definitions (2.20) of the data oscillation, (2.22) of the error estimator η, (3.1) and (3.2) of the residual and its dual norm, and finally Definition 2.1 of the equilibrated flux $\boldsymbol{\sigma}_h$.

Proposition 4.1 (Upper bound on the dual norm of the residual)**.** *The following holds true:*

$$\|\mathcal{R}(u_h)\|_{-1,\Omega} \le \left(\sum_{K\in\mathcal{T}_h} (\eta_K + \mathrm{osc}_K(f,g))^2\right)^{\frac12}. \tag{4.1}$$

Proof. We first observe that since the hat functions form a partition of unity, we have

$$\sum_{\boldsymbol{a}\in\mathcal{V}_h} \psi_{\boldsymbol{a}}(\boldsymbol{x}) = 1 \qquad \forall \boldsymbol{x}\in\overline{\Omega}.$$

The summation over all vertices $\boldsymbol{a}\in\mathcal{V}_h$ in (2.18) together with the divergence and normal trace constraints in (2.17) lead to

$$\boldsymbol{\nabla}\cdot\boldsymbol{\sigma}_h = \pi_h^p(f) + k^2 u_h \text{ in } \Omega, \quad \boldsymbol{\sigma}_h\cdot\boldsymbol{n} = -\left(\widetilde{\pi}_h^p(g) + iku_h\right) \text{ on } \Gamma_{\mathrm{A}}.$$

Then, if $v\in H^1_{\Gamma_{\mathrm{D}}}(\Omega)$, we have

$$\begin{aligned}
b(u_h,v) &= -k^2(u_h,v) - ik(u_h,v)_{\Gamma_{\mathrm{A}}} + (\boldsymbol{\nabla}u_h,\boldsymbol{\nabla}v)\\
&= (\pi_h^p(f),v) + (\widetilde{\pi}_h^p(g),v)_{\Gamma_{\mathrm{A}}} - (\pi_h^p(f)+k^2u_h,v) - (\widetilde{\pi}_h^p(g)+iku_h,v)_{\Gamma_{\mathrm{A}}} + (\boldsymbol{\nabla}u_h,\boldsymbol{\nabla}v)\\
&= (\pi_h^p(f),v) + (\widetilde{\pi}_h^p(g),v)_{\Gamma_{\mathrm{A}}} - (\boldsymbol{\nabla}\cdot\boldsymbol{\sigma}_h,v) + (\boldsymbol{\sigma}_h\cdot\boldsymbol{n},v)_{\Gamma_{\mathrm{A}}} + (\boldsymbol{\nabla}u_h,\boldsymbol{\nabla}v)\\
&= (\pi_h^p(f),v) + (\widetilde{\pi}_h^p(g),v)_{\Gamma_{\mathrm{A}}} + (\boldsymbol{\sigma}_h+\boldsymbol{\nabla}u_h,\boldsymbol{\nabla}v).
\end{aligned}$$

It follows that

$$\begin{aligned}
\langle\mathcal{R}(u_h),v\rangle &= (f-\pi_h^p(f),v) + (g-\widetilde{\pi}_h^p(g),v)_{\Gamma_{\mathrm{A}}} + (\pi_h^p(f),v) + (\widetilde{\pi}_h^p(g),v)_{\Gamma_{\mathrm{A}}} - b(u_h,v)\\
&= (f-\pi_h^p(f),v) + (g-\widetilde{\pi}_h^p(g),v)_{\Gamma_{\mathrm{A}}} - (\boldsymbol{\sigma}_h+\boldsymbol{\nabla}u_h,\boldsymbol{\nabla}v).
\end{aligned}$$

Since the restriction of $\pi_h^p(v)$ to each mesh face $F\subset\Gamma_{\mathrm{A}}$ belongs to $\mathcal{P}_p(F)$, and $v-\pi_h^p(v)$ has zero mean-value on each mesh cell K, we have

$$\begin{aligned}
&|(f-\pi_h^p(f),v)_K + (g-\widetilde{\pi}_h^p(g),v)_{\partial K\cap\partial\Gamma_{\mathrm{A}}}|\\
&= |(f-\pi_h^p(f),v-\pi_h^p(v))_K + (g-\widetilde{\pi}_h^p(g),v-\pi_h^p(v))_{\partial K\cap\Gamma_{\mathrm{A}}}|\\
&\le \|f-\pi_h^p(f)\|_{0,K}\|v-\pi_h^p(v)\|_{0,K} + \|g-\widetilde{\pi}_h^p(g)\|_{0,\partial K\cap\Gamma_{\mathrm{A}}}\|v-\pi_h^p(v)\|_{0,\partial K\cap\Gamma_{\mathrm{A}}}\\
&\le \mathrm{osc}_K(f,g)|v|_{1,K},
\end{aligned}$$

where we used (2.21). The Cauchy–Schwarz inequality now implies (4.1). □ □

At this point, the upper bound (2.23) of Theorem 2.3 follows from Propositions 3.4, 3.6, and 4.1 by setting $C_{\mathrm{up}} := \min\left(\sqrt{2}+\tilde{\theta}_1(\sigma_{\mathrm{ba}}), 1+\tilde{\theta}_2(\sigma_{\mathrm{ba}},\widetilde{\sigma}_{\mathrm{ba}})\right)$ and bounding (4.1) further by the triangle inequality.

4.2. **Local lower bound.** We first introduce a residual with projected source terms

$$\langle\mathcal{R}_h(u_h),v\rangle := (\pi_h^p(f),v) + (\widetilde{\pi}_h^p(g),v)_{\Gamma_{\mathrm{A}}} - b(u_h,v) \qquad \forall v\in H^1_{\Gamma_{\mathrm{D}}}(\Omega), \tag{4.2}$$

where the original right-hand sides f and g have been respectively replaced by their element-wise and facewise L^2 projections. We employ the same notation for the dual norms of $\mathcal{R}_h(u_h)$ as for those of $\mathcal{R}(u_h)$.

Lemma 4.2 (Data oscillations)**.** *We have*

$$\|\mathcal{R}_h(u_h)\|_{-1,\boldsymbol{a}} \le \|\mathcal{R}(u_h)\|_{-1,\boldsymbol{a}} + C(\kappa_{\mathcal{T}_{\boldsymbol{a}}})\,\mathrm{osc}_{\mathcal{T}_{\boldsymbol{a}}}(f,g) \qquad \forall \boldsymbol{a} \in \mathcal{V}_h,$$

where the constant $C(\kappa_{\mathcal{T}_{\boldsymbol{a}}})$ only depends on the shape-regularity paremeter of the elements in the patch $\mathcal{T}_{\boldsymbol{a}}$.

Proof. Fix a vertex $\boldsymbol{a} \in \mathcal{V}_h$. For all $v \in H^1_\star(\omega_{\boldsymbol{a}})$, we have

$$\langle \mathcal{R}_h(u_h), \psi_{\boldsymbol{a}} v\rangle = \langle \mathcal{R}(u_h), \psi_{\boldsymbol{a}} v\rangle - (f - \pi_h^p(f), \psi_{\boldsymbol{a}} v) - (g - \widetilde{\pi}_h^p(g), \psi_{\boldsymbol{a}} v)_{\Gamma_{\mathrm{A}}}.$$

Consequently, we infer that

$$\begin{aligned}
&|\langle \mathcal{R}_h(u_h), \psi_{\boldsymbol{a}} v\rangle| \\
&\le |\langle \mathcal{R}(u_h), \psi_{\boldsymbol{a}} v\rangle| + \|f - \pi_h^p(f)\|_{0,\omega_{\boldsymbol{a}}} \|\psi_{\boldsymbol{a}} v\|_{0,\omega_{\boldsymbol{a}}} + \|g - \widetilde{\pi}_h^p(g)\|_{0,\partial\omega_{\boldsymbol{a}}\cap\Gamma_{\mathrm{A}}} \|\psi_{\boldsymbol{a}} v\|_{0,\partial\omega_{\boldsymbol{a}}\cap\Gamma_{\mathrm{A}}} \\
&\le |\langle \mathcal{R}(u_h), \psi_{\boldsymbol{a}} v\rangle| + \|f - \pi_h^p(f)\|_{0,\omega_{\boldsymbol{a}}} \|v\|_{0,\omega_{\boldsymbol{a}}} + \|g - \widetilde{\pi}_h^p(g)\|_{0,\partial\omega_{\boldsymbol{a}}\cap\Gamma_{\mathrm{A}}} \|v\|_{0,\partial\omega_{\boldsymbol{a}}\cap\Gamma_{\mathrm{A}}},
\end{aligned}$$

and we conclude using a similar estimate as in (2.21) patchwise. □ □

In the next lemma, we observe following [7, Theorem 7], [29, Remark 3.15], or [30, Corollary 3.6] that the dual norms of the residual can be characterized using "continuous versions" of the minimization problems defining the equilibrated fluxes $\boldsymbol{\sigma}_h^{\boldsymbol{a}}$. Recall that $\Gamma_{\boldsymbol{a}}$ is the boundary $\partial\omega_{\boldsymbol{a}}$ without those faces of Γ_{D} sharing the vertex $\boldsymbol{a}$.

Lemma 4.3 (Dual characterization)**.** *We have*

$$\|\mathcal{R}_h(u_h)\|_{-1,\boldsymbol{a}} = \min_{\substack{\boldsymbol{\tau}^{\boldsymbol{a}} \in \boldsymbol{H}(\mathrm{div},\omega_{\boldsymbol{a}}) \\ \boldsymbol{\nabla}\cdot\boldsymbol{\tau}^{\boldsymbol{a}} = d_{\boldsymbol{a}} \text{ in } \omega_{\boldsymbol{a}} \\ \boldsymbol{\tau}^{\boldsymbol{a}}\cdot\boldsymbol{n} = b_{\boldsymbol{a}} \text{ on } \Gamma_{\boldsymbol{a}}}} \|\boldsymbol{\tau}^{\boldsymbol{a}} + \psi_{\boldsymbol{a}} \boldsymbol{\nabla} u_h\|_{0,\omega_{\boldsymbol{a}}}, \tag{4.3}$$

where $b_{\boldsymbol{a}}$ and $d_{\boldsymbol{a}}$ are defined in (2.15)*.*

Proof. We introduce $r_{\boldsymbol{a}}$ as the unique element of $H^1_\star(\omega_{\boldsymbol{a}})$ such that

$$(\boldsymbol{\nabla} r_{\boldsymbol{a}}, \boldsymbol{\nabla} v)_{\omega_{\boldsymbol{a}}} = \langle \mathcal{R}_h(u_h), \psi_{\boldsymbol{a}} v\rangle \qquad \forall v \in H^1_\star(\omega_{\boldsymbol{a}}).$$

Let $v \in H^1_\star(\omega_{\boldsymbol{a}})$. The definitions (2.15) and (4.2) together with the identity $\boldsymbol{\nabla}(\psi_{\boldsymbol{a}} v) = \psi_{\boldsymbol{a}} \boldsymbol{\nabla} v + v \boldsymbol{\nabla} \psi_{\boldsymbol{a}}$ show that

$$\langle \mathcal{R}_h(u_h), \psi_{\boldsymbol{a}} v\rangle \;=\; (d_{\boldsymbol{a}}, v)_{\omega_{\boldsymbol{a}}} - (b_{\boldsymbol{a}}, v)_{\partial\omega_{\boldsymbol{a}}\cap\Gamma_{\mathrm{A}}} - (\psi_{\boldsymbol{a}} \boldsymbol{\nabla} u_h, \boldsymbol{\nabla} v)_{\omega_{\boldsymbol{a}}},$$

and therefore

$$(\boldsymbol{\nabla} r_{\boldsymbol{a}}, \boldsymbol{\nabla} v)_{\omega_{\boldsymbol{a}}} = (d_{\boldsymbol{a}}, v)_{\omega_{\boldsymbol{a}}} - (b_{\boldsymbol{a}}, v)_{\partial\omega_{\boldsymbol{a}}\cap\Gamma_{\mathrm{A}}} - (\psi_{\boldsymbol{a}} \boldsymbol{\nabla} u_h, \boldsymbol{\nabla} v)_{\omega_{\boldsymbol{a}}} \qquad \forall v \in H^1_\star(\omega_{\boldsymbol{a}}).$$

Thus, $\boldsymbol{\sigma}^{\boldsymbol{a}} := -(\boldsymbol{\nabla} r_{\boldsymbol{a}} + \psi_{\boldsymbol{a}} \boldsymbol{\nabla} u_h) \in \boldsymbol{H}(\mathrm{div}, \omega_{\boldsymbol{a}})$ satisfies $\boldsymbol{\nabla}\cdot\boldsymbol{\sigma}^{\boldsymbol{a}} = d_{\boldsymbol{a}}$ and $\boldsymbol{\sigma}^{\boldsymbol{a}}\cdot\boldsymbol{n} = b_{\boldsymbol{a}}$ on $\Gamma_{\boldsymbol{a}}$ as well as

$$\left\{\begin{array}{rcll}
(\boldsymbol{\sigma}^{\boldsymbol{a}}, \boldsymbol{v})_{\omega_{\boldsymbol{a}}} - (r_{\boldsymbol{a}}, \boldsymbol{\nabla}\cdot\boldsymbol{v})_{\omega_{\boldsymbol{a}}} &=& -(\psi_{\boldsymbol{a}} \boldsymbol{\nabla} u_h, \boldsymbol{v})_{\omega_{\boldsymbol{a}}} & \forall \boldsymbol{v} \in \boldsymbol{H}_{\Gamma_{\mathrm{A}}}(\mathrm{div}, \omega_{\boldsymbol{a}}), \\
(\boldsymbol{\nabla}\cdot\boldsymbol{\sigma}^{\boldsymbol{a}}, v)_{\omega_{\boldsymbol{a}}} &=& (d_{\boldsymbol{a}}, v)_{\omega_{\boldsymbol{a}}} & \forall v \in H^1_\star(\omega_{\boldsymbol{a}}),
\end{array}\right.$$

so that $\boldsymbol{\sigma}^{\boldsymbol{a}}$ is the unique minimizer in the right-hand side of (4.3). Then, the conclusion follows since we have $\|\mathcal{R}_h(u_h)\|_{-1,\boldsymbol{a}} = |r_{\boldsymbol{a}}|_{1,\omega_{\boldsymbol{a}}} = \|\boldsymbol{\sigma}^{\boldsymbol{a}} + \psi_{\boldsymbol{a}} \boldsymbol{\nabla} u_h\|_{0,\omega_{\boldsymbol{a}}}$. □ □

The following key estimate directly follows from [7, Theorem 7] in two space dimensions and [30, Corollaries 3.3 and 3.8] in three space dimensions.

Lemma 4.4 (Stability of discrete minimization)**.** *For every vertex $\boldsymbol{a} \in \mathcal{V}_h$, we have*

$$\|\boldsymbol{\sigma}_h^{\boldsymbol{a}} + \psi_{\boldsymbol{a}} \boldsymbol{\nabla} u_h\|_{0,\omega_{\boldsymbol{a}}} \le C_{\mathrm{st},\boldsymbol{a}} \min_{\substack{\boldsymbol{\tau}^{\boldsymbol{a}} \in \boldsymbol{H}(\mathrm{div},\omega_{\boldsymbol{a}}) \\ \boldsymbol{\nabla}\cdot\boldsymbol{\tau}^{\boldsymbol{a}} = d_{\boldsymbol{a}} \text{ in } \omega_{\boldsymbol{a}} \\ \boldsymbol{\tau}^{\boldsymbol{a}}\cdot\boldsymbol{n} = b_{\boldsymbol{a}} \text{ on } \Gamma_{\boldsymbol{a}}}} \|\boldsymbol{\tau}^{\boldsymbol{a}} + \psi_{\boldsymbol{a}} \boldsymbol{\nabla} u_h\|_{0,\omega_{\boldsymbol{a}}},$$

where $C_{\mathrm{st},\boldsymbol{a}}$ only depends on $\kappa_{\mathcal{T}_{\boldsymbol{a}}}$.

The following proposition gathers intermediate results established throughout Sections 3 and 4 and proves the local lower bound (2.27) of Theorem 2.5. We denote by $\mathcal{V}_K$ the set of vertices of the mesh cell $K \in \mathcal{T}_h$.

Proposition 4.5 (Local lower bound)**.** *We have*

$$\eta_K \le C_{\mathrm{low},\omega_K} |||u - u_h|||_{1,k,\omega_K} + C(\kappa_{\mathcal{T}_K}) \operatorname{osc}_{\mathcal{T}_K}(f,g) \qquad \forall K \in \mathcal{T}_h,$$

where

$$C_{\mathrm{low},\omega_K} := (d+1) \max_{\boldsymbol{a} \in \mathcal{V}_K} C_{\mathrm{st},\boldsymbol{a}} C_{\mathrm{lb},\boldsymbol{a}}.$$

Proof. Combining Lemmas 3.7, 4.2, 4.3, and 4.4, we infer that

$$\|\boldsymbol{\sigma}_h^{\boldsymbol{a}} + \psi_{\boldsymbol{a}} \boldsymbol{\nabla} u_h\|_{0,\omega_{\boldsymbol{a}}} \le C_{\mathrm{st},\boldsymbol{a}} C_{\mathrm{lb},\boldsymbol{a}} |||u - u_h|||_{1,k,\omega_{\boldsymbol{a}}} + C_{\mathrm{st},\boldsymbol{a}} C(\kappa_{\mathcal{T}_{\boldsymbol{a}}}) \operatorname{osc}_{\mathcal{T}_{\boldsymbol{a}}}(f,g). \tag{4.4}$$

Since

$$\eta_K \le \sum_{\boldsymbol{a} \in \mathcal{V}_K} \|\boldsymbol{\sigma}_h^{\boldsymbol{a}} + \psi_{\boldsymbol{a}} \boldsymbol{\nabla} u_h\|_{0,\omega_{\boldsymbol{a}}}$$

and as each $K \in \mathcal{T}_h$ has $(d+1)$ vertices and the neighboring elements have a similar diameter, the assertion follows. □ □

Finally, the following estimate is obtained by summation of the local lower bounds (4.4) established in the proof of Proposition 4.5 and proves the global lower bound (2.28) of Theorem 2.5:

Proposition 4.6 (Global lower bound)**.** *We have*

$$\eta \le C_{\mathrm{low}} |||u - u_h|||_{1,k,\Omega} + C(\kappa) \operatorname{osc}(f,g),$$

where

$$C_{\mathrm{low}} := (d+1) \max_{\boldsymbol{a} \in \mathcal{V}_h} C_{\mathrm{st},\boldsymbol{a}} C_{\mathrm{lb},\boldsymbol{a}}.$$

Remark 4.7 (Computable lower bound)**.** *Lemma 3.7 shows that $C_{\mathrm{lb},\boldsymbol{a}} \le C_{\mathrm{lb,hat},\boldsymbol{a}}$, where the constant $C_{\mathrm{lb,hat},\boldsymbol{a}}$ is fully computable. Since we can compute an upper bound for $C_{\mathrm{st},\boldsymbol{a}}$, see* [29, Lemma 3.23]*, we are able to provide a fully computable lower bound for the error.*

5. Preasymptotic error estimates

In this section, we establish the results stated in Theorem 2.7. We only detail the proof for Cases 1a) and 1b), as the other cases (related to the interior problem) easily follow from standard properties of spectral decomposition and the regularity shift

$$|\phi|_{2,\Omega} \le \|\Delta\phi\|_{0,\Omega},$$

for all $\phi \in H_0^1(\Omega)$ with $\Delta\phi \in L^2(\Omega)$, which is valid when Ω a convex polytope, see [32] for instance. The aim of this section is thus to prove the bounds (2.31) and (2.32) of Theorem 2.7.

5.1. **A stability estimate in $L^2(\Omega)$.** Under the assumptions of Case 1a) or 1b), the cornerstone of the analysis is a stability estimate that we establish hereafter. Similar upper bounds are available in [33, 42] for the setting considered here, and we refer the reader to [12, 13, 51] for more complex geometries. However, these estimates are not as sharp as possible and/or the constant $C_{\rm stab}(\widehat{\Omega},\widehat{\Gamma}_{\rm D},\boldsymbol{x}_0)$ is not computable, since they have been derived having a priori error estimation (or simply, stability analysis) in mind. We provide here sharper, fully-computable estimates.

Lemma 5.1 ($L^2(\Omega)$ stability estimate)**.** *Let $\Omega=\Omega_0\setminus\overline{D}$, $\Gamma_{\rm A}=\partial\Omega_0$, and $\Gamma_{\rm D}=\partial D$, where $\Omega_0, D\subset\mathbb{R}^d$ are two open, bounded, and connected sets such that $\overline{D}$ is a proper subset of Ω_0. Assume that the subset $\mathcal{O}_{\Gamma_{\rm D},\Gamma_{\rm A}}$ defined in (2.29) is nonempty. For all $\phi\in L^2(\Omega)$, let the (adjoint) solution $u_\phi^\star\in H^1_{\Gamma_{\rm D}}(\Omega)$ solve (2.8), i.e., $b(w,u_\phi^\star)=(w,\phi)$ for all $w\in H^1_{\Gamma_{\rm D}}(\Omega)$. Then, we have*

$$k^2\|u_\phi^\star\|_{0,\Omega}\le\Big((d-1)+C_{\rm stab}(\widehat{\Omega},\widehat{\Gamma}_{\rm D})kh_\Omega\Big)\,\|\phi\|_{0,\Omega},\tag{5.1}$$

with $C_{\rm stab}(\widehat{\Omega},\widehat{\Gamma}_{\rm D})$ is defined in (2.30).

Proof. Let $\boldsymbol{x}_0\in\mathcal{O}_{\Gamma_{\rm D},\Gamma_{\rm A}}$, i.e., we have

$$(\boldsymbol{x}-\boldsymbol{x}_0)\cdot\boldsymbol{n}\le 0\;\forall\boldsymbol{x}\in\Gamma_{\rm D}\quad(\boldsymbol{x}-\boldsymbol{x}_0)\cdot\boldsymbol{n}>0\;\forall\boldsymbol{x}\in\Gamma_{\rm A}.$$

Let us set $\boldsymbol{y}(\boldsymbol{x}):=\boldsymbol{x}-\boldsymbol{x}_0$, $\boldsymbol{y}_{\boldsymbol{\tau}}:=\boldsymbol{y}-(\boldsymbol{y}\cdot\boldsymbol{n})\boldsymbol{n}$, $\boldsymbol{\nabla}_{\boldsymbol{\tau}}u_\phi^\star:=\boldsymbol{\nabla}u_\phi^\star-(\boldsymbol{\nabla}u_\phi^\star\cdot\boldsymbol{n})\boldsymbol{n}$. In strong form, the (adjoint) solution $u_\phi^\star$ is such that

$$\left\{\begin{array}{rcll}-k^2u_\phi^\star-\Delta u_\phi^\star&=&\phi&\text{in }\Omega,\\ u_\phi^\star&=&0&\text{on }\Gamma_{\rm D},\\ \boldsymbol{\nabla}u_\phi^\star\cdot\boldsymbol{n}+iku_\phi^\star&=&0&\text{on }\Gamma_{\rm A}.\end{array}\right.$$

The key idea of the proof is to multiply the first equation by the test function $\overline{w}:=\boldsymbol{y}\cdot\boldsymbol{\nabla}\overline{u_\phi^\star}$ (here $\bar{\cdot}$ denotes the complex conjugate) and employ integration by parts techniques. Let us point out that since Ω is a polytopal domain and $\Gamma_{\rm D}$ and $\Gamma_{\rm A}$ are well separated, we have $u_\phi^\star\in H^{\frac{3}{2}+\varepsilon}(\Omega)$ for some $\varepsilon>0$, and therefore $u_\phi^\star$ and w are sufficiently smooth to allow the operations performed hereafter (see in particular Section 3.3 of [33]).

First, applying Green's formula, we have

$$2\,\mathrm{Re}\left\{-k^2\int_\Omega u_\phi^\star\left(\boldsymbol{y}\cdot\boldsymbol{\nabla}\overline{u_\phi^\star}\right)\right\}=-k^2\int_\Omega\boldsymbol{y}\cdot\boldsymbol{\nabla}|u_\phi^\star|^2=dk^2\|u_\phi^\star\|_{0,\Omega}^2-k^2\int_{\partial\Omega}|u_\phi^\star|^2\boldsymbol{y}\cdot\boldsymbol{n},$$

where we used the fact that $\boldsymbol{\nabla}\cdot\boldsymbol{y}=d$. Recalling Rellich's identity

$$2\,\mathrm{Re}\left\{\int_\Omega\boldsymbol{\nabla}(\boldsymbol{y}\cdot\boldsymbol{\nabla}\overline{u_\phi^\star})\cdot\boldsymbol{\nabla}u_\phi^\star\right\}=-(d-2)|u_\phi^\star|_{1,\Omega}^2+\int_{\partial\Omega}|\boldsymbol{\nabla}u_\phi^\star|^2\boldsymbol{y}\cdot\boldsymbol{n},$$

which can be obtained by integration by parts (see [33, proof of Proposition 3.3] for instance), we have

$$\begin{aligned}&2\,\mathrm{Re}\left\{-\int_\Omega\Delta u_\phi^\star\boldsymbol{y}\cdot\boldsymbol{\nabla}\overline{u_\phi^\star}\right\}\\&=2\,\mathrm{Re}\int_\Omega\boldsymbol{\nabla}u_\phi^\star\cdot\boldsymbol{\nabla}(\boldsymbol{y}\cdot\boldsymbol{\nabla}\overline{u_\phi^\star})-2\,\mathrm{Re}\int_\Omega\left(\boldsymbol{\nabla}u_\phi^\star\cdot\boldsymbol{n}\right)\boldsymbol{y}\cdot\boldsymbol{\nabla}\overline{u_\phi^\star}\\&=-(d-2)|u_\phi^\star|_{1,\Omega}^2+\int_{\partial\Omega}|\boldsymbol{\nabla}u_\phi^\star|^2\boldsymbol{y}\cdot\boldsymbol{n}-2\,\mathrm{Re}\int_{\partial\Omega}\left(\boldsymbol{\nabla}u_\phi^\star\cdot\boldsymbol{n}\right)\boldsymbol{y}\cdot\boldsymbol{\nabla}\overline{u_\phi^\star}.\end{aligned}$$

It follows that

$$\begin{aligned}2\,\mathrm{Re}\int_\Omega \phi\boldsymbol{y}\cdot\boldsymbol{\nabla}\overline{u_\phi^\star} &= 2\,\mathrm{Re}\int_\Omega \left(-k^2u_\phi^\star-\Delta u_\phi^\star\right)\boldsymbol{y}\cdot\boldsymbol{\nabla}\overline{u_\phi^\star}\\ &= dk^2\|u_\phi^\star\|_{0,\Omega}^2-(d-2)|u_\phi^\star|_{1,\Omega}^2\\ &\quad -k^2\int_{\partial\Omega}|u_\phi^\star|^2\boldsymbol{y}\cdot\boldsymbol{n}+\int_{\partial\Omega}|\boldsymbol{\nabla}u_\phi^\star|^2\boldsymbol{y}\cdot\boldsymbol{n}-2\,\mathrm{Re}\int_{\partial\Omega}\left(\boldsymbol{\nabla}u_\phi^\star\cdot\boldsymbol{n}\right)\boldsymbol{y}\cdot\boldsymbol{\nabla}\overline{u_\phi^\star}.\end{aligned}$$

We now simplify the boundary term as

$$\begin{aligned}\mathscr{B} &:= \int_{\partial\Omega}|\boldsymbol{\nabla}u_\phi^\star|^2\boldsymbol{y}\cdot\boldsymbol{n}-2\,\mathrm{Re}\int_{\partial\Omega}(\boldsymbol{\nabla}u_\phi^\star\cdot\boldsymbol{n})\boldsymbol{y}\cdot\boldsymbol{\nabla}\overline{u_\phi^\star}\\ &= \int_{\partial\Omega}|\boldsymbol{\nabla}_{\boldsymbol{\tau}}u_\phi^\star|^2\boldsymbol{y}\cdot\boldsymbol{n}-\int_{\partial\Omega}|\boldsymbol{\nabla}u_\phi^\star\cdot\boldsymbol{n}|^2\boldsymbol{y}\cdot\boldsymbol{n}-2\,\mathrm{Re}\int_{\partial\Omega}(\boldsymbol{\nabla}u_\phi^\star\cdot\boldsymbol{n})\boldsymbol{y}_{\boldsymbol{\tau}}\cdot\boldsymbol{\nabla}_{\boldsymbol{\tau}}\overline{u_\phi^\star}\\ &= \int_{\Gamma_{\mathrm{A}}}|\boldsymbol{\nabla}_{\boldsymbol{\tau}}u_\phi^\star|^2\boldsymbol{y}\cdot\boldsymbol{n}-\int_{\Gamma_{\mathrm{D}}}|\boldsymbol{\nabla}u_\phi^\star\cdot\boldsymbol{n}|^2\boldsymbol{y}\cdot\boldsymbol{n}-\int_{\Gamma_{\mathrm{A}}}|iku_\phi^\star|^2\boldsymbol{y}\cdot\boldsymbol{n}+2\,\mathrm{Re}\left\{\int_{\Gamma_{\mathrm{A}}}iku_\phi^\star\boldsymbol{y}_{\boldsymbol{\tau}}\cdot\boldsymbol{\nabla}_{\boldsymbol{\tau}}\overline{u_\phi^\star}\right\}\\ &\geq \int_{\Gamma_{\mathrm{A}}}|\boldsymbol{\nabla}_{\boldsymbol{\tau}}u_\phi^\star|^2\boldsymbol{y}\cdot\boldsymbol{n}-k^2\int_{\Gamma_{\mathrm{A}}}|u_\phi^\star|^2\boldsymbol{y}\cdot\boldsymbol{n}+2\,\mathrm{Re}\left\{\int_{\Gamma_{\mathrm{A}}}iku_\phi^\star\boldsymbol{y}_{\boldsymbol{\tau}}\cdot\boldsymbol{\nabla}_{\boldsymbol{\tau}}\overline{u_\phi^\star}\right\},\end{aligned}$$

where we used that $\boldsymbol{\nabla}_{\boldsymbol{\tau}}u_\phi^\star=\boldsymbol{0}$ on Γ_{D}, $\boldsymbol{\nabla}u_\phi^\star\cdot\boldsymbol{n}=-iku_\phi^\star$ on Γ_{A}, and $\boldsymbol{y}\cdot\boldsymbol{n}\leq 0$ on Γ_{D}. We now have

$$\begin{aligned}2\,\mathrm{Re}\int_\Omega\phi\boldsymbol{y}\cdot\boldsymbol{\nabla}\overline{u_\phi^\star} &\geq dk^2\|u_\phi^\star\|_{0,\Omega}+\int_{\Gamma_{\mathrm{A}}}|\boldsymbol{\nabla}_{\boldsymbol{\tau}}u_\phi^\star|^2\boldsymbol{y}\cdot\boldsymbol{n}-(d-2)|u_\phi^\star|_{1,\Omega}^2\\ &\quad -2k^2\int_{\Gamma_{\mathrm{A}}}|u_\phi^\star|^2\boldsymbol{y}\cdot\boldsymbol{n}+2\,\mathrm{Re}\int_{\Gamma_{\mathrm{A}}}iku_\phi^\star\boldsymbol{y}_{\boldsymbol{\tau}}\cdot\boldsymbol{\nabla}_{\boldsymbol{\tau}}\overline{u_\phi^\star},\end{aligned}$$

that we can rewrite as

$$\begin{aligned}&dk^2\|u_\phi^\star\|_{0,\Omega}^2+\int_{\Gamma_{\mathrm{A}}}|\boldsymbol{\nabla}_{\boldsymbol{\tau}}u_\phi^\star|^2\boldsymbol{y}\cdot\boldsymbol{n}\\ &\leq 2\,\mathrm{Re}\int_\Omega\phi\boldsymbol{y}\cdot\boldsymbol{\nabla}\overline{u_\phi^\star}+(d-2)|u_\phi^\star|_{1,\Omega}^2+2k^2\int_{\Gamma_{\mathrm{A}}}|u_\phi^\star|^2\boldsymbol{y}\cdot\boldsymbol{n}+2\,\mathrm{Re}\,ik\left\{\int_{\Gamma_{\mathrm{A}}}u_\phi^\star\boldsymbol{y}_{\boldsymbol{\tau}}\cdot\boldsymbol{\nabla}_{\boldsymbol{\tau}}\overline{u_\phi^\star}\right\}\\ &\leq 2\,\mathrm{Re}(\phi,\boldsymbol{y}\cdot\boldsymbol{\nabla}u_\phi^\star)+(d-2)|u_\phi^\star|_{1,\Omega}^2+2k^2\int_{\Gamma_{\mathrm{A}}}|u_\phi^\star|^2\boldsymbol{y}\cdot\boldsymbol{n}+2k\int_{\Gamma_{\mathrm{A}}}|u_\phi^\star||\boldsymbol{\nabla}_{\boldsymbol{\tau}}u_\phi^\star||\boldsymbol{y}_{\boldsymbol{\tau}}|.\end{aligned}$$

At this point, since $\boldsymbol{y}\cdot\boldsymbol{n}>0$ on Γ_{A}, we use the inequality

$$\begin{aligned}2k|u_\phi^\star||\boldsymbol{\nabla}_{\boldsymbol{\tau}}u_\phi^\star||\boldsymbol{y}_{\boldsymbol{\tau}}| &= 2k|u_\phi^\star||\boldsymbol{\nabla}_{\boldsymbol{\tau}}u_\phi^\star||\boldsymbol{y}\times\boldsymbol{n}|\\ &= 2\left(k\frac{|\boldsymbol{y}\times\boldsymbol{n}|}{\sqrt{\boldsymbol{y}\cdot\boldsymbol{n}}}|u_\phi^\star|\right)\left(|\boldsymbol{\nabla}_{\boldsymbol{\tau}}u_\phi^\star|\sqrt{\boldsymbol{y}\cdot\boldsymbol{n}}\right)\\ &\leq k^2\frac{|\boldsymbol{y}\times\boldsymbol{n}|^2}{\boldsymbol{y}\cdot\boldsymbol{n}}|u_\phi^\star|^2+|\boldsymbol{\nabla}_{\boldsymbol{\tau}}u_\phi^\star|^2\boldsymbol{y}\cdot\boldsymbol{n},\end{aligned}$$

and infer that

$$\begin{aligned}dk^2\|u_\phi^\star\|_{0,\Omega}^2 &\leq 2\,\mathrm{Re}(\phi,\boldsymbol{y}\cdot\boldsymbol{\nabla}u_\phi^\star)+(d-2)|u_\phi^\star|_{1,\Omega}^2+k^2\int_{\Gamma_{\mathrm{A}}}\left(2\boldsymbol{y}\cdot\boldsymbol{n}+\frac{|\boldsymbol{y}\times\boldsymbol{n}|^2}{\boldsymbol{y}\cdot\boldsymbol{n}}\right)|u_\phi^\star|^2\\ &\leq 2\lambda(\boldsymbol{x}_0)\|\phi\|_{0,\Omega}|u_\phi^\star|_{1,\Omega}+(d-2)|u_\phi^\star|_{1,\Omega}^2+k^2\mu(\boldsymbol{x}_0)\|u_\phi^\star\|_{0,\Gamma_{\mathrm{A}}}^2\\ &\leq \lambda(\boldsymbol{x}_0)^2\|\phi\|_{0,\Omega}^2+(d-1)|u_\phi^\star|_{1,\Omega}^2+k^2\mu(\boldsymbol{x}_0)\|u_\phi^\star\|_{0,\Gamma_{\mathrm{A}}}^2,\end{aligned}$$

where, recalling that $\boldsymbol{y} = \boldsymbol{x} - \boldsymbol{x}_0$, we have set

$$\lambda(\boldsymbol{x}_0) := \sup_{\boldsymbol{x}\in\Omega} |\boldsymbol{x}-\boldsymbol{x}_0|, \quad \mu(\boldsymbol{x}_0) := \sup_{\boldsymbol{x}\in\Gamma_{\mathrm{A}}} \left(2(\boldsymbol{x}-\boldsymbol{x}_0)\cdot\boldsymbol{n} + \frac{|(\boldsymbol{x}-\boldsymbol{x}_0)\times\boldsymbol{n}|^2}{(\boldsymbol{x}-\boldsymbol{x}_0)\cdot\boldsymbol{n}} \right).$$

Moreover, we have

$$|u_\phi^\star|_{1,\Omega}^2 = \operatorname{Re} b(u_\phi^\star, u_\phi^\star) + k^2\|u_\phi^\star\|_{0,\Omega}^2 \le \|\phi\|_{0,\Omega}\|u_\phi^\star\|_{0,\Omega} + k^2\|u_\phi^\star\|_{0,\Omega}^2$$

and

$$k\|u_\phi^\star\|_{0,\Gamma_{\mathrm{A}}}^2 = -\operatorname{Im} b(u_\phi^\star, u_\phi^\star) \le \|\phi\|_{0,\Omega}\|u_\phi^\star\|_{0,\Omega}.$$

It follows that

$$k^2\|u_\phi^\star\|_{0,\Omega}^2 \le \lambda(\boldsymbol{x}_0)^2\|\phi\|_{0,\Omega}^2 + ((d-1)+k\mu(\boldsymbol{x}_0))\|\phi\|_{0,\Omega}\|u_\phi^\star\|_{0,\Omega}.$$

Lemma 3.2 with $a = k^2$, $b = (d-1)+k\mu(\boldsymbol{x}_0)\|\phi\|_{0,\Omega}$, and $c = \lambda(\boldsymbol{x}_0)^2\|\phi\|_{0,\Omega}^2$ shows that

$$\begin{aligned} k^2\|u_\phi^\star\|_{0,\Omega} &\le \left(\frac{(d-1)+k\mu(\boldsymbol{x}_0)}{2} + \sqrt{\left(\frac{(d-1)+k\mu(\boldsymbol{x}_0)}{2}\right)^2 + k^2\lambda(\boldsymbol{x}_0)^2} \right)\|\phi\|_{0,\Omega} \\ &\le \left((d-1)+k\left(\lambda(\boldsymbol{x}_0)+\mu(\boldsymbol{x}_0)\right)\right)\|\phi\|_{0,\Omega}. \end{aligned}$$

Then (5.1) follows since $C_{\mathrm{stab}}(\widehat{\Omega},\widehat{\Gamma}_{\mathrm{D}}) = \inf_{\boldsymbol{x}_0\in\mathcal{O}_{\Gamma_{\mathrm{D}},\Gamma_{\mathrm{A}}}}(1/h_\Omega)(\lambda(\boldsymbol{x}_0)+\mu(\boldsymbol{x}_0))$. □ □

5.2. **A bound on σ_{ba} for scattering by a non-trapping obstacle (Case 1a)).** We prove the bound (2.31) from Theorem 2.7. Observe first that

$$\sigma_{\mathrm{ba}} = k \sup_{\phi\in L^2(\Omega)\setminus\{0\}} \inf_{v_h\in V_h} \frac{|u_\phi^\star - v_h|_{1,\Omega}}{\|\phi\|_{0,\Omega}} \le k \sup_{\phi\in L^2(\Omega)\setminus\{0\}} \frac{|u_\phi^\star|_{1,\Omega}}{\|\phi\|_{0,\Omega}}. \tag{5.2}$$

Then, we consider an arbitrary $\phi \in L^2(\Omega)$ and the associated solution $u_\phi^\star \in H^1_{\Gamma_{\mathrm{D}}}(\Omega)$. Selecting the test function $v = u_\phi^\star$ in (2.8) and considering the real part of the equality, we see that

$$|u_\phi^\star|_{1,\Omega}^2 = \operatorname{Re}(\phi, u_\phi^\star) + k^2\|u_\phi^\star\|_{0,\Omega}^2.$$

Hence, employing (5.1), we have

$$\begin{aligned} k^2|u_\phi^\star|_{1,\Omega}^2 &\le \frac{k^2}{2\varepsilon}\|\phi\|_{0,\Omega}^2 + \frac{\varepsilon}{2k^2}k^4\|u_\phi^\star\|_{0,\Omega}^2 + k^4\|u_\phi^\star\|_{0,\Omega}^2 \\ &\le \left(F(\varepsilon) + \left((d-1) + C_{\mathrm{stab}}(\widehat{\Omega},\widehat{\Gamma}_{\mathrm{D}})kh_\Omega\right)^2 \right)\|\phi\|_{0,\Omega}^2 \end{aligned}$$

for all $\varepsilon > 0$ with

$$F(\varepsilon) = \frac{k^2}{2\varepsilon} + \frac{\varepsilon}{2k^2}\left((d-1) + C_{\mathrm{stab}}(\widehat{\Omega},\widehat{\Gamma}_{\mathrm{D}})kh_\Omega\right)^2.$$

Then, considering the equation $F'(\varepsilon) = 0$, we see that the minimum of F is achieved for

$$\varepsilon_\star = \frac{k^2}{(d-1) + C_{\mathrm{stab}}(\widehat{\Omega},\widehat{\Gamma}_{\mathrm{D}})kh_\Omega},$$

and

$$F(\varepsilon_\star) = \left((d-1) + C_{\mathrm{stab}}(\widehat{\Omega},\widehat{\Gamma}_{\mathrm{D}})kh_\Omega\right).$$

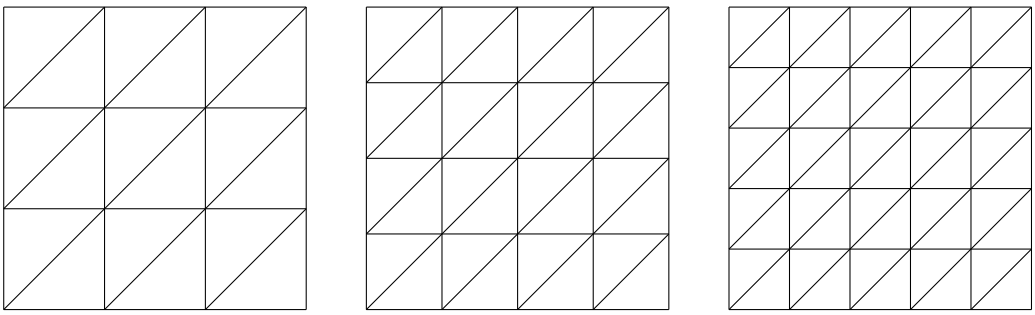

$h = \sqrt{2} \times 2/3$ $h = \sqrt{2} \times 1/2$ $h = \sqrt{2} \times 2/5$

FIGURE 2. Cartesian meshes for the plane wave problem of Section 6.1

We thus obtain that

$$k^2 |u_\phi^\star|_{1,\Omega}^2 \leq \left\{ \Big((d-1) + C_{\rm stab}(\widehat{\Omega}, \widehat{\Gamma}_{\rm D}) k h_\Omega \Big) + \Big((d-1) + C_{\rm stab}(\widehat{\Omega}, \widehat{\Gamma}_{\rm D}, \boldsymbol{x}_0) k h_\Omega \Big)^2 \right\} \|\phi\|_{0,\Omega}^2,$$

for all $\phi \in L^2(\Omega)$, and (2.31) follows from (5.2).

5.3. **A bound on $\sigma_{\rm ba}$ for wave propagation in free space (Case 1b)).** We prove here the estimate (2.32) of Theorem 2.7. We thus consider the case where $\Gamma_{\rm D} = \emptyset$ and Ω is convex. In this case (see [15]), $u_\phi^\star \in H^2(\Omega)$. Using (2.33), we observe that

$$\sigma_{\rm ba} = k \sup_{\phi \in L^2(\Omega)\setminus\{0\}} \inf_{v_h \in V_h} \frac{|u_\phi^\star - v_h|_{1,\Omega}}{\|\phi\|_{0,\Omega}} \leq k C_{\rm i}(\kappa) \frac{h}{p^\beta} \sup_{\phi \in L^2(\Omega)\setminus\{0\}} \frac{|u_\phi^\star|_{2,\Omega}}{\|\phi\|_{0,\Omega}}. \tag{5.3}$$

We can view $u_\phi^\star$ as the unique solution to

$$(\boldsymbol{\nabla} v, \boldsymbol{\nabla} u_\phi^\star) - ik(v, u_\phi^\star)_{\Gamma_{\rm A}} = (v, \widetilde{f}) \quad \forall v \in H^1_{\Gamma_{\rm D}}(\Omega),$$

with $\widetilde{f} = \phi + k^2 u_\phi^\star$. Then, Theorem 3.2 of [15] states that $u_\phi^\star \in H^2(\Omega)$ with

$$|u_\phi^\star|_{2,\Omega} \leq \|\widetilde{f}\|_{0,\Omega}.$$

Then, (5.1) shows that

$$|u_\phi^\star|_{2,\Omega} \leq \Big(d + C_{\rm stab}(\widehat{\Omega}, \widehat{\Gamma}_{\rm D}) k h_\Omega \Big) \|\phi\|_{0,\Omega},$$

and (2.32) follows from (5.3).

6. Numerical experiments

We present here two numerical experiments illustrating Theorems 2.3, 2.5, and 2.7.

6.1. **Plane wave in free space.** We consider problem (1.1) in the square $\Omega = (-1,1)^2$ with $\Gamma_{\rm D} = \emptyset$ and $\Gamma_{\rm A} = \partial\Omega$. We fix the angle $\nu := \pi/3$, set $\boldsymbol{d} := (\cos\nu, \sin\nu)$, and define the plane wave $\xi_\nu(\boldsymbol{x}) := e^{ik\boldsymbol{d}\cdot\boldsymbol{x}}$, $\boldsymbol{x} \in \overline{\Omega}$. We remark that ξ_ν is a homogeneous solution. The problem is thus to find u such that

$$\left\{ \begin{array}{rcll} -k^2 u - \Delta u &=& 0 & \text{in } \Omega, \\ \boldsymbol{\nabla} u \cdot \boldsymbol{n} - iku &=& g & \text{on } \partial\Omega, \end{array} \right. \tag{6.1}$$

where $g = \boldsymbol{\nabla}\xi_\nu \cdot \boldsymbol{n} - ik\xi_\nu$ on $\partial\Omega$. The unique solution is the plane wave $u = \xi_\nu$.

We consider different values of the wavenumber k. In each case, we discretize problem (6.1) with meshes based on Cartesian grids (see Figure 2) with different sizes h. The mesh sizes are selected so that the condition $\frac{kh}{2\pi p} \leq 1$ always holds true. For all meshes and wavenumbers, we compute the relative estimators (the factor 100 allows one to read the relative errors as percentages)

$$E_{\mathrm{est}} := 100 \cdot \frac{\eta}{|||u|||_{1,k,\Omega}}, \quad \widetilde{E}_{\mathrm{est}} := c_{\mathrm{up}} E_{\mathrm{est}},$$

where, following (2.25) of Theorem 2.3 and (2.32) of Theorem 2.7 (here $d = 2$, $\beta = 0$)

$$c_{\mathrm{up}} := \sqrt{\left(\frac{1}{2} + \sqrt{\frac{1}{4} + (c_{\mathrm{ba}})^2}\right) + \left(\frac{1}{2} + \sqrt{\frac{1}{4} + (c_{\mathrm{ba}})^2}\right)^2 + \big(c_{\mathrm{ba}}\big)^2}, \tag{6.2a}$$

$$c_{\mathrm{ba}} := c_{\mathrm{i}} \left(2 + c_{\mathrm{stab}} k h_\Omega\right) kh \tag{6.2b}$$

with

$$h_\Omega = 2\sqrt{2}, \quad c_{\mathrm{stab}} := \frac{3+\sqrt{2}}{2\sqrt{2}}, \quad c_{\mathrm{i}} := \frac{0.493}{\sqrt{2}},$$

see Remarks 2.9 and 2.10. $\widetilde{E}_{\mathrm{est}}$ is the relative percentage form of the guaranteed version of the upper bound (2.23), where C_{up} is bounded from above by $c_{\mathrm{up}} = \sqrt{2} + \tilde{\theta}_1(c_{\mathrm{ba}})$; E_{est} is the relative percentage form of the constant-free equilibrated error estimator η given by (2.22), without the prefactor C_{up} or c_{up}. According to our theoretical results, 1) E_{est} and $\widetilde{E}_{\mathrm{est}}$ are p-robust; 2) $\widetilde{E}_{\mathrm{est}}$ gives a guaranteed upper bound; and 3) c_{ba} as defined in (6.2b) tends to 0, but unfortunately only as $h \to 0$ and not as $p \to \infty$. Furthermore, as the analytical solution is known, we also introduce the relative percentage errors

$$E_{\mathrm{fem}} := 100 \cdot \frac{|||u - u_h|||_{1,k,\Omega}}{|||u|||_{1,k,\Omega}}, \quad E_{\mathrm{ba}} := 100 \cdot \frac{|||u - P_h(u)|||_{1,k,\Omega}}{|||u|||_{1,k,\Omega}},$$

where the best approximation $P_h(u) \in V_h$ to u is numerically computed by solving

$$k^2(P_h(u), v_h) + k(P_h(u), v_h)_{\Gamma_{\mathrm{A}}} + (\boldsymbol{\nabla}(P_h(u)), \boldsymbol{\nabla} v_h) = k^2(u, v_h) + k(u, v_h)_{\Gamma_{\mathrm{A}}} + (\boldsymbol{\nabla} u, \boldsymbol{\nabla} v_h)$$

for all $v_h \in V_h$. The behavior of E_{fem}, E_{ba}, E_{est}, and $\widetilde{E}_{\mathrm{est}}$ for polynomial degrees $p = 1$, 2, and 4 is respectively presented in Figures 3, 4, and 5. In addition, Tables 1, 2, and 3 present the effectivity indices $E_{\mathrm{est}}/E_{\mathrm{fem}}$ and $\widetilde{E}_{\mathrm{est}}/E_{\mathrm{fem}}$ of the prefactor-free and guaranteed relative estimators E_{est} and $\widetilde{E}_{\mathrm{est}}$, respectively.

At fixed wavenumber k, the prefactor-free estimator E_{est} is reliable and efficient for the error E_{fem} up to a constant independent of the mesh size h and polynomial degree p, so that the values of E_{est} follow those of E_{fem} up to effectivity indices independent of h and p. For instance for the wavenumber $k = 20\pi$, where the results cover the unresolved and resolved regimes, see above, the effectivity indices of E_{est} range between 0.11 and 1.00. Also, for fixed wavenumber k and mesh size h, the effectivity index actually improves and approaches the optimal value of one for higher values of p: for instance for $k = 10\pi$ and $h = 2\sqrt{2}/128$, the effectivity indices respectively read 0.20, 0.93, and 1.00 for $p = 1$, 2, and 4. Unfortunately, E_{est} can severely underestimate E_{fem}. The underestimation becomes more pronounced as the wavenumber k gets higher, which can be seen in Figures 3–5 and Tables 1–3, see in particular Table 2, where the effectivity index for $p = 2$ and $k = 60\pi$ drops to 0.07 on a rather refined mesh with $h = 2\sqrt{2}/256$, falling into the resolved regime with $\frac{kh}{2\pi p} \approx 0.17$. This can happen in the preasymptotic regime $\sigma_{\mathrm{ba}} > 1$, since the above reliability and efficiency of E_{est}, though

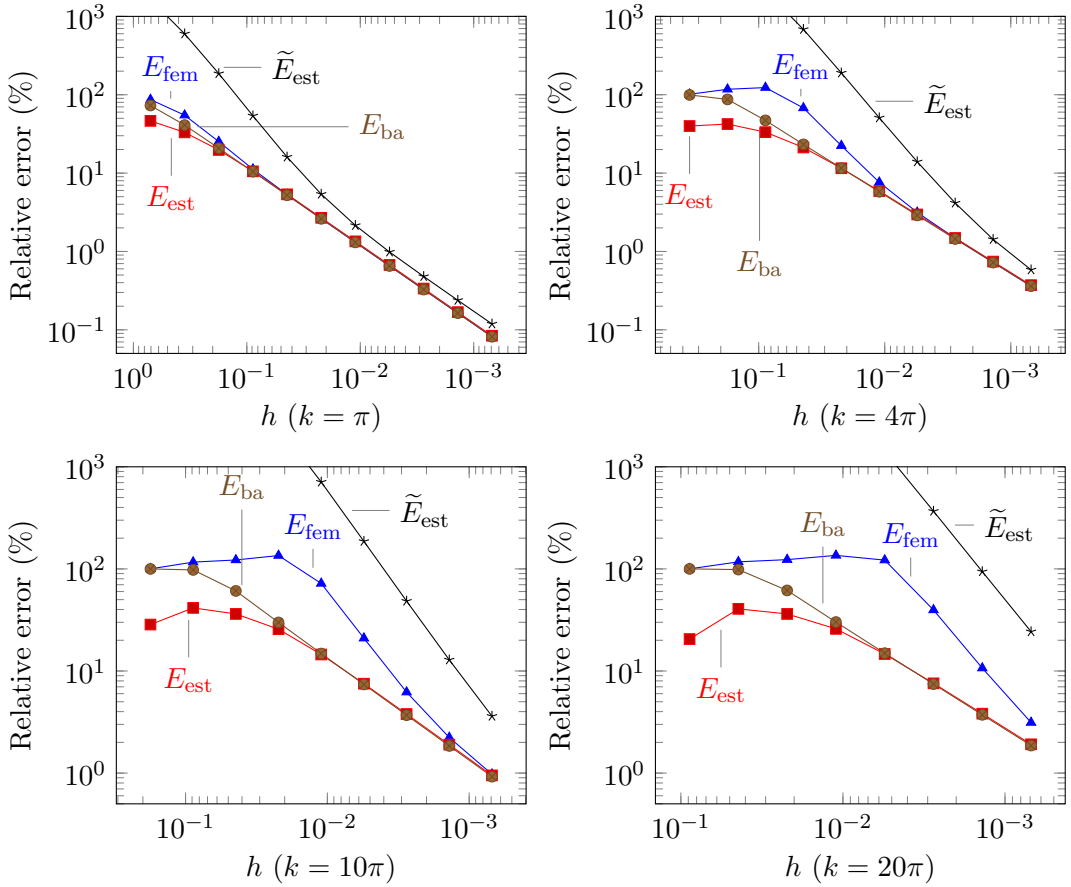

FIGURE 3. Behaviors of the estimated and analytical errors for the plane wave test case of Section 6.1 with $\mathcal{P}_1$ elements

robust with respect to h and p, is not robust with respect to k. In accordance with the theory, though, the effectivity index $E_{\text{est}}/E_{\text{fem}}$ indeed approaches the optimal value of one in the asymptotic regime.

The relative estimator $\widetilde{E}_{\text{est}}$ indeed gives a guaranteed upper bound on the finite element error E_{fem} in all situations. Its effectivity index can unfortunately reach very high values. Although it decreases rather swiftly with mesh refinement for $\mathcal{P}_1$ elements, see Table 1, we were not able to design the upper bound (2.32) on σ_{ba} to be sharp for $p > 1$: we only employ it with $\beta = 0$ which means that c_{ba} does not decrease with increasing polynomial degree p (cf. the asymptotic behavior of σ_{ba} with respect to both h and p in (2.10) where $\varepsilon = 1$ can be taken here). Consequently, the effectivity indices of $\widetilde{E}_{\text{est}}$ are relatively poor for higher-order elements in Tables 2 and 3, and, moreover, only improve with decreasing the mesh size h but not with increasing the polynomial degree p. We also see from Table 1 when $k = \pi$ that asymptotically, the effectivity index of the guaranteed estimator $\widetilde{E}_{\text{est}}$ is close to $\sqrt{2} \simeq 1.41$, which is in agreement with (2.25). Recall that theoretically, this is remedied by the use of the constant $1 + \tilde{\theta}_2(\sigma_{\text{ba}}, \widetilde{\sigma}_{\text{ba}})$ in (2.26). In practice, however, we do not have a computable estimate on $\widetilde{\sigma}_{\text{ba}}$.

	$k=\pi$		$k=4\pi$		$k=10\pi$		$k=20\pi$	
h	E_{est}	$\widetilde{E}_{\text{est}}$	E_{est}	$\widetilde{E}_{\text{est}}$	E_{est}	$\widetilde{E}_{\text{est}}$	E_{est}	$\widetilde{E}_{\text{est}}$
$2\sqrt{2}/8$	0.78	7.38	0.36	45.55	0.28	219.62	0.16	502.52
$2\sqrt{2}/16$	0.94	4.80	0.27	17.18	0.36	137.48	0.21	314.17
$2\sqrt{2}/32$	1.01	3.01	0.31	10.07	0.30	57.24	0.35	265.17
$2\sqrt{2}/64$	1.02	2.05	0.52	8.48	0.19	18.42	0.29	112.57
$2\sqrt{2}/128$	1.03	1.64	0.77	6.65	0.20	9.84	0.19	36.61
$2\sqrt{2}/256$	1.03	1.51	0.94	4.43	0.36	8.89	0.12	11.60
$2\sqrt{2}/512$	1.03	1.47	1.01	2.81	0.61	7.79	0.19	9.27
$2\sqrt{2}/1024$	1.03	1.46	1.02	1.96	0.85	5.76	0.36	8.81
$2\sqrt{2}/2048$	1.03	1.46	1.03	1.61	0.97	3.70	0.61	7.76

TABLE 1. Effectivity indices of the asymptotical and guaranteed error estimators in the plane wave test case of Section 6.1 with $\mathcal{P}_1$ elements

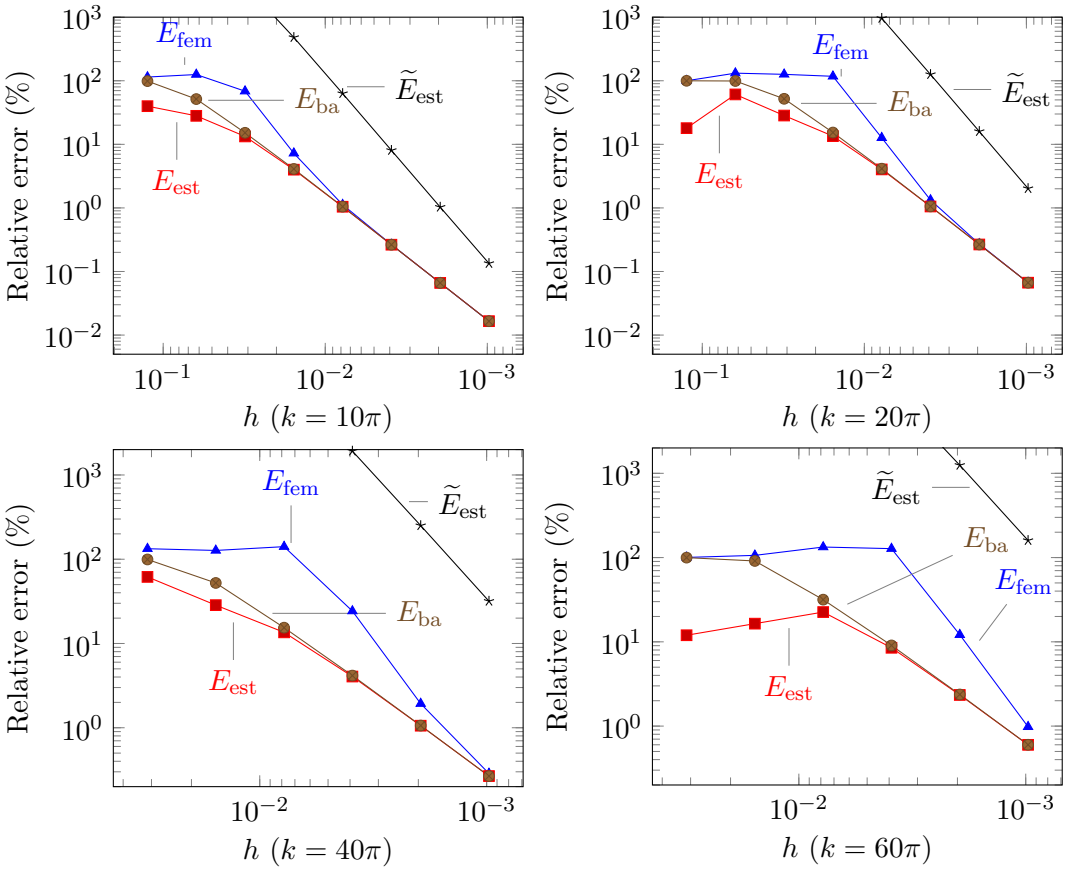

FIGURE 4. Behaviors of the estimated and analytical errors for the plane wave test case of Section 6.1 with $\mathcal{P}_2$ elements

	$k = 10\pi$		$k = 20\pi$		$k = 40\pi$		$k = 60\pi$	
h	E_{est}	$\widetilde{E}_{\text{est}}$	E_{est}	$\widetilde{E}_{\text{est}}$	E_{est}	$\widetilde{E}_{\text{est}}$	E_{est}	$\widetilde{E}_{\text{est}}$
$2\sqrt{2}/32$	0.19	46.58	0.22	213.82	0.46	1753.21	0.12	1014.61
$2\sqrt{2}/64$	0.55	66.32	0.11	54.52	0.22	424.74	0.15	658.57
$2\sqrt{2}/128$	0.93	56.13	0.32	75.82	0.10	91.05	0.17	359.92
$2\sqrt{2}/256$	1.00	30.36	0.79	94.49	0.17	79.18	0.07	70.88
$2\sqrt{2}/512$	1.00	15.57	0.98	58.91	0.55	129.81	0.19	102.77
$2\sqrt{2}/1024$	1.00	8.12	1.00	30.30	0.93	111.08	0.61	162.98

TABLE 2. Effectivity indices of the asymptotical and guaranteed error estimators in the plane wave test case of Section 6.1 with $\mathcal{P}_2$ elements

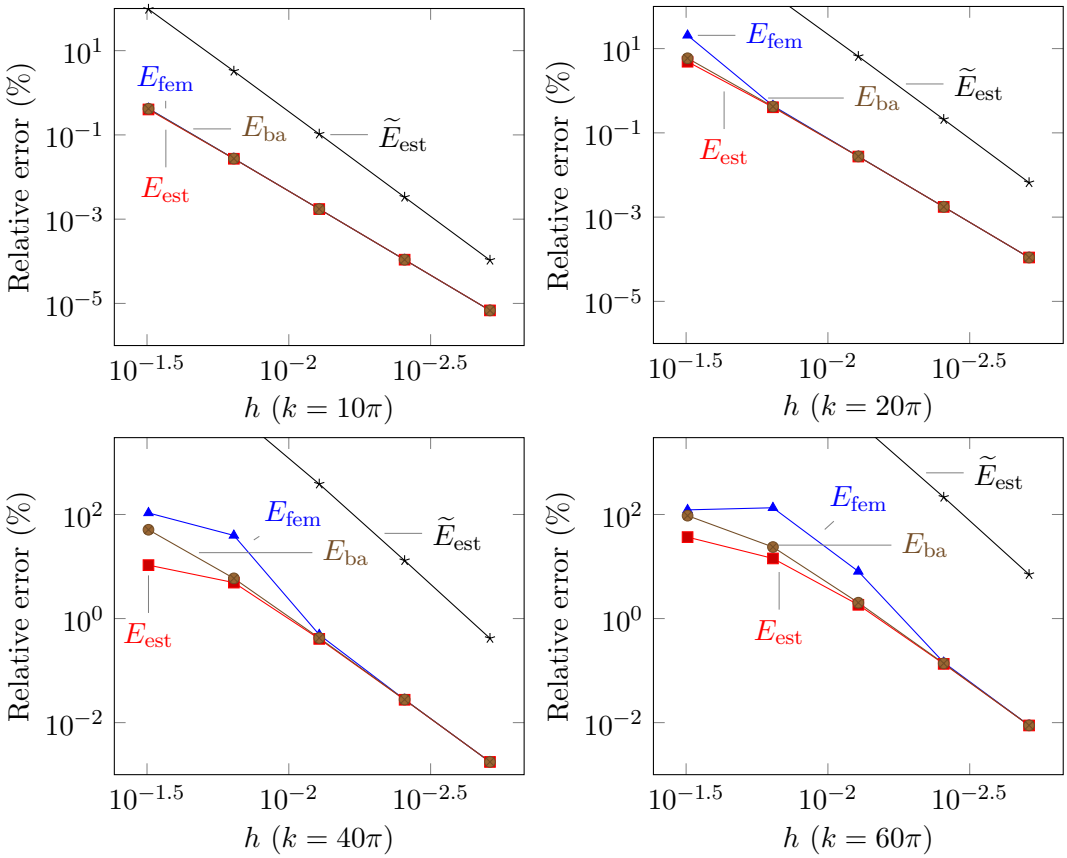

FIGURE 5. Behaviors of the estimated and analytical errors for the plane wave test case of Section 6.1 with $\mathcal{P}_4$ elements

6.2. **Scattering by a non-trapping obstacle.** We now consider the scattering of a plane wave by an obstacle. This problem consists in finding u such that

$$\left\{\begin{array}{rcll} -k^2 u - \Delta u & = & 0 & \text{in } \Omega, \\ u & = & 0 & \text{on } \Gamma_{\text{D}}, \\ \boldsymbol{\nabla} u \cdot \boldsymbol{n} - iku & = & g & \text{on } \Gamma_{\text{A}}, \end{array}\right. \tag{6.3}$$

	$k = 10\pi$		$k = 20\pi$		$k = 40\pi$		$k = 60\pi$	
h	E_{est}	$\widetilde{E}_{\text{est}}$	E_{est}	$\widetilde{E}_{\text{est}}$	E_{est}	$\widetilde{E}_{\text{est}}$	E_{est}	$\widetilde{E}_{\text{est}}$
$2\sqrt{2}/32$	0.95	227.91	0.24	224.79	0.10	376.03	0.30	2548.49
$2\sqrt{2}/64$	0.99	119.14	0.92	438.82	0.12	234.70	0.11	451.99
$2\sqrt{2}/128$	1.00	60.35	0.99	236.00	0.83	787.63	0.23	486.20
$2\sqrt{2}/256$	1.00	30.54	1.00	119.27	0.99	469.50	0.94	1000.73
$2\sqrt{2}/512$	1.00	15.58	1.00	60.06	1.00	237.14	1.00	530.32

TABLE 3. Effectivity indices of the asymptotical and guaranteed error estimators in the plane wave test case of Section 6.1 with $\mathcal{P}_4$ elements

where again $g = \boldsymbol{\nabla}\xi_\nu \cdot \boldsymbol{n} - ik\xi_\nu$ with ξ_ν given in Section 6.1. The computational domain is constructed such that $\Omega = \Omega_0 \setminus \overline{D}$, $\Gamma_{\text{D}} = \partial D$, and $\Gamma_{\text{A}} = \partial\Omega_0$, where $\Omega_0 = (-1, 1)^2$ and

$$D = \left\{ \boldsymbol{x} \in \Omega \;\middle|\; 2|\boldsymbol{x}_1| - \frac{1}{2} < \boldsymbol{x}_2 < |\boldsymbol{x}_1| \right\},$$

see the left panel of Figure 6. We see that we have $\boldsymbol{x} \cdot \boldsymbol{n} \leq 0$ on Γ_{D} and $\boldsymbol{x} \cdot \boldsymbol{n} > 0$ on Γ_{A}, so that this setting enters Case 1a) of Theorem 2.7 with $\boldsymbol{x}_0 = (0, 0)$.

We select the wavenumbers $k = 2\pi$ and 10π and employ polynomials of degree $p = 1$, 2, and 3. As the analytical solution of the problem is not available, we employ an accurate numerical solution as a reference. Specifically, for each mesh $\mathcal{T}_h$, we employ the approximation $u \simeq \widetilde{u}_h$ for the comparison, where $\widetilde{u}_h$ is computed using the mesh $\mathcal{T}_h$ with $\mathcal{P}_6$ finite elements.

In order to generate unstructured adaptive meshes, we consider a simple procedure based on the software platform `mmg` [26]. We start with the initial mesh depicted in the right panel of Figure 6. The software `mmg` allows one to impose a map of maximal allowed mesh sizes (or metric). This map is specified by defining values on the vertices of a previously introduced mesh. Thus, at each iteration, after solving the problem on the mesh $\mathcal{T}_h$ and computing the corresponding estimators η_K, we produce a metric to generate the mesh of the next iteration. We start by defining a new maximal mesh size $h_K^\star$ for each element. This is done by sorting the elements in decreasing values of η_K, setting $h_K^\star := h_K/2$ for the $|\mathcal{T}_h|/10$ first elements, and defining $h_K^\star := 1.1h_K$ for the last $|\mathcal{T}_h|/10$ elements (we set $h_K^\star = h_K$ for the remaining elements). Then, the maximal mesh size value at the vertex $\boldsymbol{a} \in \mathcal{V}_h$ is specified as $h_{\boldsymbol{a}}^\star := \min_{K \in \mathcal{T}_{\boldsymbol{a}}} h_K^\star$. Examples of meshes produced by this algorithm can be seen in Figure 9.

Figures 7 and 8 represent the relative percentage analytical and estimated errors

$$E_{\text{fem}} := 100 \cdot \frac{|||\widetilde{u}_h - u_h|||_{1,k,\Omega}}{|||\widetilde{u}_h|||_{1,k,\Omega}}, \quad E_{\text{est}} := 100 \cdot \frac{\eta}{|||\widetilde{u}_h|||_{1,k,\Omega}}$$

in the different stages of the adaptive procedure for both $k = 2\pi$ and $k = 10\pi$ and for all $\mathcal{P}_1$, $\mathcal{P}_2$, and $\mathcal{P}_3$ elements. All the observations made in the example of Section 6.1 still hold true here, even though the meshes are now unstructured and feature elements of significantly different sizes. The relative estimators E_{est} are in particular a much better match to the approximate relative errors E_{fem} for $\mathcal{P}_3$ elements than for $\mathcal{P}_1$ and $\mathcal{P}_2$ elements in the $k = 10\pi$ case.

Following (2.25) in Theorem 2.3, Case 1a) of Theorem 2.7, and Remark 2.9, we can also define

$$\widetilde{E}_{\text{est}} := c_{\text{up}} E_{\text{est}}$$

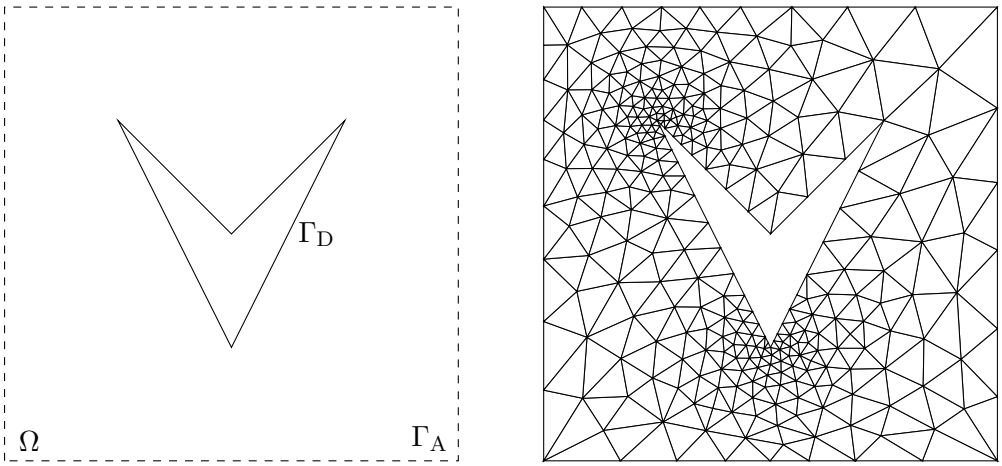

FIGURE 6. Scattering problem of Section 6.2: domain settings (left) and the initial mesh (right)

with $c_{\rm up}$ given by (6.2a) and

$$c_{\rm ba} := \Big((1 + c_{\rm stab} k h_\Omega) + (1 + c_{\rm stab} k h_\Omega)^2 \Big)^{\frac{1}{2}}, \quad c_{\rm stab} := \frac{3+\sqrt{2}}{2\sqrt{2}}, \quad h_\Omega = 2\sqrt{2},$$

where we have employed the point $\boldsymbol{x}_0 = \mathbf{0}$ in Remark 2.9. We remark that here $c_{\rm up}$ only depends on k and improves neither with the mesh size h nor with the polynomial degree p. We compute $c_{\rm up} = 42.05$ for $k = 2\pi$, and $c_{\rm up} = 198.94$ for $k = 10\pi$. We observe that with this definition, $\widetilde{E}_{\rm est}$ indeed constitutes a guaranteed upper bound for all meshes, wavenumbers, and polynomial degrees considered in this example. However, as the overestimation factor for $E_{\rm est}$ is about 1 asymptotically, the overestimation factor for $\widetilde{E}_{\rm est}$ will be about 40 and 200 for $k = 2\pi$ and $k = 10\pi$, respectively, which might unfortunately be too large for being useful in applications.

Finally, Figure 9 depicts the local estimators η_K of (2.22) compared to the actual approximate errors $e_K = |||\widetilde{u}_h - u_h|||_{1,k,K}$, evaluated using the reference numerical solution $\widetilde{u}_h$ on a sequence of adapted meshes for $k = 10\pi$ and $\mathcal{P}_3$ elements. We see that the estimators η_K provide a very good representation of the error distribution, even if the wavenumber is relatively high and the mesh is unstructured, with a significant ratio between the largest and the smallest element sizes. This result illustrates the local efficiency of the proposed estimator as stated in (2.27). The solution corresponding to the finest mesh is depicted in Figure 10.

Let us finally investigate the ability of the local estimators η_K of (2.22) to drive a mesh adaptive algorithm starting with a very coarse mesh. To this end, we still consider the scattering of an incident wave by a non-trapping obstacle (6.3), but we change the incident angle to $\nu = -\pi/12$ and work with higher wavenumbers k. We keep the same refinement algorithm as above but we start with the (much) coarser mesh depicted in Figure 11. Figures 12, 13, and 14 present the results respectively obtained with $\mathcal{P}_1$ elements and $k = 20\pi$, $\mathcal{P}_2$ elements and $k = 60\pi$, and $\mathcal{P}_4$ elements and $k = 120\pi$. The reference solutions, computed on a fine mesh with $\mathcal{P}_6$ elements, are represented in Figure 11. The left panels of Figures 12–14 show that, in all cases, the algorithm converges towards the correct solution, even though the initial mesh is very coarse and features less than one degree of freedom per wavelength.

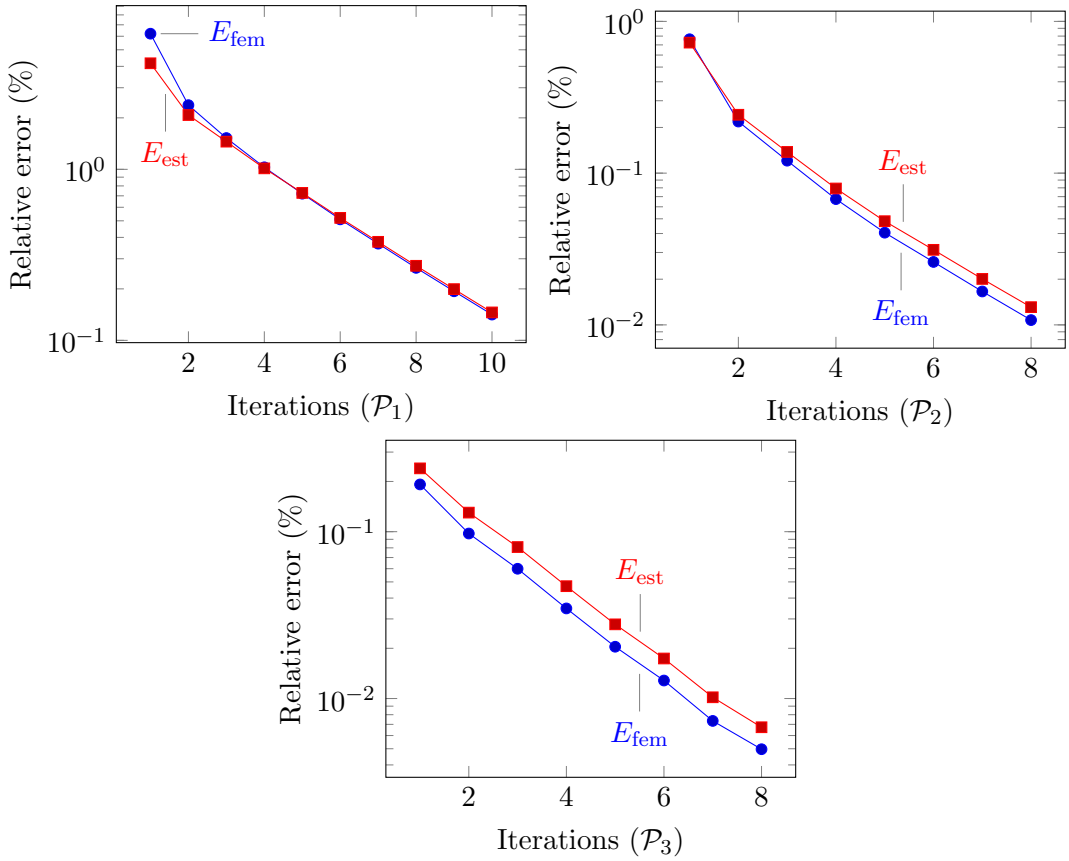

FIGURE 7. Behaviors of the estimated and analytical errors in the adaptive procedure for the scattering problem of Section 6.2 with $k = 2\pi$

In the right panels of Figures 12–14, we indicate the minimal and maximal element sizes in the mesh at each iteration (recall that the meshing package divides the mesh size by 2 in the zone selected for refinement. In each figure, we indicate by a dashed vertical line the first iteration for which the resolved regime is entered in that there holds $\frac{kh}{2\pi p} \leq 1$. In the resolved regime where $\frac{kh}{2\pi p} \leq 1$, we can see that the minimal element sizes are divided by two at each iteration, which means that the smallest elements in the mesh are always selected for refinement. This is typical of refinements close to re-entrant corners, and is expected to correctly capture the corner singularities. In the unresolved regime, however, the minimal element sizes decrease more slowly and are closer to the maximal element sizes, indicating a more uniform refinement of the mesh. This is expected since a global refinement of the mesh is required in the unresolved regime, before the local behavior of the solution can be efficiently captured. Congruently, in the first iterations of the algorithm (approximately 10), the error E_{fem} stagnates or even slightly increases, while in the remaining iterations, the error steeply decreases at each step. An interesting observation is that this seems to appear here soon after the beginning of the resolved regime where $\frac{kh}{2\pi p} \leq 1$, whereas a similar steep decrease only appeared later for uniformly refined meshes, see Figures 3 and 4. This earlier decrease of the finite element error may be explained by the fact that the resolved regime is defined only by

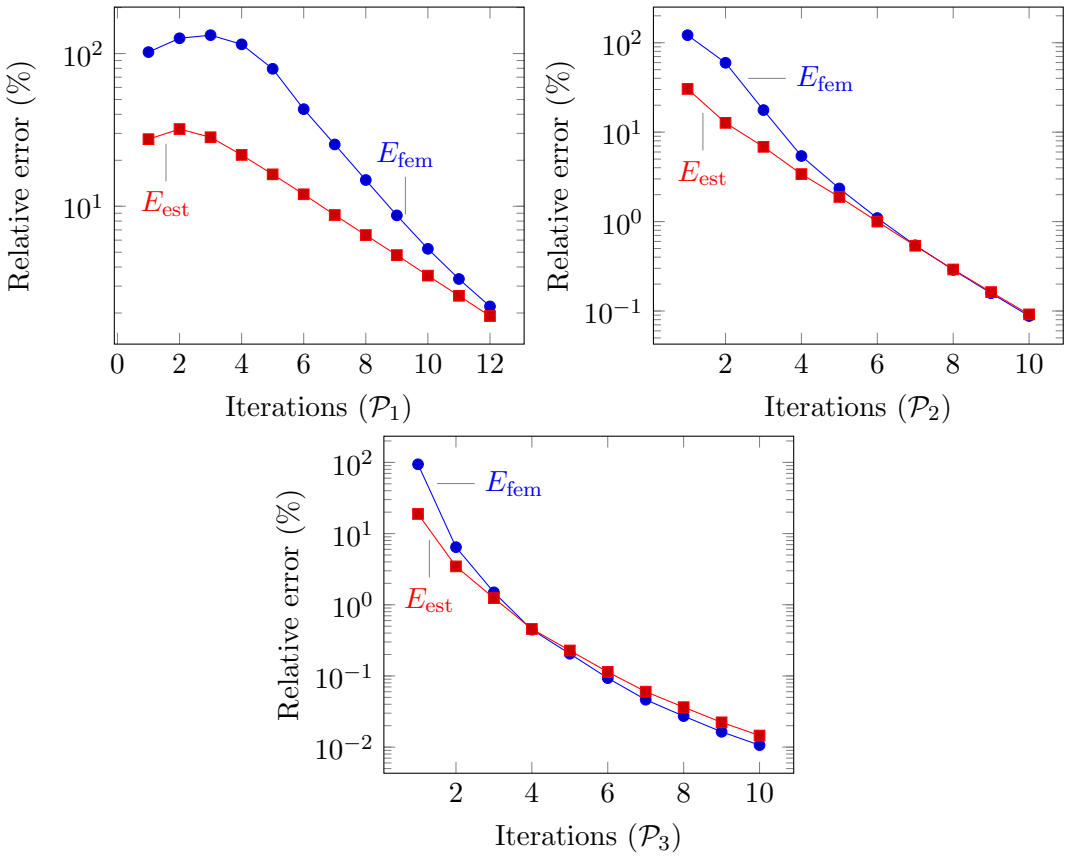

FIGURE 8. Behaviors of the estimated and analytical errors in the adaptive procedure for the scattering problem of Section 6.2 with $k = 10\pi$

the size of the largest element in the mesh, so that a large part of the mesh can be refined before entering the resolved regime.

7. CONCLUSIONS

We have proposed a novel a posteriori error estimator for the Helmholtz problem with mixed boundary conditions in two and three space dimensions. The estimator is based on equilibrated flux reconstruction that relies on the solution of patchwise mixed finite element problems. It is reliable, where the reliability constant depends on the approximation factors σ_{ba} and (possibly) $\widetilde{\sigma}_{\text{ba}}$ and tends to one when $\sigma_{\text{ba}}, \widetilde{\sigma}_{\text{ba}} \to 0$, so that the estimator becomes asymptotically unknown-constant-free. We have also proven, via arguments based on elliptic regularity shift, that the conditions $\sigma_{\text{ba}}, \widetilde{\sigma}_{\text{ba}} \to 0$ are met, for most situations of practical interest, when $\frac{h}{p} \to 0$ with fixed k. Finally, we have proven that the derived estimator is locally efficient and polynomial-degree-robust in all regimes and wavenumber-robust in the asymptotic regime $\sigma_{\text{ba}} \leq 1$.

The approximation factor(s) σ_{ba} (and $\widetilde{\sigma}_{\text{ba}}$) are unfortunately in general not computable. We have managed to provide computable upper bounds on σ_{ba} in particular settings of interest, including scattering by non-trapping obstacles and wave propagation in free space. For such configurations, our upper bound thus becomes guaranteed and fully computable with

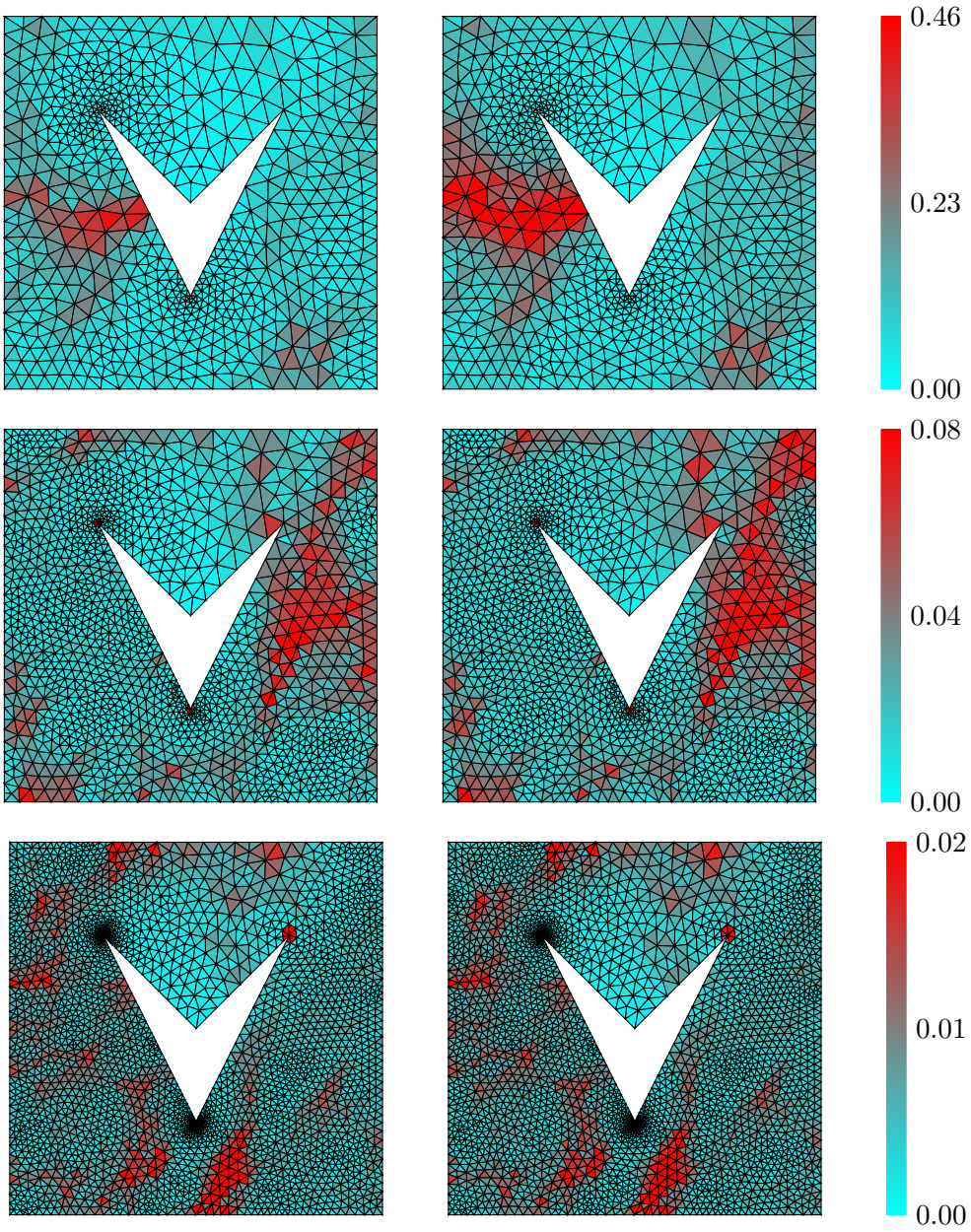

FIGURE 9. Estimators η_K (left) and elementwise errors $|||\widetilde{u}_h - u_h|||_{1,k,K}$ (right) for the scattering problem of Section 6.2 for $k = 10\pi$ with $\mathcal{P}_3$ elements

no unknown constant and no assumptions on the mesh size, the polynomial degree, or the wavenumber. Unfortunately, our computable bounds on σ_{ba} are in general too rough, not converging to zero in some cases, or only converging to 0 with mesh refinement $h \to 0$ but not with polynomial degree increase $p \to \infty$, in contrast to the property $\sigma_{\mathrm{ba}} \to 0$ when $\frac{h}{p} \to 0$ at fixed k. Consequently, an important overestimation can appear for these guaranteed bounds, though they are still locally efficient and polynomial-degree-robust. We believe that these

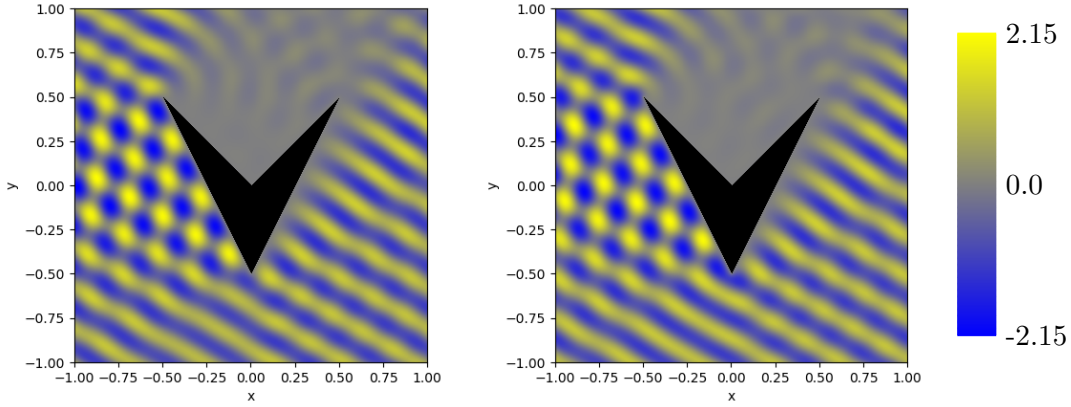

FIGURE 10. Scattering problem with $\nu = \pi/3$: real (left) and imaginary (right) parts of the solution for $k = 10\pi$

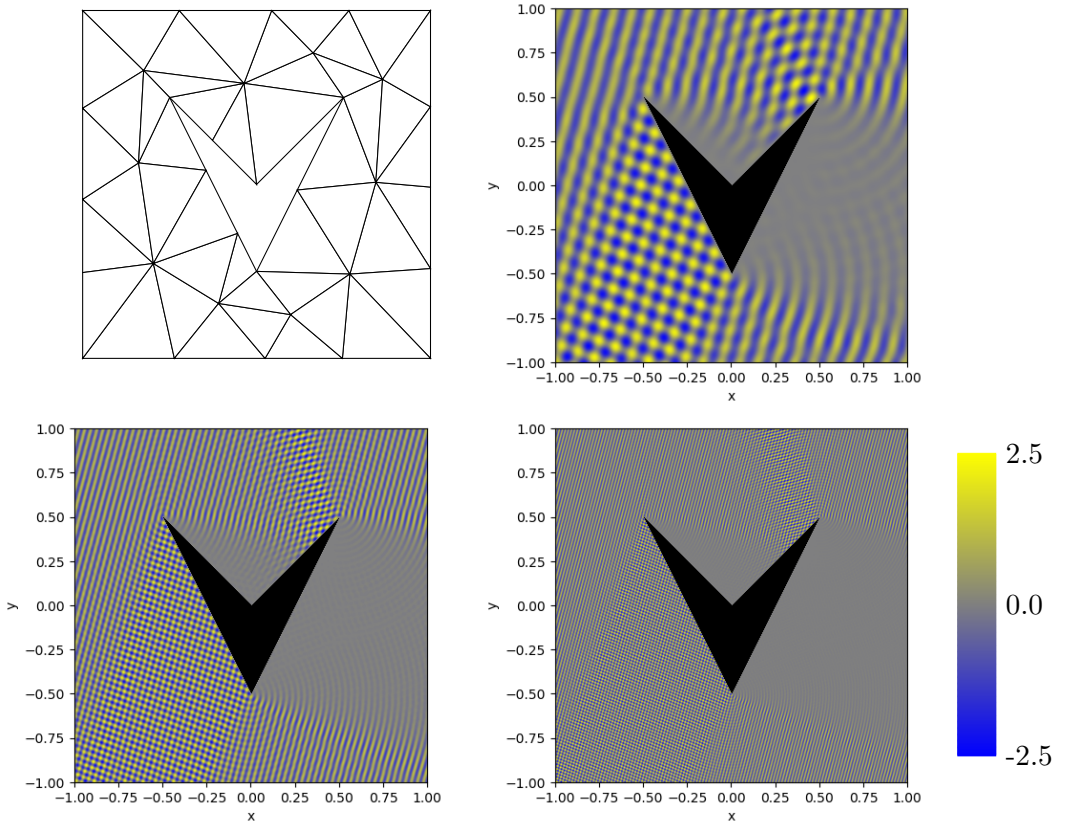

FIGURE 11. Initial mesh for the adaptivity experiment and real part of reference solution for different wavenumbers. Top right panel: $k = 20\pi$. Bottom left panel $k = 60\pi$. Bottom right panel $k = 120\pi$

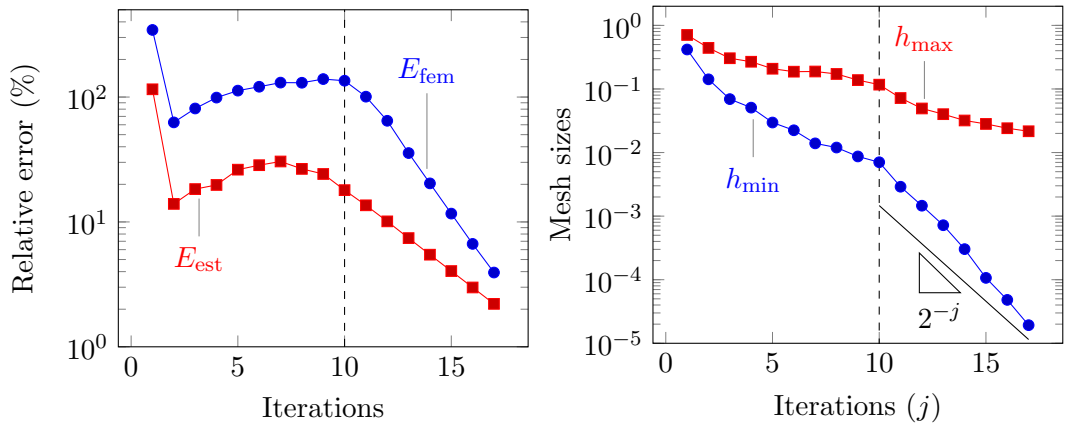

FIGURE 12. Behaviors of the estimated and approximate analytical errors and mesh sizes in the adaptive procedure for the scattering problem of Section 6.2, $\mathcal{P}_1$ elements and $k = 20\pi$

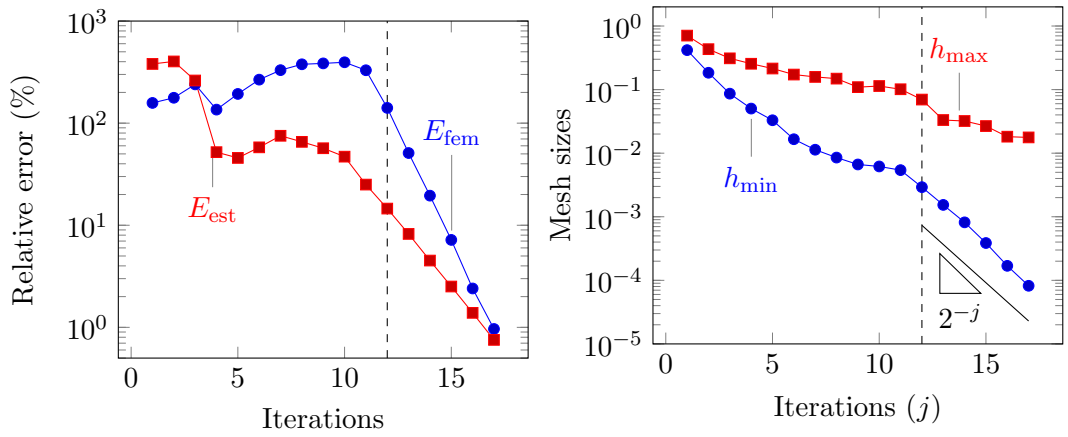

FIGURE 13. Behaviors of the estimated and approximate analytical errors and mesh sizes in the adaptive procedure for the scattering problem of Section 6.2, $\mathcal{P}_2$ elements and $k = 60\pi$

issues could be addressed in future work following [13], in particular by carefully estimating the multiplicative coefficient of corner singularities.

The presented numerical experiments illustrate our findings, and suggest that the proposed estimators additionally have the potential to be asymptotically exact, and indicate that they can drive adaptive mesh refinement starting from coarse meshes and small polynomial degrees even when starting the adaptive process in the unresolved regime where $\frac{kh}{2\pi p} > 1$.

APPENDIX A. ESTIMATE ON THE BEST-APPROXIMATION CONSTANT FOR BOUNDARY DATA

In this appendix, we analyze the behavior of the quantity $\widetilde{\sigma}_{\text{ba}}$ defined in (2.11) in terms of σ_{ba} defined in (2.7). For the sake of simplicity, in this section, the notation $C(\widehat{\Omega}, \widehat{\Gamma}_{\text{D}})$ denotes a generic constant that only depends on the geometry of Ω and Γ_{D} but may vary

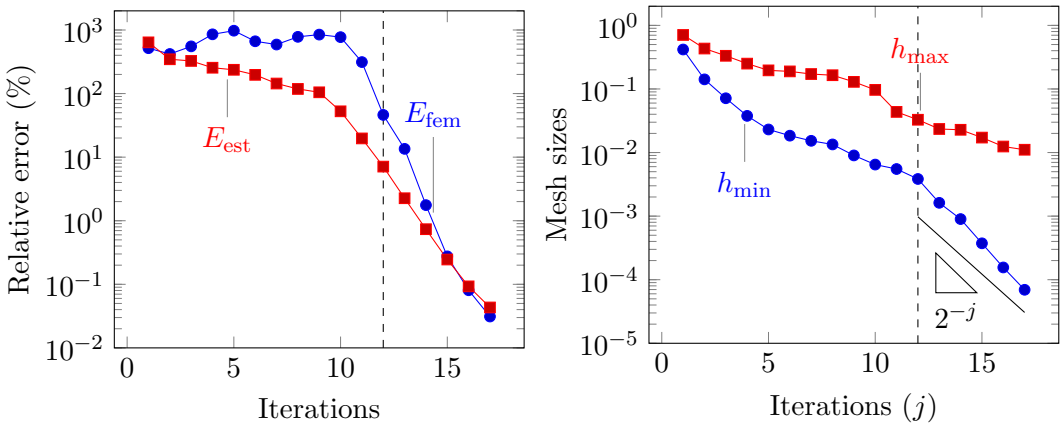

FIGURE 14. Behaviors of the estimated and approximate analytical errors and mesh sizes in the adaptive procedure for the scattering problem of Section 6.2, $\mathcal{P}_4$ elements and $k = 120\pi$

from one occurrence to the other. In addition $C_{\text{qi}}(\kappa)$ is a "quasi-interpolation" constant that only depends on the mesh shape-regularity parameter κ [34, 43].

The results derived in this appendix rely on the following regularity assumption.

Assumption A.1 (Additional regularity)**.** *Let $\phi \in L^2(\Omega)$. We assume that if $u \in H^1(\Omega)$ satisfies*

$$\left\{ \begin{array}{rcll} -\Delta u & = & \phi & \text{in } \Omega, \\ u & = & 0 & \text{on } \Gamma_{\text{D}}, \\ \boldsymbol{\nabla} u \cdot \boldsymbol{n} & = & 0 & \text{on } \Gamma_{\text{A}}, \end{array} \right.$$

then $u \in H^2(\widetilde{\Omega})$ with

$$|u|_{2,\widetilde{\Omega}} \leq C(\widehat{\Omega}, \widehat{\Gamma}_{\text{D}}) \|\phi\|_{0,\Omega},$$

where $\widetilde{\Omega} \subset \Omega$ is a neighborhood of Γ_{A} (i.e., $\widetilde{\Omega}$ is an open subset of Ω and Γ_{A} is a subset of the closure of $\widetilde{\Omega}$) and the constant $C(\widehat{\Omega}, \widehat{\Gamma}_{\text{D}})$ depends on the shape of Ω and the splitting of its boundary into Γ_{D} and Γ_{A} but not on its diameter h_Ω. Furthermore, we assume that if $\psi \in L^2(\Gamma_{\text{A}})$ and $u \in H^1(\Omega)$ solves

$$\left\{ \begin{array}{rcll} -\Delta u & = & 0 & \text{in } \Omega, \\ u & = & 0 & \text{on } \Gamma_{\text{D}}, \\ \boldsymbol{\nabla} u \cdot \boldsymbol{n} & = & \psi & \text{on } \Gamma_{\text{A}}, \end{array} \right.$$

then $u \in H^{\frac{3}{2}}(\widetilde{\Omega})$ with

$$|u|_{\frac{3}{2},\widetilde{\Omega}} \leq C(\widehat{\Omega}, \widehat{\Gamma}_{\text{D}}) \|\psi\|_{0,\Gamma_{\text{A}}}.$$

Assumption A.1 is not an important restriction. Indeed, it is typically satisfied in applications, as the boundary Γ_{A} is artificially designed to enclose the region of interest. For instance, Γ_{A} is usually selected as the boundary of a convex polytope for scattering problems, so that Assumption A.1 holds (see [15] and [21, Lemma 1]). In the case of cavity problems, Γ_{A} is typically planar, and Assumption A.1 holds if the solid angle between Γ_{A} and Γ_{D} is less than or equal to $\pi/2$ (we can perform an odd reflection across the Dirichlet boundary, and

recover a situation similar to the scattering problem, see [15]). As a result, Assumption A.1 is satisfied in all the configurations depicted in Figure 1.

Our next step is to employ a lifting operator $\mathscr{L}$ introduced in [44] that transforms the boundary right-hand side on Γ_{A}, say ψ, appearing in the definition (2.11) of $\widetilde{\sigma}_{\mathrm{ba}}$ into a volume right-hand side $\mathscr{L}_\psi$. We remark that there exists a function $\chi \in C^\infty(\overline{\Omega})$ such that $0 \leq \chi \leq 1$ in $\overline{\Omega}$, $\chi = 0$ outside $\widetilde{\Omega}$, and $\chi = 1$ in a neighborhood on Γ_{A}. In addition, a simple scaling argument shows that we can choose χ such that

$$|\chi|_{j,\infty,\Omega} \leq C(\widehat{\Omega}, \widehat{\Gamma}_{\mathrm{D}}) h_\Omega^{-j}$$

for all $j \in \mathbb{N}$. The main novelty of the following result resides when both subsets Γ_{D} and Γ_{A} have positive measure and touch each other, so that only a regularity shift to $H^{\frac{3}{2}}$ is available owing to Assumption A.1.

Lemma A.2 (Boundary lifting operator)**.** *Let Assumption A.1 hold. For all $\psi \in L^2(\Gamma_{\mathrm{A}})$, we define $\mathscr{L}_\psi$ as the unique element of $H^1_{\Gamma_{\mathrm{D}}}(\Omega)$ such that*

$$a(w, \mathscr{L}_\psi) = (w, \psi)_{\Gamma_{\mathrm{A}}} \tag{A.1}$$

for all $w \in H^1_{\Gamma_{\mathrm{D}}}(\Omega)$, where

$$a(w, \mathscr{L}_\psi) := k^2 (w, \mathscr{L}_\psi) - ik (w, \mathscr{L}_\psi)_{\Gamma_{\mathrm{A}}} + (\boldsymbol{\nabla} w, \boldsymbol{\nabla} \mathscr{L}_\psi).$$

Then we have

$$k \|\mathscr{L}_\psi\|_{0,\Gamma_{\mathrm{A}}} \leq \|\psi\|_{0,\Gamma_{\mathrm{A}}}, \tag{A.2}$$

$$k^2 \|\mathscr{L}_\psi\|^2_{0,\Omega} + |\mathscr{L}_\psi|^2_{1,\Omega} \leq \frac{1}{k} \|\psi\|^2_{0,\Gamma_{\mathrm{A}}}. \tag{A.3}$$

In addition, we have

$$k^{\frac{1}{2}} \inf_{v_h \in V_h} |\chi \mathscr{L}_\psi - v_h|_{1,\Omega} \leq C(\widehat{\Omega}, \widehat{\Gamma}_{\mathrm{D}}) C_{\mathrm{qi}}(\kappa) \left(\left(\frac{kh}{p} \right)^{\frac{1}{2}} + \frac{kh}{p} \right) \|\psi\|_{0,\Gamma_{\mathrm{A}}}, \tag{A.4}$$

where the last term is present only if Γ_{D} has positive surface measure.

Proof. We first pick $w = \mathscr{L}_\psi$ as a test function in (A.1). Taking the imaginary part yields

$$k \|\mathscr{L}_\psi\|^2_{0,\Gamma_{\mathrm{A}}} = -\operatorname{Im}(\mathscr{L}_\psi, \psi)_{\Gamma_{\mathrm{A}}} \leq \|\psi\|_{0,\Gamma_{\mathrm{A}}} \|\mathscr{L}_\psi\|_{0,\Gamma_{\mathrm{A}}},$$

and (A.2) follows. Now, we take the real part and use the above bound to obtain

$$k^2 \|\mathscr{L}_\psi\|^2_{0,\Omega} + |\mathscr{L}_\psi|^2_{1,\Omega} = \operatorname{Re}(\mathscr{L}_\psi, \psi)_{\Gamma_{\mathrm{A}}} \leq \frac{1}{k} \|\psi\|^2_{0,\Gamma_{\mathrm{A}}}.$$

This yields (A.3). Finally, we observe that we can see $\mathscr{L}_\psi$ as the unique element of $H^1_{\Gamma_{\mathrm{D}}}(\Omega)$ such that

$$(\boldsymbol{\nabla} w, \boldsymbol{\nabla} \mathscr{L}_\psi) = -k^2 (w, \mathscr{L}_\psi) + (w, \psi - ik \mathscr{L}_\psi)_{\Gamma_{\mathrm{A}}}$$

for all $w \in H^1_{\Gamma_{\mathrm{D}}}(\Omega)$.

At this point, we distinguish the case where Γ_{D} is of zero measure or not. If $|\Gamma_{\mathrm{D}}| = 0$, then Assumption A.1 together with classical arguments (see [32]) away from Γ_{A} show that

$$\begin{aligned} \|\mathscr{L}_\psi\|_{\frac{3}{2},\Omega} &\leq C(\widehat{\Omega}, \widehat{\Gamma}_{\mathrm{D}}) \left(k^2 \|\mathscr{L}_\psi\|_{\frac{1}{2},\Omega} + \|\psi\|_{0,\Gamma_{\mathrm{A}}} + k \|\mathscr{L}_\psi\|_{0,\Gamma_{\mathrm{A}}} \right) \\ &\leq C(\widehat{\Omega}, \widehat{\Gamma}_{\mathrm{D}}) \left(k^2 \sqrt{\|\mathscr{L}_\psi\|_{0,\Omega} \|\mathscr{L}_\psi\|_{1,\Omega}} + \|\psi\|_{0,\Gamma_{\mathrm{A}}} + k \|\mathscr{L}_\psi\|_{0,\Gamma_{\mathrm{A}}} \right), \end{aligned}$$

and we conclude with (A.2) and (A.3) that

$$\|\chi\mathscr{L}_\psi\|_{\frac{3}{2},\Omega} \le C(\widehat{\Omega},\widehat{\Gamma}_{\rm D})\|\mathscr{L}_\psi\|_{\frac{3}{2},\Omega} \le C(\widehat{\Omega},\widehat{\Gamma}_{\rm D})\|\psi\|_{0,\Gamma_{\rm A}}.$$

Then, (A.4) follows from standard approximation theory [34, 43].

On the other hand, when $|\Gamma_{\rm D}| \neq 0$, we split $\mathscr{L}_\psi = \phi_2 + \phi_{\frac{3}{2}}$ where $\phi_2, \phi_{\frac{3}{2}} \in H^1_{\Gamma_{\rm D}}(\Omega)$ are uniquely defined by

$$(\boldsymbol{\nabla} w, \boldsymbol{\nabla}\phi_2) = -k^2(w,\mathscr{L}_\psi), \quad (\boldsymbol{\nabla} w, \boldsymbol{\nabla}\phi_{\frac{3}{2}}) = (w, \psi - ik\mathscr{L}_\psi)_{\Gamma_{\rm A}}$$

for all $w \in H^1_{\Gamma_{\rm D}}(\Omega)$. Picking the test function $w = \phi_2$, it follows that

$$|\phi_2|^2_{1,\Omega} \le k^2\|\mathscr{L}_\psi\|_{0,\Omega}\|\phi_2\|_{0,\Omega} \le C(\widehat{\Omega},\widehat{\Gamma}_{\rm D})k^{\frac{1}{2}}h_\Omega\|\psi\|_{0,\Gamma_{\rm A}}|\phi_2|_{1,\Omega},$$

where we used the Poincaré inequality to handle $\|\phi_2\|_{0,\Omega}$ and (A.2) to estimate $k\|\mathscr{L}_\psi\|_{0,\Omega}$. Similarly, employing a multiplicative trace inequality which combined with the Poincaré inequality yields $\|\phi_{\frac{3}{2}}\|_{0,\Gamma_{\rm A}} \le C(\widehat{\Omega},\widehat{\Gamma}_{\rm D})h_\Omega^{\frac{1}{2}}|\phi_{\frac{3}{2}}|_{1,\Omega}$, we infer that

$$|\phi_{\frac{3}{2}}|^2_{1,\Omega} \le \|\psi - ik\mathscr{L}_\psi\|_{0,\Gamma_{\rm A}}\|\phi_{\frac{3}{2}}\|_{0,\Gamma_{\rm A}} \le C(\widehat{\Omega},\widehat{\Gamma}_{\rm D})h_\Omega^{\frac{1}{2}}\|\psi\|_{0,\Gamma_{\rm A}}|\phi_{\frac{3}{2}}|_{1,\Omega}.$$

Then, invoking Assumption A.1, we have

$$|\phi_2|_{2,\widetilde{\Omega}} \le C(\widehat{\Omega},\widehat{\Gamma}_{\rm D})k^2\|\mathscr{L}_\psi\|_{0,\Omega} \le C(\widehat{\Omega},\widehat{\Gamma}_{\rm D})k^{\frac{1}{2}}\|\psi\|_{0,\Gamma_{\rm A}},$$

and

$$|\phi_{\frac{3}{2}}|_{\frac{3}{2},\widetilde{\Omega}} \le C(\widehat{\Omega},\widehat{\Gamma}_{\rm D})\|\psi - ik\mathscr{L}_\psi\|_{0,\Gamma_{\rm A}} \le C(\widehat{\Omega},\widehat{\Gamma}_{\rm D})\|\psi\|_{0,\Gamma_{\rm A}}.$$

Thus, since $\operatorname{supp}\chi \subset \widetilde{\Omega}$ and invoking once again the Poincaré inequality, we infer that

$$\begin{aligned}
|\chi\phi_2|_{2,\Omega} &\le \|\chi\|_{0,\Omega}|\phi_2|_{2,\widetilde{\Omega}} + |\chi|_{1,\Omega}|\phi_2|_{1,\Omega} + |\chi|_{2,\Omega}\|\phi_2\|_{0,\Omega} \\
&\le C(\widehat{\Omega},\widehat{\Gamma}_{\rm D})\left(|\phi_2|_{2,\widetilde{\Omega}} + h_\Omega^{-1}|\phi_2|_{1,\Omega}\right) \\
&\le C(\widehat{\Omega},\widehat{\Gamma}_{\rm D})k^{\frac{1}{2}}\|\psi\|_{0,\Gamma_{\rm A}},
\end{aligned}$$

and similar arguments show that

$$|\chi\phi_{\frac{3}{2}}|_{\frac{3}{2},\widetilde{\Omega}} \le C(\widehat{\Omega},\widehat{\Gamma}_{\rm D})\|\psi\|_{0,\Gamma_{\rm A}}.$$

At this point, (A.4) follows from standard approximation theory [34, 43]. □ □

We are now ready to establish the main result of this appendix which proves the claim (A.6).

Proposition A.3 (Bound on $\widetilde{\sigma}_{\rm ba}$)**.** *Let Assumption A.1 hold. Then*

$$\widetilde{\sigma}_{\rm ba} \le C(\widehat{\Omega},\widehat{\Gamma}_{\rm D})C_{\rm qi}(\kappa)\left(\left(\frac{kh}{p}\right)^{\frac{1}{2}} + \frac{kh}{p}\right) + \left(C(\widehat{\Omega},\widehat{\Gamma}_{\rm D})\frac{1}{kh_\Omega}\left(1 + \frac{1}{kh_\Omega}\right) + 2\right)\sigma_{\rm ba}.$$

Proof. We consider an arbitrary element $\psi \in L^2(\Gamma_{\rm A})$ and define $u^\star_\psi$ as the unique element of $H^1_{\Gamma_{\rm D}}(\Omega)$ such that $b(w,u^\star_\psi) = (w,\psi)_{\Gamma_{\rm A}}$ for all $w \in H^1_{\Gamma_{\rm D}}(\Omega)$. Then, defining $\mathscr{L}_\psi \in H^1_{\Gamma_{\rm D}}(\Omega)$

following Lemma A.2, we have

$$
\begin{aligned}
&b(w,\chi\mathscr{L}_\psi)\\
&= -k^2(w,\chi\mathscr{L}_\psi) - ik(w,\chi\mathscr{L}_\psi)_{\Gamma_{\mathrm{A}}} + (\boldsymbol{\nabla} w, \boldsymbol{\nabla}(\chi\mathscr{L}_\psi))\\
&= k^2(\chi w,\mathscr{L}_\psi) - ik(\chi w,\mathscr{L}_\psi)_{\Gamma_{\mathrm{A}}} + (\boldsymbol{\nabla}(\chi w), \boldsymbol{\nabla}\mathscr{L}_\psi)\\
&\quad + (\boldsymbol{\nabla} w, \boldsymbol{\nabla}(\chi\mathscr{L}_\psi)) - (\boldsymbol{\nabla}(\chi w), \boldsymbol{\nabla}\mathscr{L}_\psi) - 2k^2(\chi w,\mathscr{L}_\psi)\\
&= a(\chi w,\mathscr{L}_\psi) + (\boldsymbol{\nabla} w, \mathscr{L}_\psi\boldsymbol{\nabla}\chi) - (w\boldsymbol{\nabla}\chi, \boldsymbol{\nabla}\mathscr{L}_\psi) - 2k^2(\chi w,\mathscr{L}_\psi)\\
&= (\chi w,\psi)_{\Gamma_{\mathrm{A}}} + (\boldsymbol{\nabla} w, \mathscr{L}_\psi\boldsymbol{\nabla}\chi) - (w\boldsymbol{\nabla}\chi, \boldsymbol{\nabla}\mathscr{L}_\psi) - 2k^2(\chi w,\mathscr{L}_\psi)\\
&= (w,\psi)_{\Gamma_{\mathrm{A}}} + (w, \mathscr{L}_\psi\boldsymbol{\nabla}\chi\cdot\boldsymbol{n})_{\partial\Omega} - (w, \boldsymbol{\nabla}\cdot(\mathscr{L}_\psi\boldsymbol{\nabla}\chi)) - (w, \boldsymbol{\nabla}\chi\cdot\boldsymbol{\nabla}\mathscr{L}_\psi) - 2k^2(w,\chi\mathscr{L}_\psi)\\
&= (w,\psi)_{\Gamma_{\mathrm{A}}} - (w, \boldsymbol{\nabla}\cdot(\mathscr{L}_\psi\boldsymbol{\nabla}\chi) + \boldsymbol{\nabla}\chi\cdot\boldsymbol{\nabla}\mathscr{L}_\psi + 2k^2\chi\mathscr{L}_\psi),
\end{aligned}
$$

where we used the fact that $\boldsymbol{\nabla}\chi\cdot\boldsymbol{n} = 0$ on Γ_{A}, as $\chi = 1$ in a neighborhood of Γ_{A}, and that $w = 0$ on Γ_{D} so that $(w, \mathscr{L}_\psi\boldsymbol{\nabla}\chi\cdot\boldsymbol{n})_{\partial\Omega} = 0$. It follows that

$$
b(w, u_\psi^\star - \chi\mathscr{L}_\psi) = (w,\widetilde{f}),
$$

with $\widetilde{f} = \boldsymbol{\nabla}\cdot(\mathscr{L}_\psi\boldsymbol{\nabla}\chi) + \boldsymbol{\nabla}\chi\cdot\boldsymbol{\nabla}\mathscr{L}_\psi + 2k^2\chi\mathscr{L}_\psi$. In particular, we have $\widetilde{f} \in L^2(\Omega)$, and using (A.3), we infer that

$$
\|\widetilde{f}\|_{0,\Omega} \le \left(C(\widehat{\Omega},\widehat{\Gamma}_{\mathrm{D}})\frac{1}{h_\Omega}\left(1+\frac{1}{kh_\Omega}\right)k^{-\frac{1}{2}} + 2k^{\frac{1}{2}}\right)\|\psi\|_{0,\Gamma_{\mathrm{A}}}. \tag{A.5}
$$

Then, we have

$$
\begin{aligned}
k^{\frac{1}{2}}\left(\inf_{v_h\in V_h}|u_\psi^\star - v_h|_{1,\Omega}\right) &\le k^{\frac{1}{2}}\left(\inf_{y_h\in V_h}|(u_\psi^\star - \chi\mathscr{L}_\psi) - y_h|_{1,\Omega} + \inf_{w_h\in V_h}|\chi\mathscr{L}_\psi - w_h|_{1,\Omega}\right)\\
&\le k^{-\frac{1}{2}}\sigma_{\mathrm{ba}}\|\widetilde{f}\|_{0,\Omega} + k^{\frac{1}{2}}\inf_{w_h\in V_h}|\chi\mathscr{L}_\psi - w_h|_{1,\Omega},
\end{aligned}
$$

where the first bound stems by taking the function $v_h = y_h + w_h$ where $y_h \in V_h$ and $w_h \in V_h$ realize the two infimums in the right-hand side. Using (A.5) and Lemma A.2, we see that

$$
\begin{aligned}
k^{\frac{1}{2}}\left(\inf_{v_h\in V_h}|u_\psi^\star - v_h|_{1,\Omega}\right) \le\ &\left(C(\widehat{\Omega},\widehat{\Gamma}_{\mathrm{D}})\frac{1}{kh_\Omega}\left(1+\frac{1}{kh_\Omega}\right)+2\right)\sigma_{\mathrm{ba}}\|\psi\|_{0,\Gamma_{\mathrm{A}}}\\
&+ C(\widehat{\Omega},\widehat{\Gamma}_{\mathrm{D}})C_{\mathrm{qi}}(\kappa)\left(\frac{kh}{p}+\left(\frac{kh}{p}\right)^{\frac{1}{2}}\right)\|\psi\|_{0,\Gamma_{\mathrm{A}}},
\end{aligned}
$$

and we conclude by taking the supremum over $\psi \in L^2(\Gamma_{\mathrm{A}})$. □ □

Corollary A.4 (Asymptotic regime)**.** *Under Assumption A.1, we have*

$$
1 + \tilde{\theta}_2(\sigma_{\mathrm{ba}},\widetilde{\sigma}_{\mathrm{ba}}) \le 1 + \widetilde{\theta}_3\left(\sigma_{\mathrm{ba}}, \frac{kh}{p}\right), \tag{A.6}
$$

where $\widetilde{\theta}_3$ is a decreasing function of its two arguments such that $\lim_{t,t'\to 0}\widetilde{\theta}_3(t,t') = 0$.

References

1. R. Adams and J. Fournier, *Sobolev spaces*, Academic Press, 2003.
2. M. Ainsworth, *Discrete dispersion relation for hp-version finite element approximation at high wave number*, SIAM J. Numer. Anal. **42** (2004), no. 2, 553–575.
3. R. Arcangeli and J.L. Gout, *Sur l'évaluation de l'erreur d'interpolation de Lagrange dans un ouvert de* $\mathbb{R}^n$, R.A.I.R.O. Analyse numérique **10** (1976), no. 3, 5–27.
4. I. Babuška, F. Ihlenburg, T. Strouboulis, and S.K. Gangaraj, *A posteriori error estimation for finite element solutions of Helmholtz equation. Part I: the quality of local indicators and estimators*, Int. J. Numer. Meth. Engrg. **40** (1997), 3443–3462.
5. ———, *A posteriori error estimation for finite element solutions of Helmholtz equation. Part II: estimation of the pollution error*, Int. J. Numer. Meth. Engrg. **40** (1997), 3883–3900.
6. H. Bériot, A. Prinn, and G. Gabard, *Efficient implementation of high-order finite elements for Helmholtz problems*, Int. J. Numer. Meth. Engng. **106** (2016), 213–240.
7. D. Braess, V. Pillwein, and J. Schöberl, *Equilibrated residual error estimates are p-robust*, Comput. Meth. Appl. Mech. Engrg. **198** (2009), 1189–1197.
8. E. Cancès, G. Dusson, Y. Maday, B. Stamm, and M. Vohralík, *Guaranteed and robust a posteriori bounds for Laplace eigenvalues and eigenvectors: conforming approximations*, SIAM J. Numer. Anal. **55** (2017), no. 5, 2228–2254.
9. C. Carstensen and J. Gedicke, *Guaranteed lower bounds for eigenvalues*, Math. Comp. **83** (2014), no. 290, 2605–2629.
10. C. Carstensen, J. Gedicke, and D. Rim, *Explicit error estimates for Courant, Crouzeix-Raviart and Raviart-Thomas finite element methods*, J. Comp. Math. **30** (2012), no. 4, 337–353.
11. C. Carstensen and J. Storn, *Asymptotic exactness of the least-squares finite element residual*, SIAM J. Numer. Anal. **56** (2018), no. 4, 2008–2028.
12. S. N. Chandler-Wilde, E. A. Spence, A. Gibbs, and V. P. Smyshlyaev, *High-frequency bounds for the Helmholtz equation under parabolic trapping and applications in numerical analysis*, SIAM J. Math. Anal. **52** (2020), no. 1, 845–893. MR 4068326
13. T. Chaumont-Frelet and S. Nicaise, *High-frequency behaviour of corner singularities in Helmholtz problems*, ESAIM Math. Model. Numer. Anal. **52** (2018), no. 5, 1803–1845.
14. ———, *Wavenumber explicit convergence analysis for finite element discretizations of general wave propagation problems*, IMA J. Numer. Anal. **40** (2020), 1503–1543.
15. T. Chaumont-Frelet, S. Nicaise, and J. Tomezyk, *Uniform a priori estimates for elliptic problems with impedance boundary conditions*, Comm. Pure Appl. Anal. **19** (2020), no. 5, 2445–2471.
16. G. Chavent, G. Papanicolaou, P. Sacks, and W.W. Symes, *Inverse problems in wave propagation*, Springer, 2012.
17. I. Cheddadi, R. Fučík, M.I. Prieto, and M. Vohralík, *Guaranteed and robust a posteriori error estimates for singularly perturbed reaction-diffusion problems*, ESAIM Math. Model. Numer. Anal. **43** (2009), 867–888.
18. P.G. Ciarlet, *The finite element method for elliptic problems*, SIAM, 2002.
19. D. Colton and R. Kress, *Inverse acoustic and electromagnetic scattering theory*, Springer, 2012.
20. S. Congreve, J. Gedicke, and I. Perugia, *Robust adaptive hp discontinuous Galerkin finite element methods for the Helmholtz equation*, SIAM J. Sci. Comput. **41** (2019), no. 2, A1121–A1147.
21. M. Costabel, *A remark on the regularity of solutions to Maxwell's equations in Lipschitz domains*, Math. Meth. Appl. Sci. **12** (1990), 365–368.
22. V. Darrigrand, D. Pardo, and I. Muga, *Goal–oriented adaptivity using unconventional error representations for the 1D Helmholtz equation*, Comput. Math. Appl. **69** (2015), 964–979.
23. R.B. Davidson, *Computational electromagnetics for RF and microwave engineering*, Cambridge University Press, 2010.
24. L. Demkowicz, *Computing with hp-adaptive finite elements*, vol. 1, Wiley, 2006.
25. Ph. Destuynder and B. Métivet, *Explicit error bounds in a conforming finite element method*, Math. Comp. **68** (1999), no. 228, 1379–1396.
26. C. Dobrzynski, *MMG3D: User guide*, Tech. Report 422, Inria, 2012.
27. V. Dolejší, A. Ern, and M. Vohralík, *hp-adaptation driven by polynomial-degree-robust a posteriori error estimates for elliptic problems*, SIAM J. Sci. Comput. **38** (2016), no. 5, A3220–A3246.

28. W. Dörfler and S. Sauter, *A posteriori error estimation for highly indefinite Helmholtz problems*, Comput. Meth. Appl. Math. **13** (2013), 333–347.
29. A. Ern and M. Vohralík, *Polynomial-degree-robust a posteriori estimates in a unified setting for conforming, nonconforming, discontinuous Galerkin, and mixed discretizations*, SIAM J. Numer. Anal. **53** (2015), no. 2, 1058–1081.
30. A. Ern and M. Vohralík, *Stable broken H^1 and $H(\mathrm{div})$ polynomial extensions for polynomial-degree-robust potential and flux reconstruction in three space dimensions*, Math. Comp. **89** (2020), no. 322, 551–594.
31. V. Girault and P.A. Raviart, *Finite element methods for Navier-Stokes equations: theory and algorithms*, Springer-Verlag, 1986.
32. P. Grisvard, *Singularities in boundary value problems*, Springer-Verlag, 1992.
33. U. Hetmaniuk, *Stability estimates for a class of Helmholtz problems*, Commun. Math. Sci. **5** (2007), no. 3, 665–678.
34. R. Hiptmair and C. Pechstein, *Discrete regular decomposition of tetrahedral discrete 1-forms*, Tech. Report 2017-47, ETH Zürich, 2017.
35. R.H.W. Hope and N. Sharma, *Convergence analysis of an adaptive interior penalty discontinuous Galerkin method for the Helmholtz equation*, IMA J. Numer. Anal. **33** (2013), 898–921.
36. S. Irimie and Ph. Bouillard, *A residual a posteriori error estimator for the finite element solution of the Helmholtz equation*, Comput. Meth. Appl. Mech. Engrg. **190** (2001), 4027–4042.
37. K. Kobayashi and T. Tsuchiya, *A Babuška-Aziz proof of the circumradius condition*, Japan J. Indust. Appl. Math. **31** (2014), 193–210.
38. P. Ladevèze, *Comparaison de modèles de milieux continus*, Ph.D. thesis, Université Pierre et Marie Curie (Paris 6), 1975.
39. X. Liu, *A framework of verified eigenvalue bounds for self-adjoint differential operators*, Appl. Math. Comput. **267** (2015), 341–355.
40. X. Liu and F. Kikuchi, *Analysis and estimation of error constants for P_0 and P_1 interpolations over triangular finite elements*, J. Math. Sci. Univ. Tokyo **17** (2010), no. 1, 27–78.
41. S. Marburg, *Developments in structural-acoustic optimization for passive noise control*, Arch. Comput. Meth. Engng. **9** (2002), no. 4, 291–370.
42. J.M. Melenk, *On generalized finite element methods*, Ph.D. thesis, University of Maryland, 1995.
43. ———, *hp-interpolation of nonsmooth functions and an aplication to hp-a posteriori error estimation*, SIAM J. Numer. Anal. **43** (2005), no. 1, 127–155.
44. J.M. Melenk and S. Sauter, *Wavenumber explicit convergence analysis for Galerkin discretizations of the Helmholtz equation*, SIAM J. Numer. Anal. **49** (2011), no. 3, 1210–1243.
45. J.C. Nédélec, *Mixed finite elements in $\mathbb{R}^3$*, Numer. Math. **35** (1980), 315–341.
46. J. Peraire and A.T. Patera, *Asymptotic a posteriori finite element bounds for the outputs of noncoercive problems: the Helmholtz and Burgers equations*, Comput. Meth. Appl. Mech. Engrg. **171** (1999), 77–86.
47. W. Prager and J.L. Synge, *Approximations in elasticity based on the concept of function space*, Quart. Appl. Math. **5** (1947), no. 3, 241–269.
48. P.A. Raviart and J.M. Thomas, *A mixed finite element method for 2nd order elliptic problems*, Mathematical Aspect of Finite Element Methods, Springer-Verlag, 1977.
49. J. Sarrate, J. Peraire, and A. Patera, *A posteriori finite element error bounds for non-linear outputs of the Helmholtz equation*, Int. J. Numer. Meth. Fluids **31** (1999), 17–36.
50. S. Sauter and J. Zech, *A posteriori error estimation of hp-dG finite element methods for highly indefinite Helmholtz problems*, SIAM J. Numer. Anal. **53** (2015), no. 5, 2414–2440.
51. E.A. Spence, *Wavenumber-explicit bounds in time-harmonic acoustic scattering*, SIAM J. Math. Anal. **46** (2014), no. 4, 2987–3024.
52. J.R. Stewart and T.J.R. Hughes, *Explicit residual-based a posteriori error estimation for finite element discretizations of the Helmholtz equation: computation of the constant and new measures of error estimator quality*, Comput. Meth. Appl. Mech. Engrg. **131** (1996), 335–363.
53. ———, *An a posteriori error estimator and hp-adaptive strategy for finite element discretization of the Helmholtz equation in exterior domains*, Finite Elem. Anal. and Des. **25** (1997), 1–26.
54. M. Taus, L. Zepeda-Nunez, R. Hewett, and L. Demanet, *Pollution-free and fast hybridizable discontinuous Galerkin solvers for the high-frequency Helmholtz equation*, Proc. SEG annual meeting (Houston), 2017.
55. A. Veeser and R. Verfürth, *Poincaré constants for finite element stars*, IMA J. Numer. Anal. **32** (2012), no. 1, 30–47.

56. R. Verfürth, *A posteriori error estimation techniques for finite element methods*, Numerical Mathematics and Scientific Computation, Oxford University Press, Oxford, 2013.
57. O. C. Zienkiewicz and J. Z. Zhu, *A simple error estimator and adaptive procedure for practical engineering analysis*, Internat. J. Numer. Methods Engrg. **24** (1987), no. 2, 337–357.